Federal Safety Investigation Authority

Final report

Accident with helicopter type MD900(902),
on 1 August 2017, at ca. 18:15 UTC on Grossglockner mountain,
municipal Heiligenblut, A-9844, Carinthia
Ref.: 2022-0.483.594

Vienna, 2022

Imprint

Media owner, publisher and editor:
Republic of Austria
Federal Ministry for Climate Action, Environment, Energy, Mobility, Innovation and Technology
Federal Safety Investigation Authority – Civil Aviation Department
Radetzkystrasse 2, 1030 Vienna
Vienna, 2022. Version: 01/08/2022

Investigation report
This report pursuant to Article 16 of Regulation (EU) No. 996/2010 was approved by the Head of the Federal Safety Investigation Authority after completion of the consultation procedure pursuant to Article 16 of Regulation (EU) 996/2010 in conjunction with § 14 para. 1 UUG 2005.

Preamble

The safety investigation took place in accordance with Regulation (EU) No. 996/2010 and Accident Investigation Act, Federal Law Gazette [*BGBl. I*] No. 123/2005 as amended.

The sole objective of the safety investigation is the prevention of future accidents and incidents. The determination of the causes does not imply the assignment of fault or of administrative, civil or criminal liability (Regulation (EU) No 996/2010 Art. 1)

This investigation report is based on the information provided. In the event that the information base is expanded, the Federal Safety Investigation Authority reserves the right to supplement or amend the present investigation report.

The scope of the safety investigation and the procedure to be applied when conducting the safety investigation shall be determined by the Federal Safety Investigation Authority in accordance with the lessons it intends to draw from the investigation in order to improve aviation safety (Regulation (EU) No 996/2010 Art. 5).

Unless stated otherwise, safety recommendations are directed at bodies in a position to implement these recommendations in the form of suitable actions. Decisions to implement these safety recommendations will be at the discretion of such bodies.

The content of the report is subject to restrictions in order to ensure the anonymity of all natural or legal persons involved in the occurrence.

All times given in this report are in 24 hour format and refer to UTC (local time = UTC + 2 hours).

This is a courtesy translation of the report of the safety investigation. As accurate as the translation may be, the original text in German is the work of reference.

Note on persons in photographs:

The photographs of objects and locations included in this report may show persons that may be uninvolved or involved with investigations into the accident or with recovery and possibly anonymized. The colors of clothing worn by these persons (e.g. luminous reflective vests) were digitally retouched as needed (e.g. greyed) since colors may distract from the purpose of the illustrations.

Content

Introduction

Aircraft operator:	Austrian commercial operator
Operating mode:	HEMS
Aircraft manufacturer:	MD Helicopters, Inc. (MDHI)
Type designation:	MD900 (902 Config) Explorer
Aircraft type:	Twin-engine helicopter, MET (H)
Nationality:	Austria
Accident site:	approx. 500 m southeast of the summit of Mount Grossglockner, near the Erzherzog-Johann lodge.
Coordinates (WGS84):	N 47° 4' 10.46", E 012° 42' 9.74"
Altitude above MSL:	approx. 3420 m (11220 ft)
Date and time:	1 August 2017, 18:15 hours UTC (20:15 hours local time)

On 1 August 2017, an accident occurred involving a rescue helicopter at an altitude of 11220 ft (3420 m) on Mount Grossglockner, during a rescue mission due to a medical emergency. The aircraft began to spin (yaw) clockwise around the vertical axis when taking off from the rescue site. The pilot could not regain control and reduced the collective pitch control. After several revolutions, the helicopter hit the ground next to the landing site and tipped over onto the right side of the fuselage. It was badly damaged in the incident, and some of the passengers suffered minor injuries. The likely cause of the accident was loss of control. Contributing factors were the operation close to the limit of aerodynamic controllability combined with the aerodynamic peculiarities of the NOTAR system compared to a helicopter with a conventional tail rotor.

The on-duty service from the Austrian Federal Safety Investigation Authority (SIA), Department for Civil Aviation, was informed of the incident at around 18:35 hours on 1 August 2017, by the Rescue Co-ordination Centre of Austro Control GmbH (ACG). A safety investigation was launched in accordance with Art. 5 paragraph 1 of Regulation (EU) No. 996/2010.

In accordance with Article 9 (2) of Regulation (EU) No. 996/2010, the following states involved were informed of the accident:

State of manufacture:	United States of America
Engine state of manufacture:	Canada

1 Factual information

1.1 Events and history of the flight

The events and history of the flight were reconstructed as follows, on the basis of statements by the pilot, the HEMS crew member, the doctor, eyewitnesses and the passenger, the inquiries by the police department of Heiligenblut, the Carinthian State Criminal Police Office, the Safety Investigation Authority, and a private video recording:

At around 18:04 hours on 1 August 2017, the rescue helicopter, stationed at Matrei heliport (LOMM) in East Tyrol, was called by the Tyrol Control Center to the Erzherzog-Johann lodge (Adlersruhe) due to a medical emergency (Figure 1).

Figure 1 Overview of the flight path from Matrei heliport to Erzherzog-Johann lodge

Source: Google Earth, SIA

The crew consisted of the pilot, a HEMS crew member (HCM) and a doctor. Based on the pilot's performance calculations, it was decided to leave a fourth crew member, who should have been on board for training, at the helipad. The helicopter reached the site, which is approximately 3420 m above MSL (11220 ft), at approximately 18:15 hours. An overflight

of the rescue site as well as a hover flight was performed, to check the helicopter's on-site performance. The rescue site was then approached, to pick up the patient. The approach from south-west direction (course approx. 225°) was stable and at a constant speed and rate of descent, with a steady and slightly gusty headwind. The helicopter was marshalled by the lodge keeper (a mountain rescuer), who was in radio contact with the HEMS crew member and reported a light wind from the south-west direction. At that point the patient was waiting next to the lodge keeper. As there was no suitable area for a stable landing, where the pilot could stop the engines, the pilot decided to hover, supported by the right skid touching the ground, to position the helicopter in order to pick up the patient. The slope gradient at the landing site was about 13 degree. The right sliding door was opened by the doctor, and the patient was assisted into the aircraft by the doctor and the lodge keeper. The doctor helped the patient onto the stretcher located in the left side of the cabin, whereby the Safety Investigation Authority could not clearly clarify where exactly in the helicopter the patient was at the time of impact.

During boarding, the helicopter began to yaw to the right by approx. 30-40° around the vertical axis for the first time, but the pilot was able to stop this movement. The cabin door was closed and the pilot initiated the take-off. The helicopter began to yaw to the right again. As the rotation progressed, the rotation of the helicopter was no longer exclusively around its vertical axis due to significant attitude excursions. This movement could not be stopped by the pilot, despite fully depressing the left pedal. Due to the then uncontrolled rotation around the vertical axis at around 60° per second (corresponding to 6 seconds per revolution), and because the altitude above ground was still too low at this time, no maneuver could be initiated to end this critical flight condition. The lodge keeper was able to move far enough away from the helicopter in time to avoid being hit or injured by it. After approximately 2 ¼ turns around the vertical axis, the helicopter, which was still rotating, landed hard at approximately the point where the patient had boarded, tipped over onto the right side of the fuselage due to the spinning motion, and came to rest. The helicopter was severely damaged (see section 1.3). The pilot switched off the engines and inquired about the condition of the other people on board. The pilot and other people who rushed to the scene helped the doctor and the patient out of the helicopter. The patient was taken to the Erzherzog-Johann lodge where he received further care.

A few minutes after the accident, smoke and a slight fire was noticed at the right engine exhaust. The pilot was able to extinguish the fire immediately using the onboard handheld fire extinguisher, so that no further damage occurred. The wreck was secured with ropes by the lodge keeper and the crew, to prevent the wreckage from slipping down the mountain slope.

1.1.1 Pre-Flight preparation

A weather briefing was carried out in accordance with section 1.7.4 “Pilot weather briefing”. Written flight information documents for LOMM (consisting of NOTAM, SNOWTAM, DOC), created on 1 August 2017 at 05:00 hours, as well as an Airspace Use Plan (AUP) for 1 August 2017 were also submitted to the Safety Investigation Authority. A performance calculation was made in accordance with section 1.6.7.

1.2 Injuries to persons

Table 1 Injuries to persons

Injuries	Crew	Passengers	Others
Fatal	0	0	0
Serious	0	0	0
Minor	1	1	0
None	2	0	–

1.3 Damage to aircraft

The rolling-over of the helicopter and the resulting impact caused damage to the right side of the fuselage, in particular the right engine, engine cowling, the right cockpit and cabin door and the right cockpit windows. The skid landing gear was broken in several places. The tail boom was broken near the fuselage attachment and the right side of the tail section was badly damaged. All the rotor blades were completely destroyed. Parts of them were scattered across a radius of up to 50 m. Overall, the helicopter was a write-off.

1.4 Other damage

There was no other damage.

1.5 Personnel information

1.5.1 Pilot

Age / Gender:	36 years / male
Type of civil aviation license:	ATPL(H)
Ratings:	Helicopter
Model / type rating:	AS350/EC130, Bell206, BO105, EC135/635, MD900/902
Instrument rating:	IR(H)
Training authorization:	FI(H): CPL, PPL, Night, IR, FI, Bell206, BO105, EC135/635, AS350/EC130
Other authorizations:	MCC
Validity:	All licenses were valid on the date of the accident
Checks:	
Medical check:	Class 1, issued on 28 June 2017, valid on the date of the accident

Overall flying experience (including accident flight):	ca. 3541	hours
of which in the last 90 days:	39.5	hours, 204 landings
of which in the last 24 hours:	ca. 24	minutes
Flight experience on the accident type:	ca. 531	hours
of which in the last 24 hours:	ca. 24	minutes
Rest period before the date of the accident:	ca. 9.25	hours

1.6 Aircraft information

The MD900 Explorer is an eight-seat helicopter with skid landing gear from the US manufacturer MD Helicopters Inc. (MDHI). It is powered by two EEC-controlled turboshaft engines of the type Pratt & Whitney P&W 207E, with a continuous shaft horsepower of 500 hp (373 kW). The main rotor rotates counter-clockwise. A unique feature of this type is the utilized anti-torque system. Instead of a conventional tail rotor, a NOTAR® (No Tail Rotor) system developed by McDonnell Douglas is used (see section 1.6.2).

Aircraft type:	Helicopter
Manufacturer:	MD Helicopters, Inc.
Manufacturer designation:	MD900 (902 Config) Explorer
Certification basis:	Small rotorcraft according to JAR-27 Category A
Year of construction:	1995
MTOM:	6500 lb (2948 kg)
Aircraft operator:	Austrian commercial operator
Total flight hours:	ca. 3102.85
Landings:	ca. 12523

Engines	
Manufacturer:	Pratt & Whitney
Manufacturer designation:	P&W 207E
Total flight hours (Engine 1/2):	ca. 1836.1 / ca. 1836.1

1.6.1 Aircraft documents

Certificate of Registration:	issued 3 March 2011, by ACG, valid on the date of the accident
Certificate of Airworthiness:	issued on 4 April 2011, by ACG, valid on the date of the accident
Airworthiness Review Certificate:	issued on 4 April 2017, by the helicopter operator's maintenance organization, valid on the date of the accident
Noise Certification:	issued on 11 April 2011, by ACG, valid on the date of the accident
Qualification Certificate:	issued on 11 April 2011, by ACG, valid on the date of the accident

Permitted types of use:	Helicopter emergency medical services (HEMS), aerial work, external cargo transportation, external passenger transportation, day and night VFR flights and night VFR flights in aerodrome areas, parachute-dropping
Certificate of Insurance:	valid since 04 February 2017, valid on the date of the accident
Aircraft Radio Station License:	issued on 3 August 2016 by the telecommunications office for Upper Austria and Salzburg, valid on the date of the accident

1.6.2 NOTAR anti-torque

The NOTAR system is used instead of a conventional tail rotor to compensate the torque of the main rotor system and for yaw control of the helicopter. The system consists of an air intake, a Variable-Pitch Fan located in the rear of the fuselage with a variable pitch angle, a tail boom through which air flows, a Direct Jet Thruster and a variable vertical stabilizer (VSCS) (Figure 2).

Figure 2 Components of the NOTAR® system

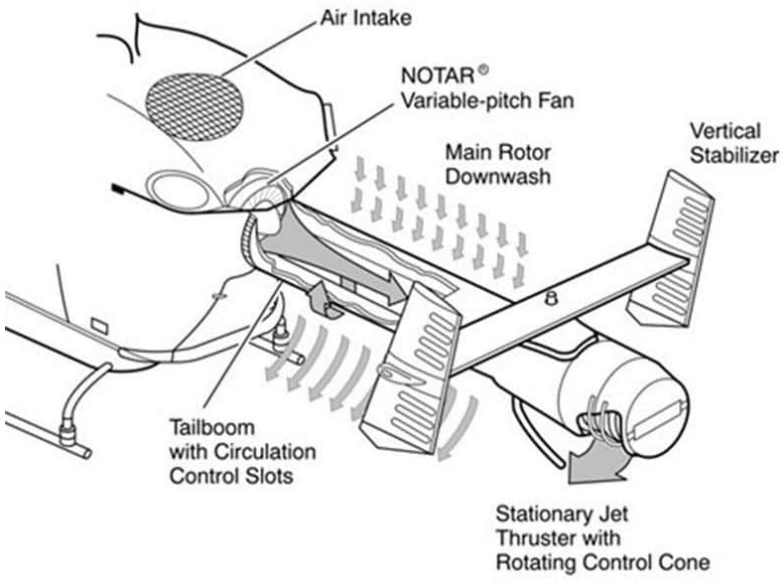

Source: MDHI

Figure 3 Flow around the tail boom

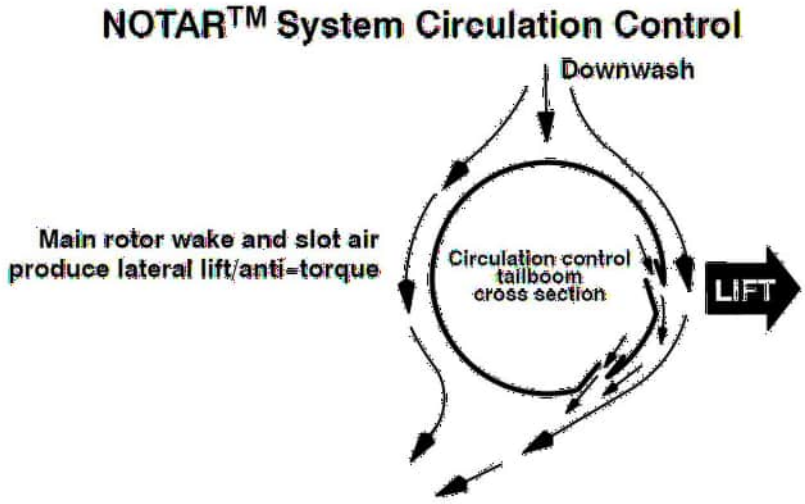

Source: MDHI

The fan is driven by the main gearbox and generates an air stream (low pressure, high volume) that flows through two longitudinal Circulation Control Slots in the tail boom (Figure 3) and exits through the Rotating Control Cone. The Circulation Control Slots run nearly the entire length of the tail boom. The pitch angle of the fan blades and the Rotating Control Cone are pedal-controlled. If the pedals are moved from the neutral position in one of the two directions, the pitch angle of the fan blades and the volume of the air flow is increased, the Control Cone is rotated in the appropriate direction and the outflowing air mass generates a torque around the helicopter's vertical axis. In hover, around 60% of the anti-torque moment is generated via the two longitudinal slots along the tail boom. According to the Coandă effect, the main rotor wake is deflected around the tail boom to the side opposite the slots, and thus creates a lift perpendicular to the direction of flow (to the right in the picture), similar to the flow around a wing flying in the downwash of the main rotor.

During the transition from hovering to forward flight, this lift or torque compensation effect, resulting from the longitudinal slots and the Coandă effect, decreases. The necessary torque compensation is provided by the inflow towards the vertical stabilizer. The upper and lower endplates of the vertical stabilizers are movable control surfaces that help control yaw of the helicopter in forward flight. In forward flight, the vertical stabilizers provide the majority of the anti-torque, however directional control remains a function of the Direct Jet Thruster.

According to MD Helicopters, during the development testing and certification of the MD900, an uncommanded yaw excursion of more than 90 degrees was never encountered. When full left pedal was applied and was unable to stop right yaw, the yaw excursion rarely exceeded 40 degrees.

1.6.3 Certification and operating limitations

The MD900 model was first approved on 2 December 1994 by the Federal Aviation Administration (FAA) with Type Certificate Data Sheet (TCDS) H19NM. On 11 February 1998, an extended version was approved under the designation MD900 (902 Configuration) or MD902, which can be used for Category A operations according to FAR Part 27. On 18 February 1999, the holder of the type certificate changed from McDonnell Douglas Helicopter Company (MDHC), a subsidiary of Boeing Company, to MDHI. During the certification by the FAA, two equivalent level of safety findings (ELOS) were raised. One ELOS related to the fireproof bulkheads of the engines. The second ELOS with the designation TD9369LA-R/F-2 related to the controllability of the helicopter at low speeds.

According to CFR 14 Part 27.143, the aircraft must be able to be operated at wind speeds of 17 kt and below, with critical mass (MTOM), center of gravity and rotor speed up to an altitude of 7000 ft without loss of control (see Appendix 6.1). As this could not be demonstrated for the MD900 model with MTOM up to 7000 ft, in order to achieve an equivalent safety level, operating limits for take-off and landing procedures were specified in the Limitations section of the RFM, in the form of the chart in Figure 2-2 (see this report's Figure 4). This chart applies to hover maneuvers in ground effect (HIGE), and to take-off and landing maneuvers. This chart shows that the take-off and landing WAT limit is independent of the aircraft mass at a density altitude of 12400 ft. However, this operating limit does not apply to flights outside the ground effect. For example, a cruise or hover flight can also take place at a higher density altitude than 12400 ft, provided that sufficient engine power is available. Figure 2-2 is a combined representation of the mentioned WAT limits and crosswind operations limits.

Further approved maximum flight altitudes (density altitudes) are 20,000 ft for aircraft masses up to 6250 lb, and 14,000 ft for aircraft masses between 6251 and 6500 lb.

No separate TCDS was issued by EASA or JAA. The FAA's TCDS (H19NM) was recognized by the JAA and EASA, and is valid in the EASA area.

Figure 4 WAT and Crosswind Limits

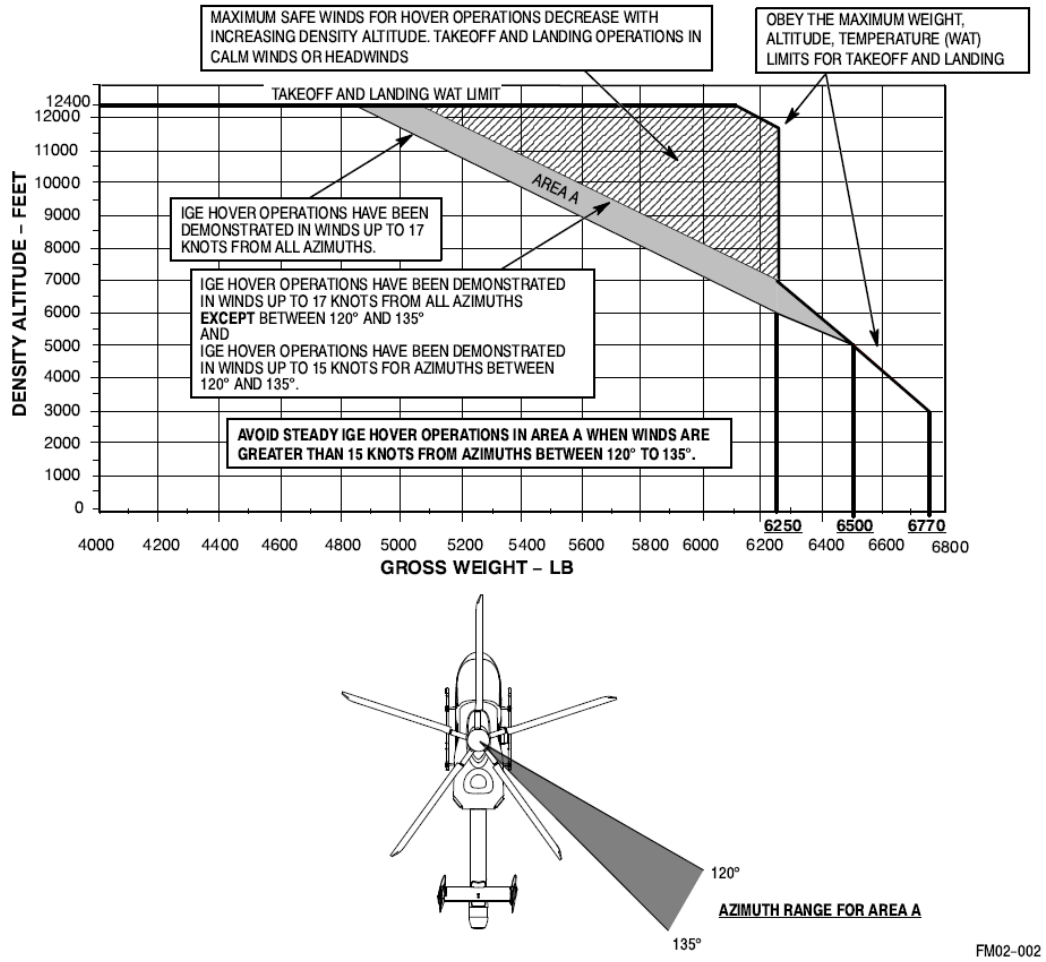

Figure 2–2. WAT Limit and "Area A" Azimuth For Crosswind Operations

Source: MDHI CSP-902RFM207E-1

1.6.4 Airworthiness directives and service bulletins

The following Airworthiness Directives (ADs) and Service Bulletins (SBs) are relevant with regard to directional control of the helicopter or the NOTAR system:

- SB900-094 / EASA AD US-2004-16-08
  Installation of a Fan Input Force Limiting Control Rod Fail-Safe Device.
  SB / AD implementation date: 2 April 2004

- SB900-095 / EASA AD US-2006-18-01
  Reduction of the service life limits of certain NOTAR Fan System Torque Tension Straps (TT Straps) and periodic X-ray inspections of the TT Straps.
  SB / AD implementation date: 25 January 2007

- SB900-100 / EASA AD US-2008-08-11
  Modification of the Pilot and Co-Pilot Dual Control Directional Pedal Assemblies and the Pilot Single-Control Directional Pedal Assembly (Directional Control Pedal Assembly).
  SB / AD implementation date: 25 January 2007

- SB900-108R1 / EASA AD US-2008-17-51
  Performing a fluorescence magnetic particle test to determine possible cracks on the threads of the Directional Control Cable.
  SB / AD implementation date: 16 September 2008

- SB900-096 / EASA AD US-2010-06-06
  Determination of the service life limits of certain components, including parts of the VSCS (Vertical Stabilizer Control System).
  AD implementation date: 22 March 2005

- SB900-110R1 / EASA AD US-2011-22-08
  Operating restrictions and replacement of the VSCS Tube Adapters.
  SB / AD implementation date 15 May 2009

- SB900-107R1 / EASA AD US-2013-03-03
  Determination of the maximum life span of the TT Straps.
  SB implementation date: 25 April 2008, AD implementation date: 3 September 2015

- SB900-099R1 / EASA AD US-2009-07-13
  On 27 December 2006, MDHI issued a mandatory service bulletin (SB) to adapt the rigging of the Directional Control System, to install the Thruster Extension Kit and to check the Fan Felt Seal. In the Airworthiness Directive (AD) 2009-07-13, the FAA stipulated the mandatory implementation of this SB. In the associated FAA Docket No. FAA-2008-0772, a further explanation is given to justify the issue of the AD: during flight tests it was found that the actual controllability limits are not consistent with those in the WAT and crosswind limits diagram (Figure 4).
  SB implementation date: 25 January 2007, AD implementation date: 15 May 2009

1.6.5 Aircraft maintenance

The last annual maintenance inspection (1-year inspection or periodic inspection), was carried out on 15 July 2016, with a total of 2755 hours on the airframe. The type certificate holder allows the date of the next annual maintenance to be exceeded by 14 days. The annual maintenance would thus have been due on 29 July 2017. On the date of the accident, that period had been exceeded by 3 days. No additional deadline extension was requested from Austro Control (Civil Aviation Authority). On 2 June 2017, the last 300 hours / 6 month inspection was carried out with a total of 3060 hours on the airframe.

1.6.6 Aircraft loading and center of gravity

The maximum take-off mass (MTOM) according to the type certificate and flight manual is 6500 lb (2948 kg).

The total basic weight[1] with built-in EMS kit is 3960.6 lb (1796.5 kg), according to the last weight report from 9 July 2016, the longitudinal arm of the center of gravity was 208.605 in. The pilot weighed 85 kg, the HEMS crew member 83 kg, the doctor 73 kg, the patient 104 kg (including baggage) and additional baggage weighing 40 kg was included in the calculation. According to the pilot's assessment, the patient's weight was well below 104 kg. The crew and passengers thus came to a total weight of 345 kg.

[1] According to RFM 6-2, the basic weight includes oil, hydraulic fluid and non-usable fuel.

The usable fuel available at the accident site was estimated at 429 litres, as per section 1.15.1.9. According to section 1.15.1.9 this corresponds to a mass of 340 kg. The mass and center of gravity were calculated according to the above data, as follows:

Table 2 Calculation of mass and center of gravity for the flight from the rescue site

	Weight [lb] (*[kg]*)		**Lever arm (longitudinal) [in] (*[mm]*)**		**Moment [in-lbs]**
Total Basic Weight	**3960.6**	**(*1796.5*)**	**208.605**	**(*5298.6*)**	**826202.8**
+ pilot	187.4	(*85*)	130.7	(*3319.8*)	24492.3
+ HEMS crew member	183.0	(*83*)	130.7	(*3319.8*)	23916.0
+ doctor	160.9	(*73*)	213.0	(*5410.2*)	34279.7
+ patient	229.3	(*104*)	193.0	(*4902.2*)	44251.2
+ baggage	88	(*40*)	245.6	(*6238.2*)	21658.2
Zero Fuel Weight	**4808**	**(*2181*)**	**202.7**	**(*5148.6*)**	**974800.2**
+ fuel	749.6	(*340*)	190.1	(*4828.5*)	142493.7
Total Weight	**5558**	**(*2521*)**	**201.0**	**(*5106.2*)**	**1117293.9**

Source: SIA

Figure 5 Mass and center of gravity

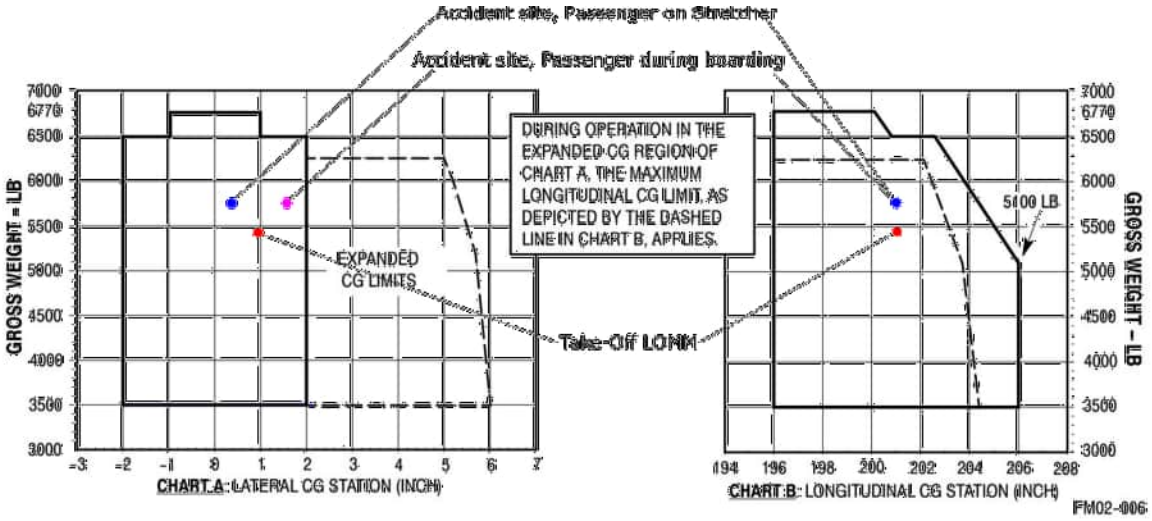

Figure 2-6. Center of Gravity Envelope

Source: MDHI CSP-902RFM207E-1, SIA

When taking off at LOMM without the patient, the center of gravity (CG) lever arm was 201.1 in, the take-off mass was 2481 kg (Figure 5). The lateral CG lever arm was +0.98 in when taking-off at LOMM, +1.74 in at the site of the accident when boarding the patient, and +0.18 in when the patient was on the stretcher.

The mass and center of gravity were therefore within the permissible range during the entire flight.

1.6.6.1 Pilot calculations

The pilot filled out a weight and balance sheet for the flight from the Matrei heliport (LOMM) to the rescue site, and from the rescue site to a hospital.

Table 3 Pilot's mass and center of gravity calculation for the flight from the rescue site

	Weight [kg]	**Lever arm (longitudinal) [mm]**
Total Basic Weight	**1796**	**5248**[(1)]
+ pilot	85	
+ HEMS crew member	83	
+ doctor	73	
+ Other crew member	85	
+ patient	104	
+ baggage	40	
Zero Fuel Weight	**2266**	**5080**
+ fuel	300.7	
Total Weight	**2566.7**	**5050**

Source: Pilot

An additional 85 kg was included for another crew member who was to receive training, but who remained on the ground at LOMM. In addition, a fuel weight of 300.7 kg at the

[1] The lever arm used in the pilot's calculation sheet differs by 51 mm from the lever arm on the last weight report

rescue site was calculated, which is approx. 40 kg less than the amount of fuel discharged from the helicopter. In total, the pilot expected a mass that was higher than the actual mass.

A lateral CG calculation could not be presented.

1.6.7 Performance calculation

The pilot filled out the following data on the operator's performance calculation sheet (underlined values from pilot):

Date : 01.08.2017

ECET : LOKL / LOWI loc. 21:16

Sunset : LOKL / LOWI loc. 20:14

QNH : 1020 10000 ft 14 o'clock Loc 10 °C

LOMM @ 2513 kg PC 1 to ____ °C

OPS - AEO HOGE

@ 2567 kg Crew+PAT	/	@ 2671 kg Crew+PAT+PAX	/	@ 2409 kg HEC-only HCM+PAT
10°C to 10500 ft	/	10 °C to 9000 ft	/	10 °C to 12000 ft
15 °C to 10000 ft	/	15 °C to 9000 ft	/	15 °C to 11500 ft
20 °C to 9000 ft	/	20 °C to 8000 ft	/	20 °C to 10500 ft

PC 1 HOSP @ 2512 kg Crew+PAT		PC 1 HOSP @ 2616 kg Crew+PAT+PAX	
KH LOKJ	PC 1 to + 35 °C	KH LOKJ	PC 1 to 30 °C
KH LOSS	PC 1 to + 40 °C	KH LOKJ	PC 1 to 35 °C
KH LOIU	PC 1 to + 40 °C	KH LOKJ	PC 1 to 35 °C

The values determined by the pilot are based on Figure 5-44 (*Hover Ceiling, OGE, IPS Installed, Takeoff Power, Cabin Heat Off*) from the flight manual (RFM), Section 5, (Performance). The altitude data are thus pressure altitudes.

1.7 Meteorological information

1.7.1 METAR, meteorological service of Austro Control GmbH

Table 4 AUTOMETAR data station Zell am See

VAMES AUTOMETAR message history for Station 11144 Zell am See between 17:40 – 18:40
SAOS61 LOWM 011740 METAR 11144 011740Z AUTO 25010KT 9999 NCD 27/13=
SAOS61 LOWM 011750 METAR 11144 011750Z AUTO 26010KT 9999 NCD 27/13=
SAOS61 LOWM 011800 METAR 11144 011800Z AUTO 26008KT 9999 NCD 27/12=
SAOS61 LOWM 011810 METAR 11144 011810Z AUTO 24007KT 9999 NCD 26/12=
SAOS61 LOWM 011820 METAR 11144 011820Z AUTO 27002KT 9999 FEW180 26/13=
SAOS61 LOWM 011830 METAR 11144 011830Z AUTO 28002KT 9999 SCT180 26/13=
SAOS61 LOWM 011840 METAR 11144 011840Z AUTO 27006KT 9999 FEW180 25/13=

Table 5 AUTOMETAR data station Lienz

VAMES AUTOMETAR message history for Station 11204 Lienz between 17:40 – 18:40
SAOS61 LOWM 011740 METAR 11204 011740Z AUTO 12005KT 9999 NCD 30/16=
SAOS61 LOWM 011750 METAR 11204 011750Z AUTO 13004KT 9999 NCD 29/16=
SAOS61 LOWM 011800 METAR 11204 011800Z AUTO 13005KT 9999 NCD 29/16=
SAOS61 LOWM 011810 METAR 11204 011810Z AUTO 13006KT 9999 NCD 29/16=
SAOS61 LOWM 011820 METAR 11204 011820Z AUTO 12005KT 9999 NCD 28/16=
SAOS61 LOWM 011830 METAR 11204 011830Z AUTO 11004KT 9999 NCD 28/16=
SAOS61 LOWM 011840 METAR 11204 011840Z AUTO 13001KT 9999 NCD 27/16=

Table 6 AUTOMETAR data station Kals

VAMES AUTOMETAR message history for Station 11200 Kals between 17:40 – 18:40
SAOS61 LOWM 011740 METAR 11200 011740Z AUTO 08001KT 9999 NCD 23/14=
SAOS61 LOWM 011750 METAR 11200 011750Z AUTO 08004KT 9999 NCD 23/14=
SAOS61 LOWM 011800 METAR 11200 011800Z AUTO 06003KT 9999 NCD 23/13=
SAOS61 LOWM 011810 METAR 11200 011810Z AUTO 05004KT 9999 NCD 22/13=
SAOS61 LOWM 011820 METAR 11200 011820Z AUTO 06004KT 9999 NCD 22/13=
SAOS61 LOWM 011830 METAR 11200 011830Z AUTO 06004KT 9999 NCD 23/13=
SAOS61 LOWM 011840 METAR 11200 011840Z AUTO 02002KT 9999 NCD 21/13=

Table 7 AUTOMETAR data station Sillian

VAMES AUTOMETAR message history for station 11201 Sillian between 17:40 – 18:40
SAOS61 LOWM 011740 METAR 11201 011740Z AUTO 08002KT 9999 NCD 27/14=
SAOS61 LOWM 011750 METAR 11201 011750Z AUTO 24001KT 9999 NCD 26/15=
SAOS61 LOWM 011800 METAR 11201 011800Z AUTO 24002KT 9999 NCD 25/15=
SAOS61 LOWM 011810 METAR 11201 011810Z AUTO 26002KT 9999 NCD 24/15=
SAOS61 LOWM 011820 METAR 11201 011820Z AUTO 24002KT 9999 NCD 23/15=
SAOS61 LOWM 011830 METAR 11201 011830Z AUTO 21001KT 9999 NCD 23/15=
SAOS61 LOWM 011840 METAR 11201 011840Z AUTO 22001KT 9999 NCD 23/15=

Table 8 TAWES data station Sonnblick

TAWES station Sonnblick 11343 (station height 10200 ft, 3109 m) at 18:00
11343 45/// /2210 10110 20079 37082 47212 55006 333 10122 20087 55310 90760 91117==
Wind (/ *2210*): Direction 220°, 10 m/s or 19 kt
Temperature (*10110*): + 11.0°C
Air pressure at station height (*37082*): 708.2 hPa

Table 9 TAWES data station Rudolfshütte

TAWES station Rudolfshütte 11138 (station height 7579 ft, 2310 m) at 18:00
SMOS42 LOWM 011800 CCA 11138 41/81 31711 10182 20080 37784 47221 58001 70600 83070 333 10201 20135 55303 83450 90760 91120==
Horizontal visibility (*41/81*): 35 km
Wind (*31711*): Direction 170 °, 11 m/s or 21 kt
Temperature (*10182*): + 18.2°C
Air pressure at station height (*37784*): 778.4 hPa

Table 10 ACG data station Rudolfshütte

Data from station Rudolfshütte provided by ACG
17:50: 170/20 kt
18:00: 180/24 kt Gusts 34 kt
18:10: 180/25 kt
18:20: 180/24 kt

Table 11 METAR data LOWS

METAR weather observations LOWS
METAR LOWS 011750Z VRB02KT CAVOK 32/17 Q1013 NOSIG=
METAR LOWS 011820Z 30005KT CAVOK 28/20 Q1013 NOSIG=

Table 12 TAF data LOWS

TAF weather forecast LOWS
FTOS53 LOWS 012300 TAF LOWS 012315Z 0200/0224 15006KT 9999 FEW050 BKN120 TX28/0215Z TN20/0203Z TEMPO 0200/0206 28010KT -SHRA SCT045TCU BKN080 PROB30 TEMPO 0200/0205 29015G25KT TSRA SCT040CB BKN050 BECMG 0207/0209 35006KT SCT060 TEMPO 0213/0218 34015G25KT 6000 TSRA SCT040CB BKN080 BECMG 0218/0220 15007KT=
FTOS53 LOWS 011700 AMD TAF LOWS 011715Z 0118/0218 03006KT CAVOK TX31/0118Z TN20/0205Z TEMPO 0119/0121 29015G25KT PROB40 TEMPO 0121/0204 30020G35KT 4000 TSRA SCT035CB BKN050 TEMPO 0204/0207 15006KT -SHRA BKN050 BECMG 0207/0209 35006KT 9999 SCT060 TEMPO 0214/0218 34015KT 6000 TSRA SCT045CB BKN070=
FTOS53 LOWS 011700 AMD TAF AMD LOWS 012025Z 0120/0218 03006KT 9999 FEW070 BKN140 TX28/0215Z TN20/0205Z TEMPO 0120/0124 30020G40KT 2500 TSRA SCT035CB BKN050 TEMPO 0200/0207 15006KT -SHRA BKN050 BECMG 0207/0209 35006KT 9999 SCT060 TEMPO 0214/0218 34015KT 6000 TSRA SCT045CB BKN070=
FTOS53 LOWS 011100 TAF LOWS 011115Z 0112/0212 03006KT CAVOK TX33/0115Z TN20/0205Z TEMPO 0112/0117 04010KT 9999 FEW080 BECMG 0117/0119 15007KT TEMPO 0121/0201 29015G25KT 9999 FEW070 SCT150 PROB30 TEMPO 0203/0212 SHRA SCT040CB BKN060 BECMG 0207/0209 02005KT=
FTOS53 LOWS 010500 TAF LOWS 010515Z 0106/0206 15007KT CAVOK TX34/0112Z TN21/0106Z BECMG 0108/0110 03006KT TEMPO 0111/0117 04010KT 9999 FEW080 BECMG 0117/0119 15007KT TEMPO 0121/0203 29015G25KT 9999 FEW070 SCT150 PROB30 TEMPO 0203/0206 31020G35KT 4000 TSRA SCT040CB BKN060=

Table 13 METAR data LOWK

METAR weather observations LOWK
METAR LOWK 011750Z AUTO 20003KT 160V230 9999 NCD 31/16 Q1017 NOSIG=
METAR LOWK 011820Z AUTO 20004KT 160V240 9999 NCD 30/16 Q1017 NOSIG=

Table 14 TAF data LOWK

TAF weather forecast LOWK
FTOS56 LOWK 012300 TAF LOWK 012315Z 0200/0224 VRB02KT CAVOK TX32/0212Z TN20/0204Z TEMPO 0213/0218 20007KT 9999 FEW070 FEW070CB PROB30 TEMPO 0215/0218 36020G35KT 5000 TSRA SCT030CB BKN040=
FTOS56 LOWK 011700 TAF LOWK 011715Z 0118/0218 VRB02KT CAVOK TX32/0212Z TN20/0204Z TEMPO 0213/0218 20007KT 9999 FEW070 FEW070CB PROB30 TEMPO 0215/0218 36020G35KT 5000 TSRA SCT030CB BKN040=
FTOS56 LOWK 011100 TAF LOWK 011115Z 0112/0212 VRB02KT CAVOK TX33/0114Z TN20/0204Z TEMPO 0112/0117 20008KT 9999 FEW070=
FTOS56 LOWK 010500 TAF COR LOWK 010515Z 0106/0206 VRB02KT CAVOK TX33/0115Z TN18/0106Z BECMG 0107/0109 09006KT 9999 FEW080 TEMPO 0112/0116 20008KT BECMG 0117/0119 VRB02KT CAVOK=
FTOS56 LOWK 010500 TAF LOWK 010515Z 0106/0206 VRB92KT CAVOK TX33/0115Z TN18/0106Z BECMG 0107/0109 09006KT 9999 FEW080 TEMPO 0112/0116 20008KT BECMG 0117/0119 VRB02KT CAVOK=

Table 15 METAR data LOWI

METAR weather observations LOWI
METAR LOWI 011750Z 10011G24KT 050V180 9999 FEW080 SCT150 BKN300 32/13 Q1015 NOSIG=
METAR LOWI 011820Z 13009G20KT 070V200 9999 FEW080 SCT130 BKN300 32/13 Q1015 NOSIG=

Table 16 TAF data LOWI

TAF weather forecast LOWI
FTOS54 LOWI 012300 TAF LOWI 012315Z 0200/0224 27005KT 9999 FEW080 SCT120 BKN300 TX32/0213Z TN17/0203Z TEMPO 0200/0208 -SHRA FEW070TCU BKN080 BECMG 0207/0209 10007KT SCT080 TEMPO 0213/0220 VRB12G25KT TSRA SCT070CB BKN080=
FTOS54 LOWI 011700 AMD TAF LOWI 011715Z 0118/0218 VRB12KT 9999 FEW080 TX33/0118Z TN16/0203Z PROB30 TEMPO 0119/0122 27015G25KT TS SCT080CB BECMG 0122/0124 27007KT TEMPO 0209/0214 -SHRA FEW070TCU SCT090 TEMPO 0214/0218 VRB12G25KT TSRA SCT070CB BKN080=
FTOS54 LOWI 011700 AMD TAF AMD LOWI 012007Z 0120/0218 VRB12KT 9999 SCT080 SCT300 TX28/0120Z TN16/0203Z TEMPO 0200/0206 -SHRA FEW070TCU BKN080 TEMPO 0214/0218 VRB12G25KT TSRA SCT070CB BKN080=
FTOS54 LOWI 011700 AMD TAF AMD LOWI 011957Z 0119/0218 VRB12KT 9999 FEW080 TX33/0118Z TN16/0203Z PROB30 TEMPO 0119/0122 27015G25KT TS SCT080CB BECMG 0122/0124 27007KT TEMPO 0200/0206 -SHRA FEW070TCU SCT090 TEMPO 0214/0218 VRB12G25KT TSRA SCT070CB BKN080=
FTOS54 LOWI 011100 TAF LOWI 011115Z 0112/0212 09010KT CAVOK TX33/0115Z TN18/0203Z TEMPO 0112/0118 12015G25KT 9999 FEW080 BECMG 0118/0120 27008KT TEMPO 0209/0212 -SHRA FEW070TCU SCT090=
FTOS54 LOWI 010500 TAF LOWI 010515Z 0106/0206 27010KT CAVOK TX35/0115Z TN18/0203Z BECMG 0108/0110 09009KT 9999 FEW080 TEMPO 0110/0118 12015G25KT BECMG 0118/0120 27007KT CAVOK=

Figure 6 GAFOR chart

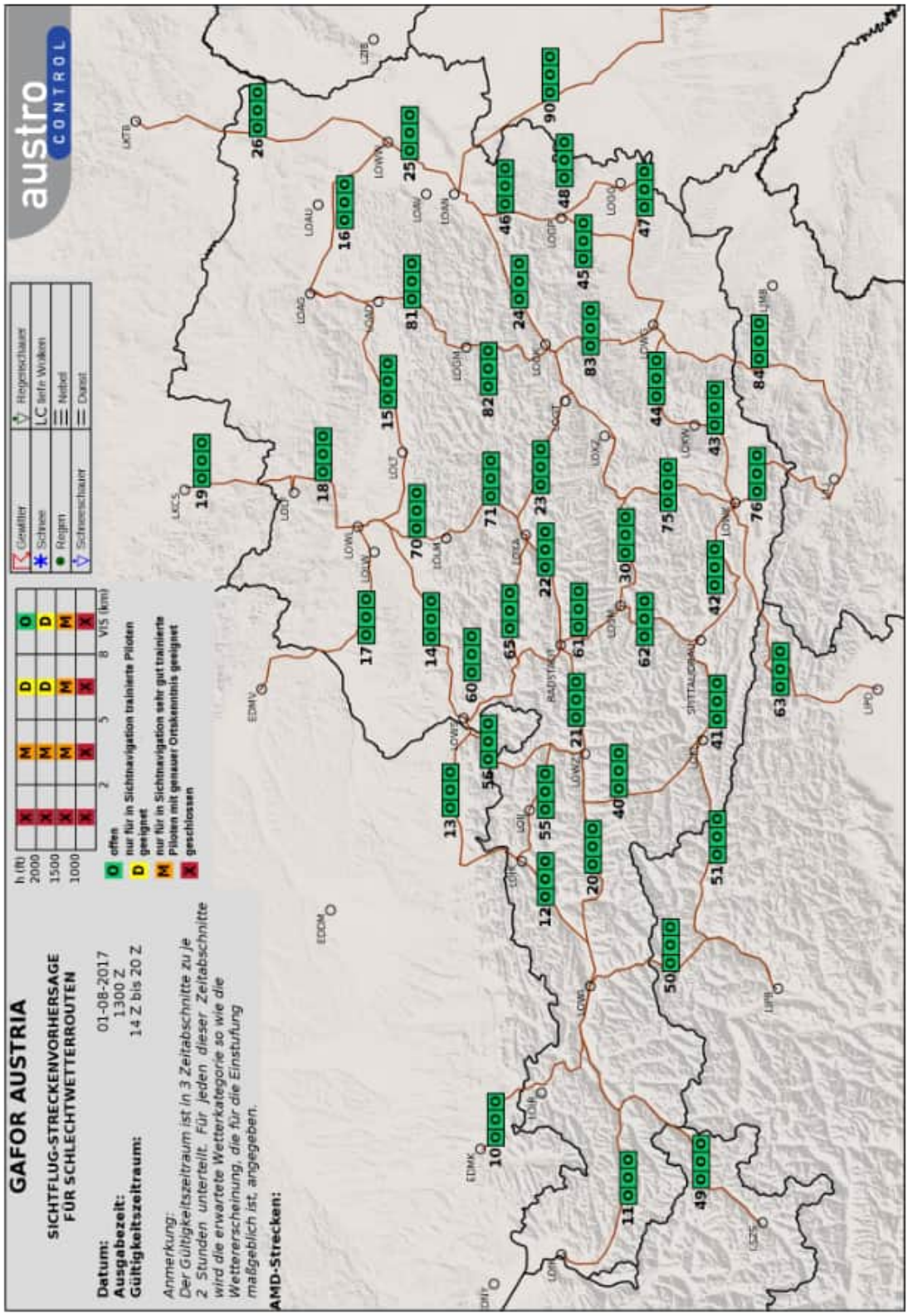

Source: ACG

Figure 7 Wind / temperature chart

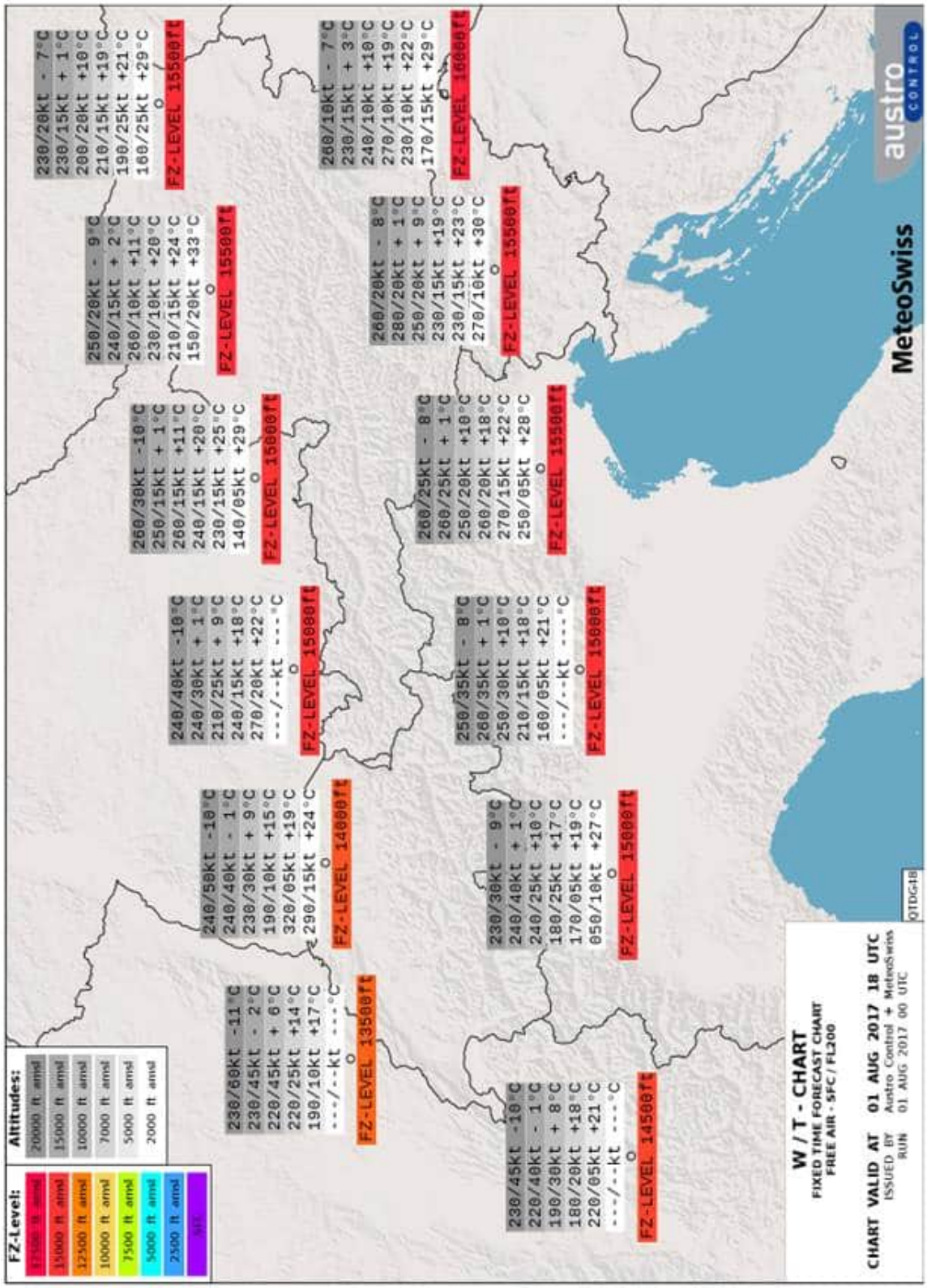

Source: ACG

Figure 8 Low-Level SWC

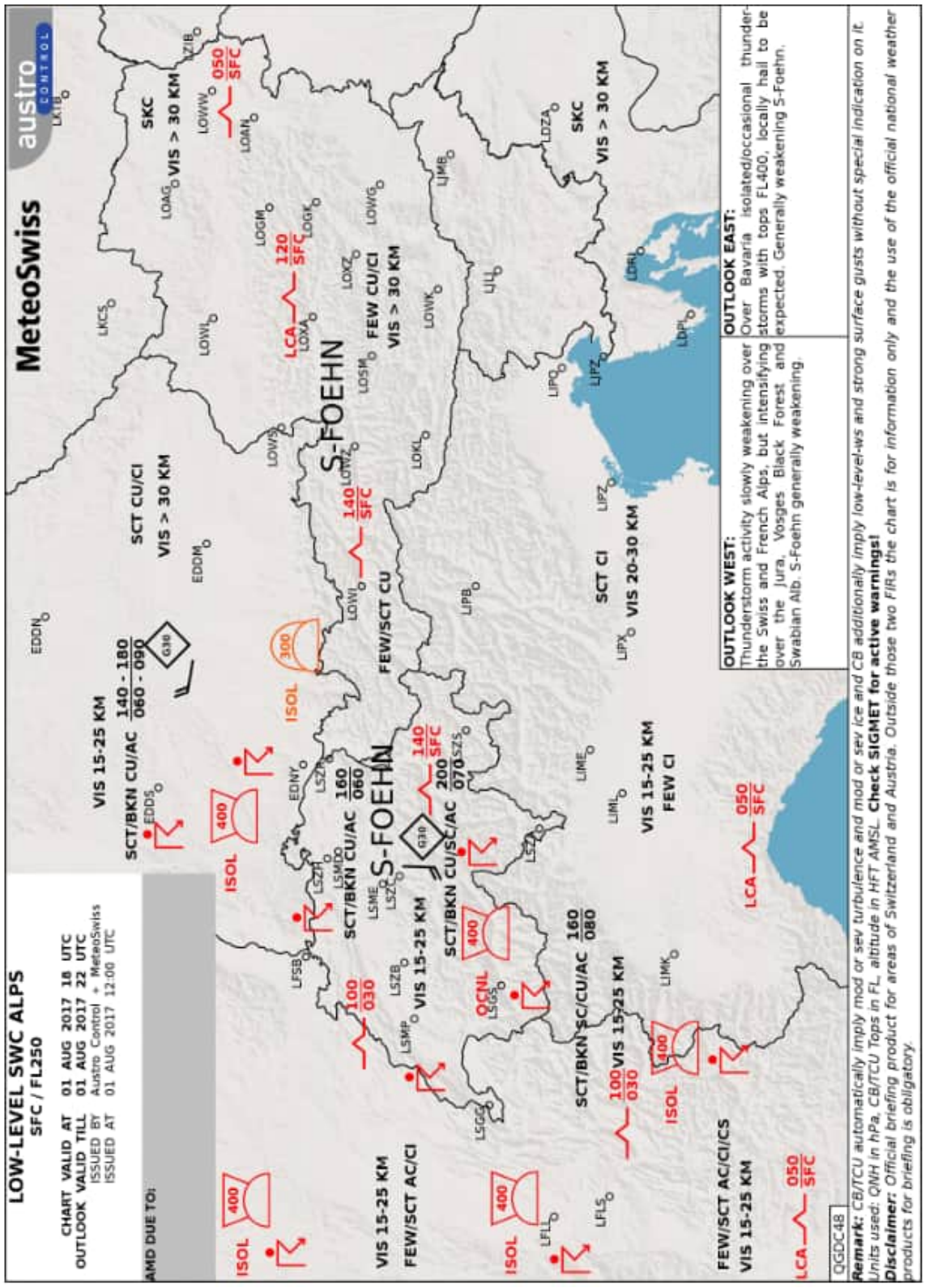

Source: ACG

Figure 9 Wind Barbs

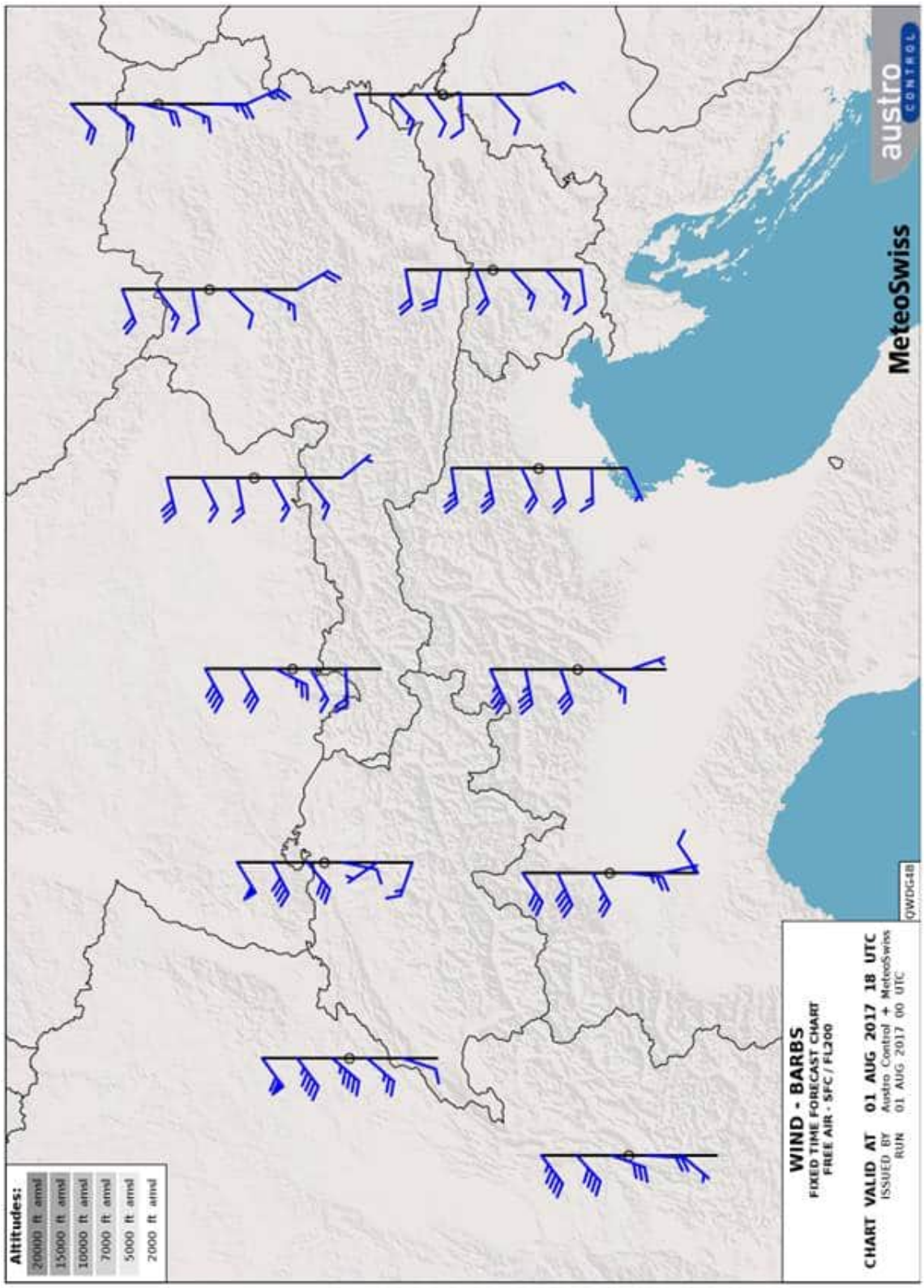

Source: ACG

Figure 10 QNH / Foehn potential chart

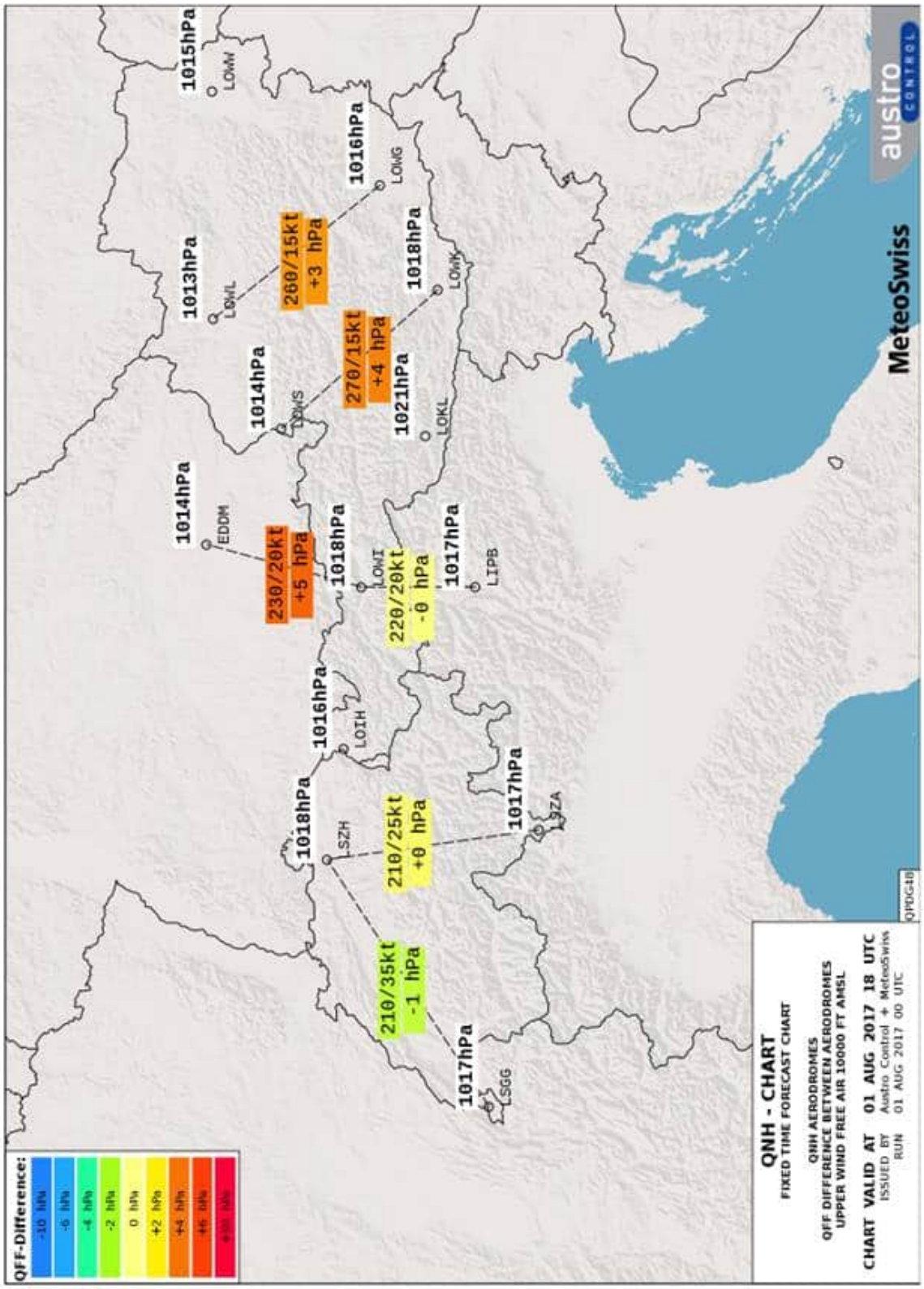

Source: ACG

1.7.2 Weather station Stüdlhütte

A weather station at Stüdlhütte (station height 9193 ft, 2802 m) automatically records weather data every minute and makes it available via the Stüdlhütte website.

Table 17 Stüdlhütte weather data from 1 August 2017 (excerpts)

Time (local)	Temp. outside	Humidity outside	Precipitation	Wind speed	Wind direction	Wind Gusts	Relative air press.
19:50	14.6°C	66.0%	0.0mm	6.0km/h	184°	1.4km/h	1016.4hPa
19:55	14.1°C	69.5%	0.0mm	6.5km/h	185°	11.2km/h	1016.4hPa
20:00	13.8°C	72.0%	0.0mm	7.9km/h	183°	9.7km/h	1016.5hPa
20:05	13.6°C	72.0%	0.0mm	7.9km/h	180°	11.2km/h	1016.4hPa
20:10	13.5°C	72.0%	0.0mm	5.1km/h	182°	13.0km/h	1016.4hPa
20:15	13.4°C	72.0%	0.0mm	6.8km/h	183°	1.4km/h	1016.3hPa
20:20	13.3°C	72.0%	0.0mm	4.7km/h	184°	6.5km/h	1016.2hPa

Source: stuedlhuette.info

1.7.3 Wind calculation from witness video

From an eyewitness video, the wind speed and direction could also be determined due to the dust cloud formed during the impact (Figure 11). The length of the helicopter from the leading edge to the trailing edge is known and was measured as the corresponding pixel length of 147.5 px. This results in a scaling factor of 0.0695 to 0.0714 m/px with a measurement error of ± 2 px. The movement of the dust cloud was measured between certain individual images of the video, here 37.8 px (= 2.66 m) and 30.1 px (= 2.12 m). With a constant frame rate of 30 frames per second and using frame numbers 01711, 01721 and 01731, there is a time interval of 0.33 seconds between the images. From the movement of the dust cloud between the images, a movement speed of 15.5 kt or 12.4 kt (± approx. 1 kt) can be calculated.

It can also be seen that the dust cloud is moving against the approach direction, over the mountain ridge. This observation is identical to the statements made by the pilot and the lodge keeper.

Figure 11 Wind calculation from video

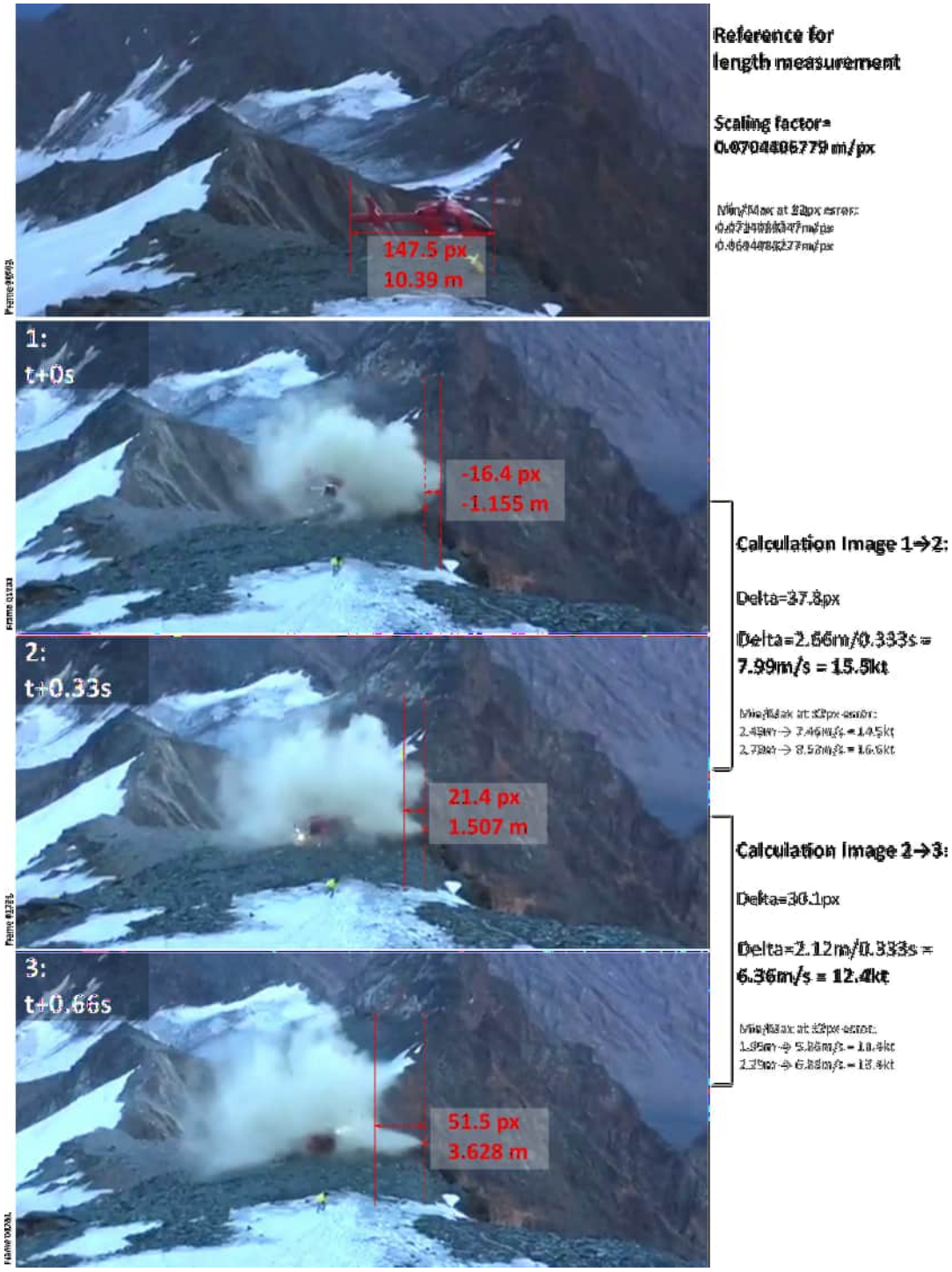

Source: witness video, SIA

1.7.4 Pilot weather briefing

The pilot's weather briefing, which was submitted in writing to the Federal Safety Investigation Authority, included the W/T chart for 18:00 hours, the low-level significant weather charts for 06:00 hours to 14:00 hours, METAR data for the day of the accident for the North and South Alps from 04:56 hours, and the flight weather overviews for the northern and southern Alps region. Further weather information was requested by the pilot before the flight, but was not saved or printed out. The QNH setting on the altimeter was 1020 hPa.

1.7.5 Natural light conditions

At the scene of the accident, twilight began on 1 August 2017 at around 18:39 hours (20:39 hours local time) and civil twilight (ECET) ended at around 19:18 hours (21:18 hours local time). At the time of the accident, natural daylight conditions prevailed at dusk. At the time of the accident, the sun was approx. 3.4° above the horizon at an azimuth of approx. 293° (west-north-west).

According to the AIP Austria, the ECET time on 1 August for LOWI is 19:24 hours and for LOWK 19:10 hours. The pilot indicated an ECET (LOKL / LOWI) of 21:16 hours and a sunset of 20:41 hours (local time in both cases) (see section 1.6.7).

1.8 Aids to navigation

The flight was conducted under visual flight rules (VFR). Apart from a GPS-based moving map system, no navigation aids were used.

1.9 Aerodrome information

The flight started at the Matrei heliport in East Tyrol (LOMM, altitude 3054 ft MSL). The direct distance to the scene of the accident is around 15 km (Figure 1).

1.10 Flight recorders

A flight recorder was not mandatory and not installed.

The prescribed ELT (Emergency Locator Transmitter) was carried and ready for operation. The ELT did not trigger because the required acceleration values were not reached on impact.

The aircraft records data on multiple devices under certain conditions.

1.10.1 DCU (Data Collection Unit)

Engine data is stored in the DCU by the engine's EEC. This happens in a snapshot format whenever an event is triggered. An event is triggered, for example, when the absolute limit of an engine parameter such as torque, engine rpm or exhaust measured gas temperature (MGT) is exceeded. The DCUs were read out by the engine manufacturer at the hangar facility of the Federal Safety Investigation Authority. The data were evaluated by the engine manufacturer and made available to the Federal Safety Investigation Authority. At the time of the accident, the DCU of the left engine recorded data for 10 events for a period of 7.254 s, the DCU of the right engine recorded 8 events for a period of 43.7256 s. Based on the data read out, the engine manufacturer concluded that both engines were providing the required power at the time of impact and that there was no indication of a problem with either engine.

The data in Table 18 and Table 19 were read from the DCUs of the engines and made available by the engine manufacturer. The "Time" column was calculated from the engine run time, with "0" corresponding to the time of the first event associated with the accident for the respective engine. The parameters are:

- NG: Gas generator speed
- NFFLT: Filtered power turbine speed
- QLFLT: Torque of the local engine, i.e. the left DCU records the left engine and the right DCU records the right engine (Filtered local engine torque)
- QRFLT: Torque of the other engine, i.e. the left DCU records the right engine and the right DCU records the left engine (Filtered remote engine torque)
- MGT: Measured gas temperature
- CLP: Collective lever position
- PAMB: Ambient pressure
- T1: Engine inlet temperature

The QRFLT parameter is not recorded when an error occurs. A value of -100 means data loss.

Table 18 Recorded engine data from the right DCU

Time [s]	NG [%]	NFFLT [%]	QLFLT [%]	QRFLT [%]	MGT [°C]	CLP [%]	PAMB [psia]	T1 [°C]	Comments
0	102.5	99.1641	86.3906	86.8906	956.375	97.4414	9.8574	9.0625	Ng peak during flight
1.098	102.4648	96.8984	86.4531	87.9688	963.375	89.3359	9.8623	8.75	MGT peak value during flight
6.1524	94.9414	77.1875	101.2578	103.8438	869.25	19.9375	9.8633	9.4688	torque peak value during flight
7.9128	95.6992	119.2266	28.2656		907.5	106.7813	9.8682	9.5625	NFQA fault
7.9128	95.6992	119.2266	28.2656		907.5	106.7813	9.8682	9.5625	NFQB fault
8.1324	91.5469	125.9766	14.3516	-100	865	106.832	9.8691	9.4375	npt peak value during flight
8.1324	90.3789	126.582	12.3125		849.125	106.832	9.8701	9.2188	LCF fault
43.7256	17.8086	0	-0.0391		379.3125	106.7539	9.874	13.9063	ARI fault

Table 19 Recorded engine data from the left DCU

Time [s]	NG [%]	NFFLT [%]	QLFLT [%]	QRFLT [%]	MGT [°C]	CLP [%]	PAMB [psia]	T1 [°C]	Comments
0	102.4688	96.668	89.625	88.5156	964.0625	93.457	9.8955	8.7813	MGT peak value during flight
0	102.4883	96.6992	88.8906	87.2969	965.0625	91.8984	9.8975	8.8125	Ng peak during flight
3.2976	101.8398	95.582	89.6641	91.1641	957.125	98.3008	9.9082	8.25	auto mode to manual mode
3.2976	101.6523	94.1445	92.6719	95.2031	959.625	87.457	9.9082	8.9375	manual to auto mode transition
5.274	96.5547	77.7813	105.184	95.3203	880.3125	19.7344	9.9033	8.875	torque peak value during flight
6.1524	94.4336	60.7734	61.6094	80.625	856	43.7305	9.9004	8.375	auto mode to manual mode
7.0344	95.9648	118.8633	39.1484		867.625	106.6016	9.9082	9	NFQB fault
7.0344	95.8594	122.3203	39.5156		863.3125	106.6719	9.9082	8.2188	NFQA fault
7.254	95.3008	126.2383	33.8438	-100	862.1875	106.6719	9.9092	9.0313	npt peak value during flight
7.254	94.5039	126.9531	30.6328		851.875	106.6719	9.9102	8.4375	LCF fault

1.10.2 IIDS (Integrated Instrumentation Display System)

The primary function of the IIDS is to display all engine parameters relevant to the pilot on the instrument panel, e.g. engine rpm, torques, exhaust measured gas temperatures (MGT). The amount of fuel available, the generator load and various information and warning messages are also displayed.

Various aircraft data can also be shown on the integrated two-line, alphanumeric display. The menu can be used to switch to a display in which the pressure altitude is displayed in the first line and the density altitude in the second line, as a numerical value, i.e. without graphical representation such as a pointer. The various options for displaying data are described in Chapter 7 (System Description) of the RFM. It should be noted, however, that the alphanumeric display is also used to display warnings, advisories and cautions, which may be displayed with priority and can (temporary) prevent the display of the pressure and density altitude.

The IIDS also offers access to the ASCM (Aircraft Systems Condition Monitoring). Various data are accumulated or stored in the permanent memory of the IIDS, in order to offer the possibility of records for aircraft maintenance, and also for performing engine trend analyses. In addition to the ASCM, the IIDS also offers access to the BMS (Balance Monitoring System) for vibrational analysis of the main rotor system and the NOTAR system. The IIDS was not designed as a flight recorder for accidents and the manufacturer cannot guarantee that data can be saved and successfully read in such cases.

The IIDS offers access to the following records within the ASCM:

- **Exceedance log**: As soon as certain engine parameters exceed limit values, an entry is made in the exceedance log. Thereby, a snapshot of the relevant parameters is stored.
- **Data log**: If an exceedance occurs, or if the "REC" button on the IIDS is pressed, all relevant parameters are recorded at 1 Hz or 4 Hz for 1.5 minutes. A maximum of 5 such data logs can be saved; older data logs are overwritten by new entries.
- **Fault log**: Should errors occur in the EECs, in the BMS, on sensors of the aircraft or in the IIDS itself, up to 100 such faults can be stored in the IIDS in the form of bit codes.
- **Trend log**: A trend log is generated when a power assurance check is performed. This must be triggered by the pilot. These logs are used for aircraft trend analysis, engine performance analysis and the analysis of the vibration spectrum.
- **Cumulative log**: This log contains data on the aircraft configuration, as well as operational data such as accumulated flight hours and engine cycles.

The IIDS was installed and data was read out on an intact aircraft of the same type by an employee of the operator, under the instructions of the manufacturer and under the supervision of a SIA investigator. The exceedance, data, fault, trend and cumulative logs were successfully downloaded with no error messages. 5 exceedance logs were recorded by the IIDS. One of these exceedances can be assigned to an event on 12 June 2017. The other 4 exceedances were recorded when several parameter limits were exceeded during the impact on the day of the accident. 1 data log was recorded, which can be assigned to the event on 12 June 2017. No further data logs were recorded from the time of the accident.

There may be different causes for this. As described above, the logging of data in the event of an accident is not a function of the IIDS, and is therefore not guaranteed. Another readout attempt by the manufacturer, under the supervision of the NTSB, was also unable to provide any further data.

4 data records can be assigned to the accident from the fault log. There was one trend log from 18 May 2017 and one from 2 June 2017. The cumulative log was last updated on 1 August 2017 at 20:17:28 hours. The last recorded flight time was 0.19 hours (corresponds to 11.4 minutes). 2526 flights with a total flight time of 3047.89 hours were also recorded. For the left engine, 1555.55 total hours of operation were recorded, for the right one 1767.76 total hours of operation were recorded. The number of recorded flights and the total hours do not necessarily have to correspond to the values mentioned in section 1.6.

1.11 Wreckage and impact information

1.11.1 Site of the accident

The site of the accident is at approx. 3420 m (11220 ft) above MSL, approx. 500 m south-east of the summit of Mount Grossglockner, near the Erzherzog-Johann lodge at the WGS84 coordinates 47° 4' 10.46" North and 012° 42' 9.74" East (Figure 12 and Figure 13). The slope gradient at the accident site is about 13°.

In the vicinity of the Erzherzog-Johann lodge there is no paved landing site for helicopters, which is why, in the event of a medical emergency, as in the present case, patients and passengers have to be picked up and dropped off in a hover flight (with the skids barely touching the ground) or by rope. The accident site is characterized by rocky, loose and stony ground. The terrain is continuously steep and uneven. At approximately 6 m south-south-east of the accident site there is a steeply sloping rock face, approximately 200 m high.

Figure 12 Site of the accident, map

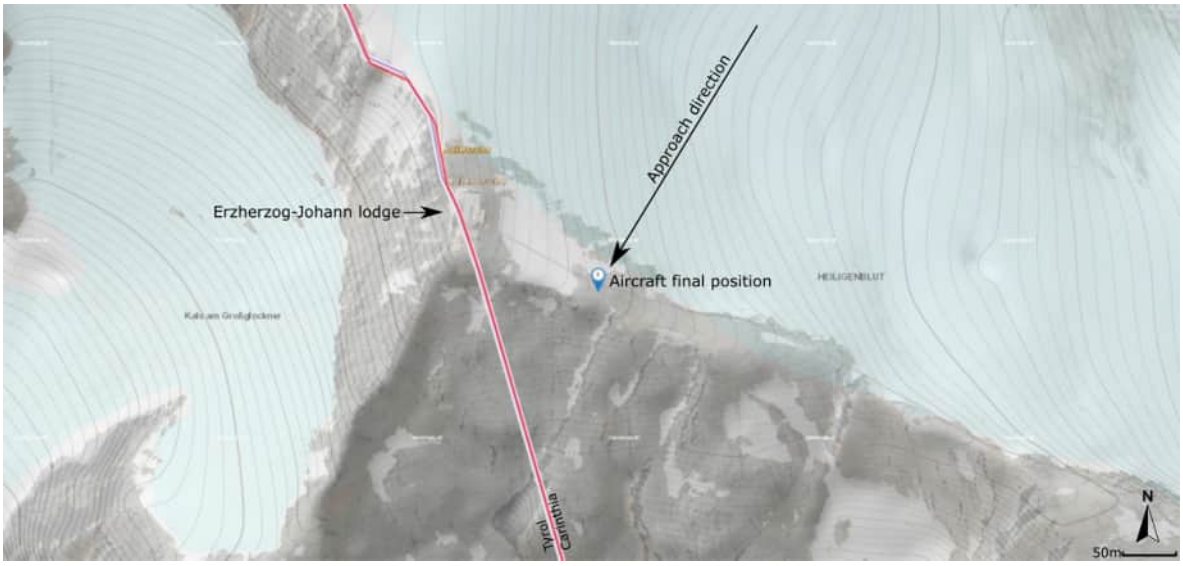

Source: geoland.at, SIA

Figure 13 Site of the accident and Erzherzog-Johann lodge

Source: SIA

1.11.2 Distribution and condition of the wreckage

Figure 14 Final position of the wreck (operator logo redacted)

Source: SIA

Apart from parts of the Main Rotor Blades and smaller parts of the Cockpit Window and the Fuselage Fairing, no parts came off the aircraft. The remains of the Rotor Blades had already been collected and placed next to the wreck, when the team from the Federal Safety Investigation Authority arrived. The Tail Boom showed a crack of approximately 0.5 m behind the Fuselage Attach Frame, which encompassed the entire circumference of the Tail Boom. The structure of the aircraft remained largely intact. The medical equipment and cabin equipment were partly scattered around the cabin and partly still in the designated place in the cabin.

1.11.3 Aircraft and equipment – failure, malfunctions

At the site of the accident, a plastic plate of about 20 x 20 cm in size was found in the Tail Boom, directly in front of the Stationary Cone, which could have influenced the air flow or could have become wedged. This plate was identified as the Upper Inlet Ramp, and was the subject of further investigation (see Section 1.15.2 Inlet Ramps). The wreck was fully examined in the presence of a representative of the manufacturer, in the hangar facility of the Federal Safety Investigation Authority (see Section 1.15 Tests and research).

1.12 Medical and pathological information

There are no indications of any pre-existing mental or physical impairment of the pilot.

1.13 Fire

A few minutes after the accident, smoke and a slight fire was noticed at the right engine exhaust. The pilot put out the fire using the on-board handheld fire extinguisher. The fire could be extinguished immediately. When the Federal Safety Investigation Authority arrived at the site of the accident, no traces of this fire could be found.

1.14 Survival aspects

The crew members or the patient were at the positions in the helicopter indicated in Figure 15.

Figure 15 Occupants' positions at the time of the accident

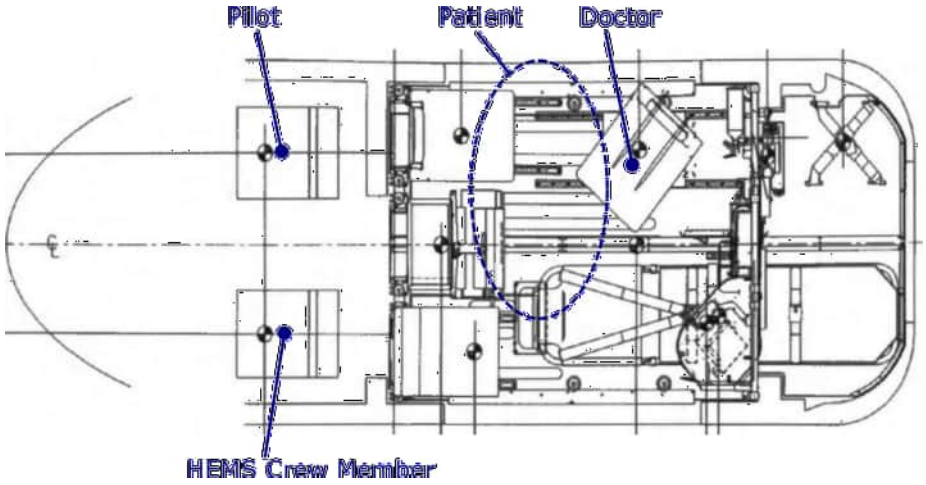

Source MD900 Flight Manual Supplement, SIA

The pilot was in the front right of the cockpit in the pilot's seat, the HEMS crew member at the front left. The doctor was sitting in his swivel chair. The patient was just about to get on the rescue stretcher and was somewhere between the sliding door and the stretcher.

1.14.1 Restraint systems

Belts, inertia reels, the attachment points of the belts and seats of the pilot and the doctor as well as the belts of the HEMS crew member withstood the forces of the impact without damage, and protected the occupants. Both side tubes of the HEMS crew member's seat were found broken.

1.14.2 Evacuation

After the pilot had switched off the engines and inquired about the condition of the other people on board, he was able to leave the cockpit on his own. Then he and other people who had rushed over helped the doctor and the patient to get out of the helicopter. The patient was taken to the Erzherzog-Johann lodge, where he received further care from the doctor. The HEMS crew member was able to open his belt after several attempts and leave the wreckage on his own with little help from the other rescuers.

1.15 Tests and research

1.15.1 Technical investigation

The wreck was examined in detail in the hanger facility of the Federal Safety Investigation Authority, in the presence of a representative of the manufacturer. The helicopter was equipped with a cargo hook and with an inlet particle separator (IPS) per engine.

1.15.1.1 Airframe

The left side of the fuselage was unremarkable in terms of damage, apart from minor damage to the Chin Bow Assembly (fuselage nose at the bottom left) and the Rear Door. The left Cockpit Window and the window on the left cockpit and Cabin Door were not broken. The right side of the fuselage showed damage to the right Chin Bow Assembly, the frame of the Pilot Door, the Pilot Door and Cabin Door itself, and various parts of the airframe fairing (especially on the upper deck) and the engine. The right Cockpit Window,

the windows of the right Cockpit and Cabin Door, as well as the right and left Chin Window were broken and parts of it were completely destroyed.

The tail section was separated from the fuselage for removal from the site of the accident, and showed a circumferential crack of about 0.5 m behind the Fuselage Attach Frame. The Tailboom Bumper was still mounted on the rear and showed scratches and contact marks. On the left side of the Vertical Stabilizer, there was no damage apart from slight scratches. The Upper and Lower Endplates on the right side of the Tail Empennage were badly damaged.

The Skid Tubes on the landing gear were removed from the Crosstubes for transport. The left Skid Tube broke off completely about 20 cm aft of the front Crosstube. The right Skid Tube was completely broken about 0.5 m in front of the forward Crosstube. The landing gear was equipped with Bear Paws, with the right Bear Paw rotated about 60° clockwise.

1.15.1.2 Cockpit and Instruments

The cockpit instruments showed no signs of damage. The IIDS was removed and read out by the team from the Federal Safety Investigation Authority (see section 1.10.2). The engine control switch for the left engine was found between the positions IDLE and FLY, the switch for the right engine in the position FLY. The BOOST PUMPS were each found in the ON position. The right engine FUEL SHUTOFF switch safety cap was open and the switch was in the RIGHT OFF position. The left engine FUEL SHUTOFF switch safety cap was closed. The BOTTLE DISCHARGE switch was in the OFF position. The indicators for the position of the left and right Vertical Stabilizers were both approximately in the middle. The following switch positions were also found at the accident site: NACA INLET: NORMAL, IPS: OFF, L and R VSCS: both ON, AVIONICS: ON, L and R GEN: both ON, POWER: OFF, CAB HEAT: OFF.

A Garmin G500H and a GNC255 COM/NAV were installed in the helicopter. The set QNH pressure was 1020 hPa. The set active COM frequency was 120.100 MHz, the standby COM frequency was 123.100 MHz. The set active NAV frequency was 112.00 MHz, the standby NAV frequency was 109.70 MHz. The HVR LGT circuit breaker was in the open position, the AHRS 1 AUX circuit breaker was in the open position and secured with a cable tie.

1.15.1.3 Engine, Main Rotor and Drive Train

The helicopter was powered by two Pratt & Whitney P&W 207E engines. The engine mount was not damaged, the engines themselves and all the connecting lines were properly connected to the helicopter. The power turbines of both engines could be rotated freely without any problems. As far as can be seen from the outside, no turbine blades were damaged.

The DCUs (data collection units) on both engines were read out by the engine manufacturer in the hangar facility of the Federal Safety Investigation Authority (see section 1.10.1) and were analyzed by the engine manufacturer. No indications of engine problems were found.

The main rotor head was badly damaged. All five rotor blades and the associated Flexbeams broke directly at the rotor head attachment; they were each broken into several parts and showed different degrees of destruction. The swashplate linkage (control rods, scissors, etc.) was for the most part completely destroyed.

The Transmission assembly showed no obvious signs of damage and all connecting elements to the fuselage cell were intact. The gear oil level was within the limits. The drive train was mechanically connected throughout from the engines to the main rotor head. The NOTAR fan was also mechanically connected throughout to the main gearbox. The flexible couplings on the driveshaft showed no damage.

1.15.1.4 Flight Controls

The helicopter was configured for control from the right pilot seat, the cyclic control stick on the left side was removed. The pedals on the left were not connected, so that no control could be made from the left seat. The control for the cyclic and collective pitch was mechanically connected throughout up to the broken control rods on the swashplate. No damage or leaks were found on the associated hydraulic actuators. Sufficient hydraulic fluid was visible in the sight glasses of the hydraulic system.

1.15.1.5 NOTAR Fan

The linkage of the NOTAR Fan Pitch Change Mechanism was damage-free and smooth-running, safety wire was properly in place. Splinters of 3-10 mm in length were found sticking in the front edge of several Fan Blades. Similar material was found in the Fan Inlet Duct. It is highly probable that this material is a carbon fiber material such as is used in

fairing parts or the Main Rotor Blades. Traces of erosion were found on the Stator Blades and rotor Fan Blades. The plastic Sleeves in the Fan Hub were heavily worn, with some segments of the plastic missing. Signs of wear could also be detected in the associated bores in the Fan Hub. The Torque Tension Straps (TT Straps) and Pitch Plate showed neither damage nor wear. Neither cracks nor detached material was found on the Fan Liner Felt Metal Seal. The distance between the fan blades and the Felt Seal was between 1.0 and 1.4 mm (permitted range: 0.76 - 1.65 mm).

The rigging of the Fan was checked by the Federal Safety Investigation Authority together with the representative of the manufacturer. The decision to also check the rigging was only made after the technical inspection of the Fan Hub, so it had to be reinstalled first. The measured values should therefore be interpreted with reservations. In addition, no appropriate external hydraulic unit was available, which is why the inspection of the rigging was carried out without hydraulics, in deviation from the instructions in the maintenance manual. When the left pedal was fully depressed, an angle of approx. 85° was measured on the Fan Blades (permitted range: 86° - 87°), with the right pedal fully depressed, an angle of approx. 76° was measured (permitted range: 79° - 81°). With the pin set in the rig position, an angle of approx. 33° was measured (permitted range: 33° - 35°).

When the owner picked up the wreck, the rigging was checked again with an active hydraulic system. When the left pedal was fully actuated, an angle of approx. 86° was measured (permitted range: 86° - 87°) and approx. 80°with the right pedal fully depressed (permitted range: 79° - 81°).

1.15.1.6 Circulation Control Tail Boom

All the Vortex Generators along the Tail Boom were present and undamaged or partially bent by up to approx. 10°. Both (Circulation Control) Slots along the Tail Boom were undamaged, apart from the point where the Tail Boom had broken. The Slots were free of foreign objects and the slot width was constant throughout. The Diverter Plate, the Tailboom Upper and Lower Airfoils and the Slot Vanes showed no abnormalities. The Upper Inlet Ramp had detached from the Tail Boom and was found in the rear end of the Tail Boom, directly in front of the Cascade Vanes. The Lower Inlet Ramp was missing and could not be found. The Upper Inlet Ramp underwent further investigation by the Bundeswehr

Research Institute for Materials, Fuels and Lubricants (“Wehrwissenschaftliches Institut für Werk- und Betriebsstoffe” - WIWeB) of the German Armed Forces (section 1.15.2).

1.15.1.7 Direct Jet Thruster

The Directional Control Push Pull Cable Bracket in the rear part of the Tail Boom was badly deformed, so that it was no longer possible to check the rigging of the Direct Jet Thruster with regard to the pedal deflections. The Directional Control Push Pull Cable was cut off to salvage the helicopter from the accident site. Contact traces were found on the Thruster Control Rod, in the area of the passage through the Upper Thruster Duct and Upper Thruster Bulkhead. The Rotating Cone was freely rotatable, but showed some scratches and scuff marks on the rear end from the 1 o’clock to the 6 o’clock position. The Stationary Cone showed no abnormalities, the 10 Cascade Vanes per side were without visible damage and free from foreign objects. The Forward and Aft Thruster Control Cable and the Control Cable Drum and Control Cable Sector were intact and could be moved easily. The Direct Jet Thruster was controllable from the Directional Control Push Pull Cable up to the Rotating Cone.

1.15.1.8 Vertical Stabilizer

The left Upper and Lower Endplates were undamaged except for scratches. The right Upper and Lower Endplates were badly damaged. The left VSCS Actuator and the associated Actuator Control Rod were undamaged, the right VSCS Actuator was undamaged, the associated Control Rod was bent by about 10°.

1.15.1.9 Fuel

The fuel capacity of the helicopter is 611 liters (161.3 US gallons), 11 liters of which are not usable. As far as can be seen, the fuel system showed no signs of leaks, clogs, or corrosion.

In the hangar facility of the Federal Safety Investigation Authority, the Jet A-1 fuel in the tank of the helicopter was emptied via the drain and the amount of fuel was measured. There was neither water nor visible contamination in the fuel.

No leakage of fuel was detected at any time, so it can be assumed that the measured fuel corresponds to the quantity that was on board at the time of the accident. The quantity of fuel measured was approximately 440 liters (116.2 US gallons) with an accuracy of approximately ± 1%. With a fuel density of 792.6 kg/m³ at 25°C (corresponding to the temperature at the time of measurement and 800 kg/m³ at 15°C) this corresponds to approx. 349 kg. Of these 440 liters, 429 liters would have been usable, which corresponds to 340 kg.

1.15.2 Inlet Ramps

During the examination as per section 1.15.1.6 it was found that the bonding areas of the Upper Inlet Ramp and the Lower Inlet Ramp in the Tail Boom differ significantly (Figure 16). Residues of the adhesive used (according to the information from the manufacturer "HMS16-1147", also available under the designation "3M Scotchweld EC 2216 B/A") can be found at both bonding areas, as well as adhesive beads, which are clearly more pronounced at the bonding area of the Lower Inlet Ramp. However, in contrast to the bonding area of the Lower Inlet Ramp, a greenish base coat can be seen on the bonding area of the Upper Inlet Ramp.

Figure 16 Upper and Lower Inlet Ramp

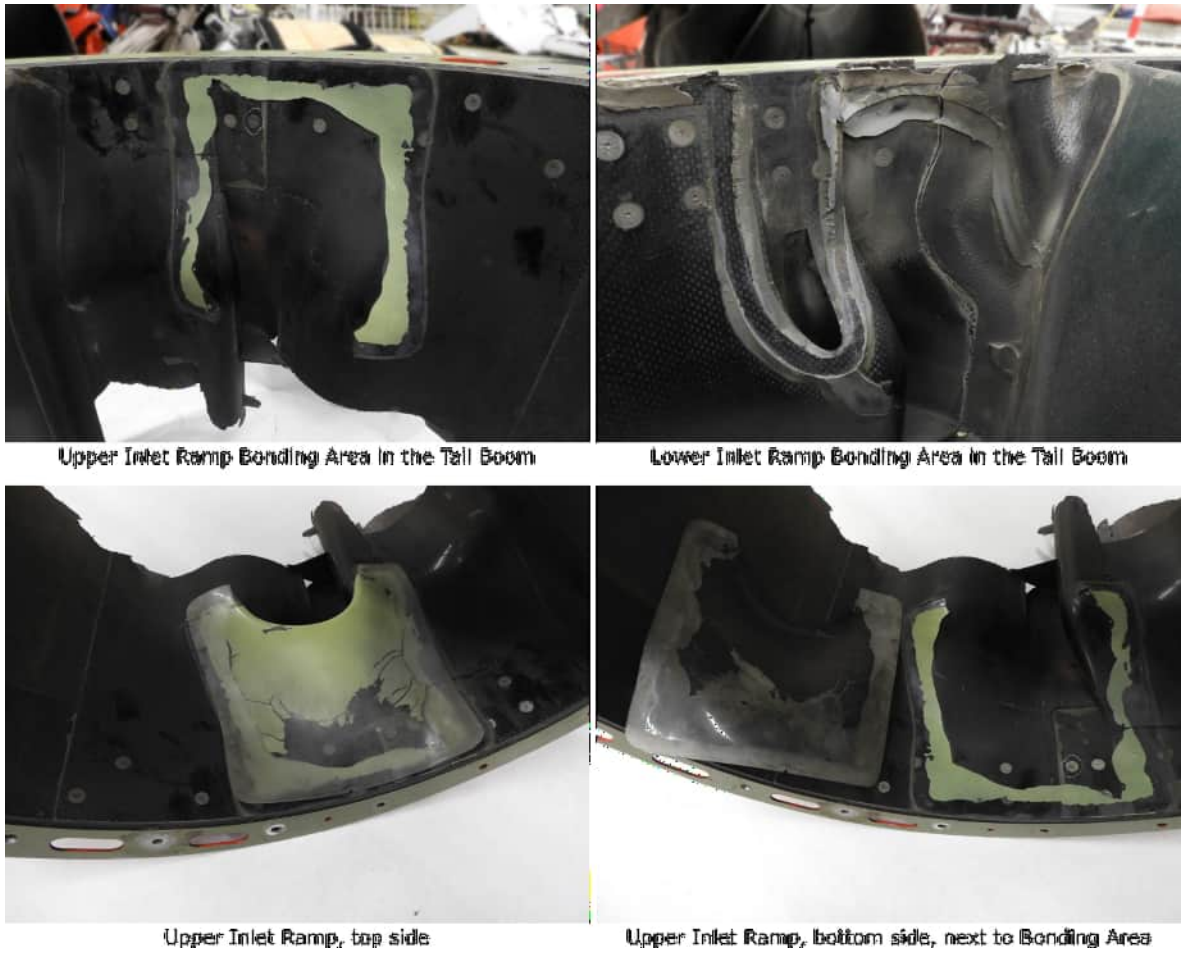

Source: SIA

The material of the Inlet Ramps, according to the manufacturer's information, is polycarbonate. The bonding area were further examined by the Bundeswehr Research Institute for Materials, Fuels and Lubricants.

The Bundeswehr Research Institute came to the following conclusion (Original German Text in Appendix **Fehler! Verweisquelle konnte nicht gefunden werden.**):

> "The test results show that the top of the UIR [Note: *Upper Inlet Ramp*] was sanded. The underside has been painted. This paintwork had been roughly removed around the edge. The sanding and painting of the UIR have no recognizable function. It can therefore be assumed that the top and bottom were confused during production. This was evidently noticeable during the bonding process, as the paint was roughly

removed from the edge of the bonding. However, there was insufficient surface pretreatment, as the bond shows adhesive failure at the interface between the tail boom and the UIR.

This means that the UIR's adhesive layer structure differs significantly from that of the LIR [Note: *Lower Inlet Ramp*], which has no paint residue. The McDonnell Douglas gluing instructions state that the UIR and LIR should not be sanded. This is in contrast to the adhesive data sheet, which provides for the surface to be roughened.

A statement as to whether the failure occurred before or after the aircraft accident cannot be made." (Report from the Bundeswehr Research Institute for Materials, Fuels and Lubricants)

In the course of the investigation, 4 other MD900s of the operator concerned were examined by the Federal Safety Investigation Authority with regard to the bonding of the Inlet Ramps. No helicopter was found to have the paint applied on the wrong side.

1.15.3 Flow simulation

Based on the information in the RFM for the Takeoff and Landing WAT limit of 12400 ft (RFM Figure 2-2, see Section 1.6.3) a more detailed investigation of the flow around the Tail Boom was carried out by flowdynamics e.U. on behalf of the Federal Safety Investigation Authority, using numerical simulation ("Investigation of the ground effect on the aerodynamic characteristics of a helicopter with a NOTAR system", see Appendix 6.3). In particular, the change in the airflow and a possible impact on the NOTAR anti torque performance should be examined based on various stationary flow states. Various simplifications were made to reduce the calculation complexity: Only the Tail Boom with the longitudinal Circulation Control Slots and the fuselage were modeled, the empennage, the Rotating Cone at the end of the Tail Boom and the landing gear were removed from the model. The geometry of the longitudinal slots was measured by the Federal Safety Investigation Authority on the accident wreckage. The exhaust gas flows from the turbines were not taken into account due to the lack of data. The rotor downwash was simulated by a constant pressure jump, which is why the rotor downwash remains constant over the entire rotor diameter. The ground was simulated as a smooth, homogeneous, horizontal wall. The complete list of restrictions, assumptions and boundary conditions is contained in Appendix 6.3. The aim of the calculation is the qualitative comparison of the change in the flow and the resulting air forces when approaching the ground, and not the calculation of

exact numerical results. The simulation was calculated for four different heights above ground (0 m, 3 m, 6 m and 15 m).

The result of the simulation is shown in Figures 17 and 18. The forces in Figure 17 result from the calculated pressure distribution around the entire aircraft. *Fy is* the force acting laterally on the helicopter (in the direction of the aircraft transverse axis), which is responsible for the torque compensation. It is clearly visible that *Fy* increases with increasing distance to ground.

Figure 17 Resulting air forces, simulation

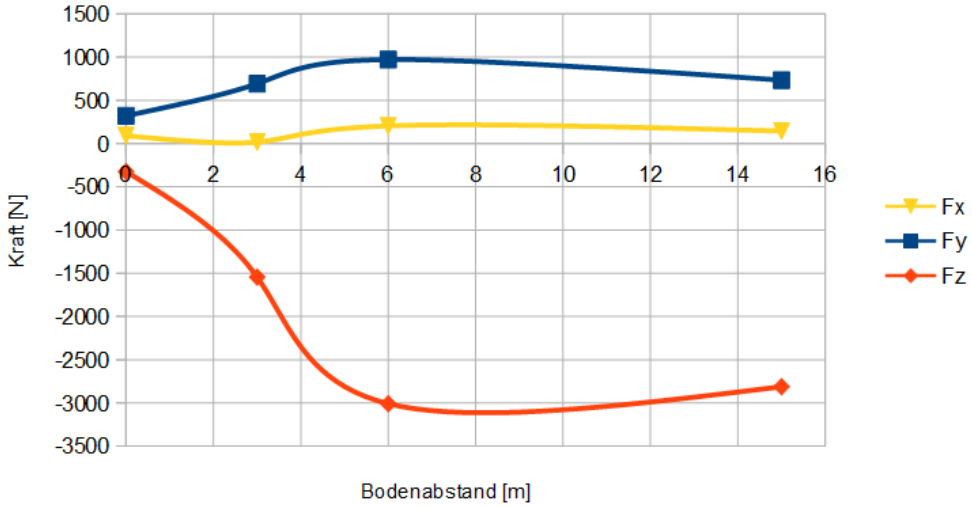

Source: flowdynamics

The same applies to the resulting yaw moment Mz around the vertical axis of the helicopter (Figure 18). An increase in distance to ground from 0 m to 4 m results in a three times larger yaw moment around the vertical axis. With a distance to ground of more than 4 m, the height above ground has practically no more influence on the yaw moment.

Figure 18 Resulting torques, simulation

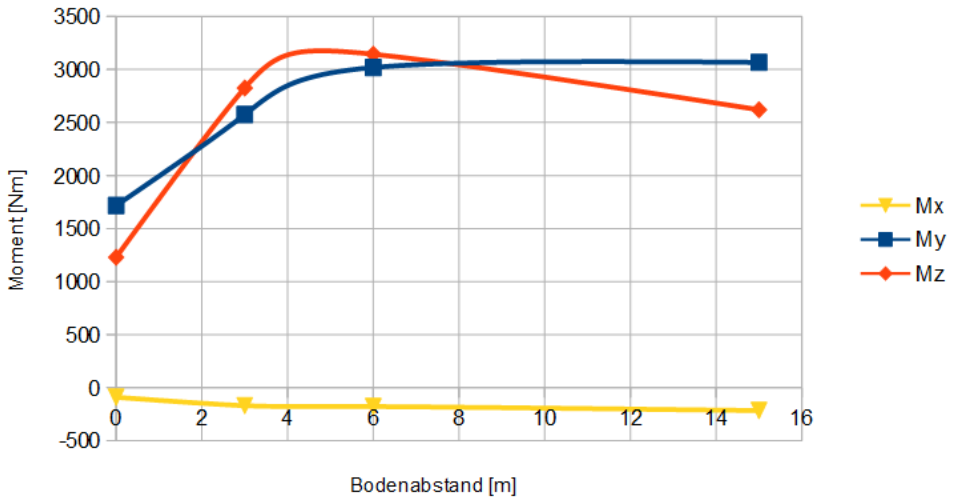

Source: flowdynamics

The figures show that both the force Fy and the yaw moment Mz increase in the course of the takeoff process. From a mathematical-analytical point of view, an aerodynamically generated lift (frictionless) can be described using the Kutta-Joukowski formula:

$$F_A = -\rho \cdot \Gamma \cdot q_\infty$$

Here, F_A is the generated lift force, ρ the air density, Γ the circulation (i.e. the result of the displacement of the stagnation point or the flow separation) and q_∞ inflow velocity. From this formula it can be seen that a reduction in the inflow velocity results in a reduced lift (here the side force generated by the NOTAR system is referred to as lift). With the NOTAR system, the inflow velocity is proportional to the velocity of the downwash. The fact that the downwash velocity or, equivalently, the required thrust and the required power, decrease with decreasing distance to ground (i.e. IGE) was proven by Tanner, Philip E. et al. ("Experimental Investigation of Rotorcraft Outwash in Ground Effect.", 2015). As a result, with constant density and circulation, the force generated by the Circulation Control Tail Boom is lower near the ground (IGE) than far away from the ground (OGE). The above frictionless approach was investigated and experimentally proven by Vernard E. Lockwood ("Effect of Groundboard Height On The Aerodynamic Characteristics Of A Lifting Circular Cylinder Using Tangential Blowing From Surface Slots For Lift Generation", 1961).

The generation of the lateral force and the yaw moment around the vertical axis is carried out by the entire NOTAR system. For a hover flight (i.e. without a horizontal inflow, e.g. from wind), this is done using the Circulation Control Tail Boom and the Rotating Cone. The latter is used primarily for trimming and direction control. The pilot has to compensate the part of the side force that is less generated by the Circulation Control Tail Boom near the ground, by actuating the Rotating Cone and the NOTAR Fan accordingly (pedals). This is only possible up to the point where the Rotating Cone fully opens. The limits of the controllability of the helicopter around the vertical axis are set by the aerodynamics of the Circulation Control Tail Boom in connection with the Direct Jet Thruster and Rotating Cone, whereby the flight altitude above ground (HOGE vs. HIGE) has an influence on the effectiveness of the Circulation Control Tail Boom.

1.16 Organisation, procedures and aircraft operation

The helicopter was used by the company for helicopter emergency medical service (HEMS) operations. The corresponding procedures were defined in the Operations Manual (OM) Part A and Part B. Part A of the operations Manual (OM-A) contains the general section “Helicopter Operating Procedures” (Section 8), “Mountain Flying” (Appendix E) and “Helicopter Emergency Medical Service (HEMS)” (Appendix F). Part B of the Operations Manual (OM-B) contains the type-specific operating instructions, including those for helicopters of the type “MD 900 Explorer (902 Config. w/PW207E)”.

1.16.1 Operations Manual Part B

Regarding the operational limitations, emergency procedures and normal procedures for the Type MD900, the OM-B refers to the flight manual of the MD900 (RFM), without any restrictions or more precise specifications.

Regarding performance, reference is made to the RFM. The conditions under which the helicopter must be operated with performance classes 1, 2 or 3 are also specified. Accordingly, performance class 2 is required for the operation of the helicopter at the present operation site. A power assurance check must also be carried out every 100 flight hours, after maintenance work and after an engine wash.

With regard to the calculation of mass and CG, reference is made to the RFM, whereby the manual calculation according to the RFM, a “load plan method” and the calculation using the M&B application as part of the EFB are available as calculation variants. Mass and CG are to be calculated for each sector.

The flight planning section contains, among other things, information on the types of fuel that can be used, the tank capacities, information on fuel consumption and fuel quantities to be taken into account in the planning.

Although correct reference was made to the RFM with regard to the operating limits and power calculation, the OM-B did not specifically indicate that the MD900 type has an absolute operating limit (density height) with regard to controllability during take-off and landing (RFM Figure 2-2, this report Figure 4). This operating limit is atypical for helicopters that are certified as small rotorcraft according to JAR-27.

1.16.2 HEMS operations

To operate a rescue helicopter (HEMS operations), the requirements of Regulation (EU) No. 965/2012 must be met. Consequently, according to SPA.HEMS.125 (b) (3), performance class 2 shall be met for the HEMS operation of a helicopter in a “hostile environment”. Performance class 2 is defined as:

> “[...] an operation that, in the event of failure of the critical engine, performance is available to enable the helicopter to safely continue the flight, except when the failure occurs early during the take-off manoeuvre or late in the landing manoeuvre, in which cases a forced landing may be required; […]” (Regulation (EU) 965/2012, Annex I, 89)

According to “CAT.POL.H.300 General”, the helicopter must be approved in category A or in an equivalent category for operation in performance class 2. Category A is defined as:

> “17. ‘category A with respect to helicopters’ means a multi-engined helicopter designed with engine and system isolation features specified in the applicable airworthiness codes and capable of operations using take-off and landing data scheduled under a critical engine failure concept that assures adequate designated surface area and adequate performance capability for continued safe flight or safe rejected take-off in the event of engine failure;” (Regulation (EU) 965/2012, Annex I, 17)

The EASA Guidance Material on Regulation (EU) 965/2012 contains more detailed information about what is to be understood by safe flight continuation according to performance class 2 (GM to Section 2, Chapter 3 performance class 2). Accordingly, a minimum climb rate of 150 ft/min up to 1000 ft above the take-off point is required for a take-off in performance class 2 in the event of an engine failure. In the RFM there are various diagrams in the performance section to determine the rate of climb for different altitudes, temperatures and helicopter masses, but these always relate to the airspeed for best climb (V_Y). It is not possible to give a realistic indication of which rate of climb is possible starting from a hover flight at the present pressure altitude, temperature and helicopter mass. For this reason, the RFM cannot be used to determine whether performance class 2 can actually be complied with at a specific location and altitude for a MD900 helicopter. Just looking at the climb rate at V_Y with the conditions given in the present case (altitude, temperature, etc.) shows that a climb rate of 150 ft/min is not achievable if one engine fails.

2 Analysis

2.1 Meteorological analysis

The accident in question took place in the mountains at an altitude of 3420 m. Localized differences in terms of weather phenomena and data are not uncommon in the mountains at such heights. In addition, there are usually few or no weather stations available at such locations. Nevertheless, data could be saved and evaluated from a sufficient number of surrounding measuring stations at different heights (see section 1.7). The weather stations are located within a radius of 2–40 km from the scene of the accident, the measuring stations at the airports Innsbruck, Salzburg and Klagenfurt are further away. The positions of the measuring stations in the immediate vicinity are shown in Figure 19. The wind directions measured by the respective stations are shown as green arrows.

Figure 19 Weather measuring stations around the site of the accident

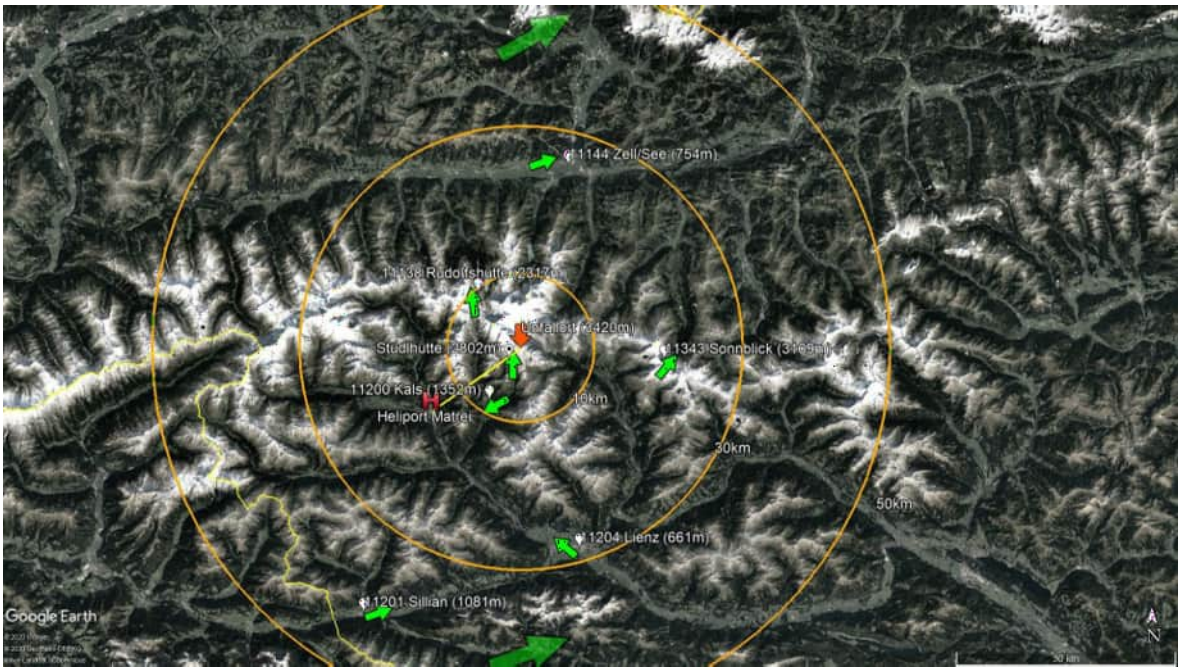

Source SIA, Google Earth

Although the onset of twilight was imminent and the lighting conditions on the witness video also indicate the onset of twilight, the conditions for visual flight in daylight conditions

(VMC) were met. Visibility ranges of more than 10 km were stated from all measuring stations.

With regard to wind directions, it should be noted that especially at the measuring stations in the valleys wind is strongly channeled and thus the measured wind directions and strengths can deviate strongly from the situation prevailing over a larger area (wind barbs, Figure 9). In the present case, this mainly applies to the Lienz and Kals measuring stations. When looking at the data of the higher-lying stations Stüdlhütte (2802 m) and Sonnblick (3109 m), as well as the witness video (section 1.7.3) and the other stations at the site of the accident, a wind direction from the southwest can most likely be assumed. The wind force was determined to be around 12 to 15 kt, mainly based on the video (Stüdlhütte 4.3 kt, Sonnblick 19 kt, Rudolfshütte 21 kt). The approach was therefore correctly carried out exactly against the prevailing wind direction. It should be noted, however, that a degree-accurate determination of the wind direction is not possible both for the pilot in flight as well as in the course of the investigation.

Figure 20 Temperature profile based on measurement data at the accident site at 18:10 hours UTC

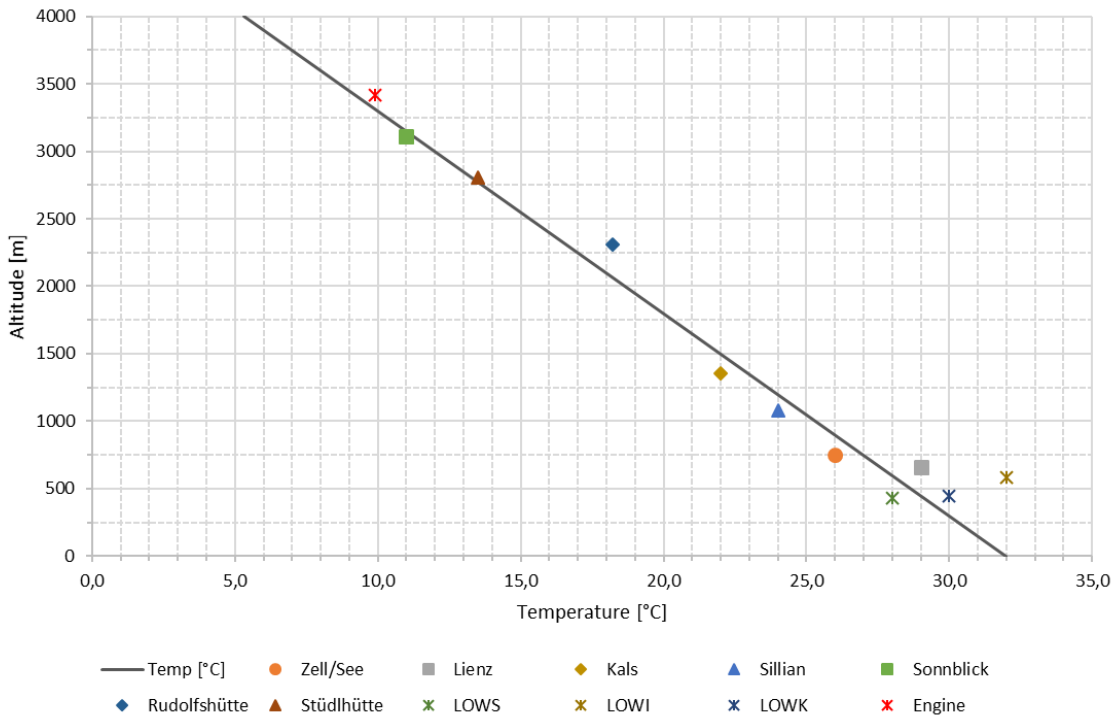

Source: SIA

Due to the availability of a number of weather stations in the vicinity of the accident site, the atmospheric temperature profile and also the temperature at the accident site can be determined with good precision.

The respective temperatures and geographical elevations of the measuring stations and the resulting vertical atmospheric temperature profile for 18:10 hours are shown in Figure 20. In addition, lower-lying stations (especially Lienz, Zell/See, Sillian and Kals), higher-lying stations (Rudolfshütte, Stüdlhütte and Sonnblick) and data from Salzburg (LOWS), Innsbruck (LOWI) and Klagenfurt (LOWK) airports were also included. The air temperature measured at the engine inlet can also be seen, for comparison. From this data, a ground temperature at MSL of 32°C (ISA + 17) and a temperature gradient of -6.67°C/km were calculated. The temperature at the site of the accident at an elevation of 3420 m corresponds to 9.2°C (ISA + 16). This value correlates very well with the measured engine temperature, which is approximately 0.4°C higher. This is realistic because air is slightly warmed up when it is sucked into the engines. The Austro Control wind and temperature chart (Figure 7) shows temperatures of 9 to 11°C at 10000 ft (3048 m) at the surrounding measuring points, whereby these measuring points are located at distances of over 100 km.

The air pressure (QNH), back-calculated to MSL, was specified by the pilot for his performance calculation as 1020 hPa and was also set on the altimeter (see sections 1.6.7 and 1.7.4). At the time of the accident, a value of 1013 hPa was measured at Salzburg Airport, a value of 1015 hPa at Innsbruck Airport and a value of 1017 hPa at Klagenfurt Airport (see Section 1.7). The QNH and Foehn chart (Figure 10) for 18:00 hours forecast 1014 hPa for Salzburg, for Innsbruck 1018 hPa, for Klagenfurt 1018 hPa and for Lienz 1021 hPa. The large-scale weather situation corresponded to a classic southern foehn situation. The QNH value used by the pilot was chosen primarily due to the close proximity of Lienz to the Matrei heliport, where the helicopter was stationed and from where the flight started. A QNH of 1020 corresponds to an air pressure of 685 hPa at the altitude of the accident site. Since the DCUs recorded the values 680 and 683 hPa (9.86 and 9.91 psia, respectively, see section 1.10.1) at the accident site, the site of the accident is closer to Innsbruck and Salzburg in a north-south direction, and the forecast was about 1-3 hPa above the actual values, it must rather be assumed that the QNH was approximately 1017 hPa at the accident site.

The density, pressure altitude and density altitude at the accident site can be calculated from the data for air temperature, temperature profile and ambient air pressure. With an air temperature of 9.2°C, a temperature gradient of -6.67°C/km and an air pressure at MSL

of 1017 hPa, the air pressure at the accident site can be determined with the aid of the barometric altitude formula[1] (683 hPa). This corresponds to a display on the altimeter of 10605 ft (3256 m, QNH setting 1020), a pressure altitude[2] of 10511 ft (3203 m) and a density altitude[3] of 12231 ft (3728 m). The density altitude is relevant in that because it is necessary to be able to assess at which point one is in the WAT and crosswind Limits chart (Figure 4) and whether the Takeoff and Landing WAT Limit has been met or exceeded. The correct relation between the values for pressure altitude and density altitude can also be verified using Fig. 5-1 *Density Altitude Chart* from the MDHI RFM.

2.2 Flight crew

At the time of the accident, the pilot held the necessary licenses, ratings and medicals to perform the flight. At the time of the accident, he had 3541 hours of flight experience, of which 531 hours were completed on the type involved in the accident. He can thus be described as an experienced pilot, both in general, and on the type involved in the accident. With 9.25 hours, there was sufficient rest time before the accident flight. During all conversations with the Federal Safety Investigation Authority, the pilot left a competent impression, he was always safety-conscious. No indications of physiological or psychological influencing factors, lack of flight experience or lack of safety awareness emerged from the pilot's interview.

2.3 Aircraft

2.3.1 Technical investigation

Although an incorrectly installed or bonded Upper Inlet Ramp was found during the technical investigation, no significant influence of this approximately 1 mm thick, and 20 by 20 cm-wide polycarbonate sheet on the accident could be proven. The Upper and Lower

[1] See also Appendix 6.4

[2] Pressure altitude: Altitude in the standard atmosphere with the same atmospheric pressure

[3] Density altitude: Altitude in the standard atmosphere with the same air density

Inlet Ramps are mounted approximately at the front end of the Tail Boom, directly behind the NOTAR Fan. Only the Upper Inlet Ramp was found in the rear part of the Tail Boom. The Lower Inlet Ramp remained unlocatable. This suggests that the detachment mechanisms of the two Inlet Ramps are different and that they detached at different times. The absence of the Lower Inlet Ramp could indicate that it broke into several small parts when exiting the sharp-edged Stationary Jet Thruster, and/or was thrown far away. In any case, no traces could be found on the Stationary Jet Thruster that would indicate that an object there had moved in the air stream for a significant period of time. This suggests that both the Upper and the Lower Inlet Ramp sheets did not represent any significant resistance to the airflow through the Stationary Jet Thruster and passed it without resistance when the aircraft was intact. The time of detachment of the inlet ramps (before the accident or during the accident) could not be determined in the course of the investigations by the Bundeswehr Research Institute for Materials, Fuels and Lubricants and the Federal Safety Investigation Authority. Although a negative influence on the airflow in the tail boom cannot be proven and must therefore be considered unlikely, this possibility remains at least conceivable and cannot be completely ruled out.

Apart from the findings about the Inlet Ramps, no technical anomalies could be found on the helicopter in the course of the investigations supported by the manufacturer that could have contributed to the accident (see Section 1.15). To determine the correct rigging, the fan hub first had to be reinstalled, as it had previously been removed for technical examination. For this reason, and because a suitable hydraulic unit was not initially available, the measured values could be subject to excessive tolerances. In a second measurement with a connected hydraulic unit, the measured values were in the permitted range (see Section 1.15.1.5). The period of the annual maintenance inspection that was exceeded by three days also had no technical influence on the accident and is not causally connected to the specific accident.

2.3.2 Certification and airworthiness directives

The aircraft type was first certified by the FAA in 1994, i.e. 23 years before the accident. MD Helicopters (formerly: McDonnell Douglas) was then and is still now the only manufacturer to offer certified helicopters with a NOTAR system, which was developed and patented by McDonnell Douglas (and before that Hughes Helicopters). The knowledge of the exact functioning and aerodynamic characteristics of the NOTAR system is thus held by MD

Helicopters. A method to achieve the required safety level had to be selected for certification, which was chosen for the first time for a FAR Part 27-certified helicopter. As the required controllability according to CFR 14 Part 27.143 (see Appendix 6.1) could not be demonstrated during certification at an altitude up to 7000 ft, the WAT and Crosswind Limits chart (Figure 4) was set as an operating limit in the flight manual. This is also reflected in the Type Certificate Data Sheet as an ELOS finding with the designation TD9369LA-R/F-2 regarding the low speed controllability of the helicopter.

Several airworthiness directives and service bulletins relating to the directional control system of the helicopter have been issued by the manufacturer and the FAA (Section 1.6.4). All the service bulletins were duly implemented by the helicopter operator. It should be noted that the FAA and EASA require the mandatory implementation of Bulletin SB900-099R1 with Airworthiness Directive AD US-2009-07-13. This is justified in the FAA Docket No. FAA-2008-0772 by the fact that during flight tests it was determined that the actual controllability limits are not consistent with the limits specified in the WAT and Crosswind Limits diagram. This is remarkable in that it concerns the same area that already received attention with the ELOS Finding TD9369LA-R/F-2 mentioned above. However, the Type Certificate Data Sheet makes no mention of the limitation for take-offs and landings at 12400 ft density altitude, nor does it contain an illustration similar to RFM Figure 2-2. Especially a limitation which is rather uncommon for helicopters of this category should be specifically highlighted in the Type Certificate Data Sheet.

2.3.3 Aerodynamics

Different forces and aerodynamic effects act on a helicopter in flight. A practical description of e.g. induced inflow, the ground effect or the transverse flow effect can be found in the FAA Helicopter Flying Handbook. Effective translational lift[1] describes the effect that above an inflow air velocity (forward flight or wind) of 16-24 kt, the power required for level flight is lower compared to a hover due to a change in induced flow and a changed angle of attack at the rotor blades. In the present case, the helicopter was hovering with an inflow from the front of 12-15 kt, resulting from wind. At the time of the accident, the helicopter was therefore in an area in which the positive influence of effective translational lift was not yet effective.

[1] e.g. “More Helicopter Aerodynamics” by RW Prouty, 1988

When a helicopter is operated close to the ground, considerably less power is required to hover. This influence of the ground effect[1] is difficult to assess in the present case. On the one hand, the effectiveness of the ground effect is largely influenced by the surface (structure, slope angle, obstacles). A flat, smooth ground favors the ground effect. The slope angle at the site of the accident is about 13°, and the slope itself is uneven and partly covered by larger rocks, which in turn dampens the influence of the ground effect. The influence of obstacles or the surrounding terrain on the rotor wake is also known as thrust augmentation. On the other hand, the influence of the ground effect decreases relatively quickly as the horizontal flow velocity around the helicopter increases[2]. A velocity of 12-15 kt already has a significant influence here. It can therefore be assumed that at the time of the take-off – despite the proximity to the ground – the ground effect was noticeable, but contributed less to the lift than under ideal conditions.

With the NOTAR system, there are further aerodynamic peculiarities. The system generates a large proportion of the anti-torque force in a hover flight by diverting the downwash of the main rotor around the Circulation Control Tail Boom in order to generate a lateral force. This means that the effectiveness of the Circulation Control Tail Boom depends to a large extend on the downwash and the influencing factors associated with it. These are, among other things, the ground effect and the horizontal inflow due to the wind from the front. From an analytical point of view, entering the ground effect leads to a lower required lift (and power), and likewise to a lower downwash[3]. As the circulation control system depends on the downwash, this in turn leads to a reduced performance of the anti-torque system. This relationship was also experimentally proven by Vernard E. Lockwood in Technical Note D-969 (“Effect Of Groundboard Height On The Aerodynamic Characteristics Of A Lifting Circular Cylinder Using Tangential Blowing From Surface Slots For Lift Generation”, 1961). This reduced performance of the anti-torque system is partially offset in a static hover by the fact that the main rotor causes less torque in the ground effect. In a dynamic flight condition, e.g. during the transition from hover to climb (e.g. taking off from the landing site), a greater torque must also be compensated for by using the pedal (Direct Jet Thruster and Rotating Cone).

[1] e.g. “More Helicopter Aerodynamics” by RW Prouty, 1988

[2] “The Effect of the Ground on a Helicopter Rotor in Forward Flight” by IC Cheeseman and WE Bennett, 1957

[3] e.g. “Experimental Investigation of Rotorcraft outwash in Ground Effect” by PE Tanner et al., 2015

In addition, an inflow from the front causes the downwash around the Circulation Control Tail Boom to be carried away to the rear[1]. Stabilization around the vertical axis in forward flight (or with wind from the front) is then taken over by the vertical stabilizer (VSCS). In between there is a transition area in which the vertical stabilizer cannot yet take over the full torque compensation, but the Circulation Control Tail Boom is no longer fully effective. The exact transition speed at which this happens is not known to the Federal Safety Investigation Authority, but a source ("Evaluation Of A Circulation Control Tail Boom For Yaw Control", 1978) cites 30 kt as the speed at which the Circulation Control Tail Boom of a similar helicopter model is no longer effective. It can therefore be assumed that a flow from the front of 12-15 kt impairs the effectiveness of the Circulation Control Tail Boom (Note: This refers to the Circulation Control Tail Boom itself, not the NOTAR system as a whole).

In order to be able to better estimate the influence of the ground effect on a helicopter with NOTAR system in the course of the investigation, a flow simulation was commissioned (section 1.15.3). In order to be able to carry out the calculation and keep the calculation complexity within reasonable limits, and in consideration of the results to be expected, simplifications and restrictions were set up. Nevertheless, the results are suitable for drawing conclusions about the behavior of the system when approaching or taking off from the ground. The result of this flow simulation is that as the distance to the ground decreases, the lateral anti-torque force generated by the tail boom decreases.

In section 2-2 "Environmental Operating Conditions" from chapter 2 "Limitations" of the flight manual (RFM), reference is made to Figure 2-2 of the RFM, for the operating limit for "maximum altitude for HIGE[2]/takeoff and landing operations". That figure indicates a "TAKEOFF AND LANDING WAT LIMIT" of 12400 ft density altitude. In comparison, the RFM specifies a "maximum operating altitude" of 20000 ft with an aircraft mass of 6250 lb or less. A flight is therefore possible at higher altitudes than 12400 ft, only take-off and landing is prohibited. This leads to the conclusion that the issue of the reduced performance of the

[1] "Evaluation Of A Circulation Control Tail Boom For Yaw Control" by A. H. Logan, 1978; "Design, Development, And Testing Of The No Tail Rotor (Notar) Demonstrator" by AH Logan, KM Morger, EP Sampatacos, 1983

[2] Hover in ground effect

NOTAR system when operating near the ground ("HIGE/takeoff and landing operations") is known. This finding corresponds to the above aerodynamic considerations, technical reports and the flow simulation. In the case of the helicopter type in question, there is indeed an operating limit with regard to the density altitude, which is aerodynamically induced. If this is considered in conjunction with the helicopter's performance data (RFM Chapter 5), it can be seen that operation of the helicopter is certainly possible at altitudes higher than 12400 ft, but due to the limitations on controllability the operation in ground effect and thus landing or take-off at a density altitude of 12400 ft and above is prohibited.

2.3.4 Rotorcraft flight manual

Although the helicopter and its flight manual have been properly certified by the FAA, there are passages in the flight manual that could be misinterpreted under certain circumstances.

To determine the hover ceiling inside and outside the ground effect (IGE and OGE), the Figures 5-38 to 5-45 are given in Chapter 5 of the RFM ("Performance Data") for different aircraft configurations. The information in Chapter 5 basically represents the technological limits that cannot be exceeded, for example due to the available engine power, while the information in Chapter 2 ("Limitations") represents the operational limits that must be adhered to for safe operation.

Figure 5-37 refers to hovering in the ground effect in wind. The content of the figure largely corresponds to Figure 2-2 (this report Figure 21). Although only the information from the Limitations chapter of the RFM is to be regarded as mandatory operating limits in the sense of type certification, the note "TAKEOFF AND LANDING WAT LIMIT" at 12400 ft is also shown in Figure 5-37.

Figure 21 RFM Figure 2-2 and Figure 5-37, Flight Manual MD900

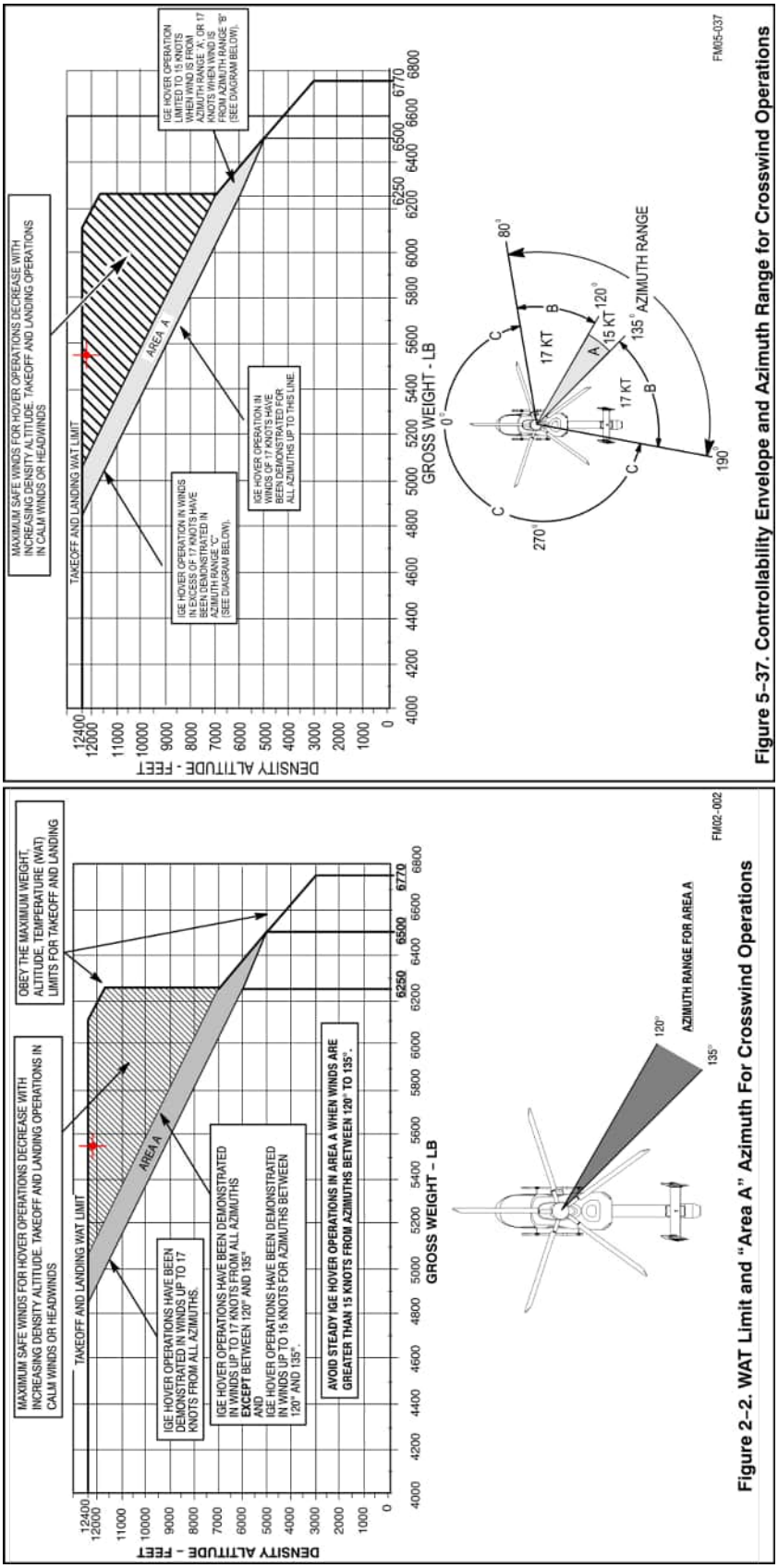

Source: MDHI RFM, supplemented by SIA

The two figures also differ in certain details. The wind information in Figure 5-37 is a little more detailed. While Figure 2-2 states “IGE HOVER OPERATIONS HAVE BEEN DEMONSTRATED IN WINDS UP TO 17 KNOTS FROM ALL AZIMUTHS”, Figure 5-37 contains the contradicting statement “IGE HOVER OPERATION IN WINDS IN EXCESS OF 17 KNOTS HAVE BEEN DEMONSTRATED IN AZIMUTH RANGE ‘C’ […]”. Consequently, according to Figure 5-37, hovering in the ground effect would also be possible with wind strengths greater than 17 knots (“demonstrated”, i.e. proven in the course of certification). On the other hand, Figure 5-37 shows that “IGE HOVER OPERATION LIMITED TO 15 KNOTS WHEN WIND IS FROM AZIMUTH RANGE ‘A’, OR 17 KNOTS WHEN WIND IS FROM AZIMUTH RANGE ‘B’ [...]”. The fact that an operating limit is mentioned in the Performance Data section of the RFM, which is not mentioned in the same diagram in the Limitations section, could be misleading. Both diagrams also show that “MAXIMUM SAFE WINDS FOR HOVER OPERATIONS DECREASE WITH INCREASING DENSITY ALTITUDE. TAKEOFF AND LANDING OPERATIONS IN CALM WINDS OR HEADWINDS”, with a reference to the hatched area in the diagram. This would also apply to wind from the front.

Since no definition for “safe winds” is given and no precise information is given here as to the ratio in which the safe wind conditions decrease with increasing altitude, based on the remaining information in the diagram, it could be assumed that wind from the front with 17 kt at an altitude of 12400 ft is also within the permitted range. However, this contradicts the basic statement of the sentence, according to which safe wind conditions decrease with increasing altitude.

Figure 2-2 is titled “WAT Limit and “Area A” Azimuth For Crosswind Operations”, while Figure 5-37 is titled “Controllability Envelope and Azimuth Range for Crosswind Operations”. Here it would make sense to name the same content the same way and thereby ensure consistency. In addition, the designation “[...] For Crosswind Operations” allows the erroneous conclusion that these two diagrams should only be used in crosswind conditions.

In the present incident, the helicopter was operated in the area marked with a red cross (this report Figure 21). The choice of the wording “take-off” and “landing” in the figures implies, according to the manufacturer, that the helicopter usually also enters the ground effect. However, there are also cases where this is not the case, e.g. on a raised landing platform, rock walls or rope or winch operations. The extent to which the ground effect was effective in this specific case was already discussed in section 2.3.3.

It could not be determined in the course of the accident investigation whether safety margins were taken into account in Figure 2-2 or Figure 5-37. Since the information on wind conditions is listed as “demonstrated” in the diagrams, it can be assumed that the values used here were those that were achievable and flyable by the test pilot during certification. It is conceivable that a pilot who has not received test pilot training and who flies in difficult real-world conditions (HEMS operations, high mountains, single-pilot operation, etc.) will reach these operational limits at an earlier stage. In addition, it must be assumed that altitude typically can only be precisely determined to about 100 ft[1] with a common altimeter (depending on the tolerances and accuracy of the altimeter and QNH setting). The same applies for the temperature (density altitude). Whether the determination of the wind direction to ±5° and the wind speed to ±1 kt is possible at the site of operation, i.e. without a windsock or other measuring devices, can in any case be doubted.

This report’s Figures 22 and 23 from the “Performance Data” section of the RFM are required to determine the maximum possible hover ceiling for inside and outside the ground effect. The data relating to the incident in question are shown in red. The maximum possible weight as the result of the intersection between the current temperature and the current altitude is shown in blue.

[1] Depending on the actual altitude and altimeter model

Figure 22 RFM Figure 5-42, Hover Ceiling, IGE, Flight Manual MD900

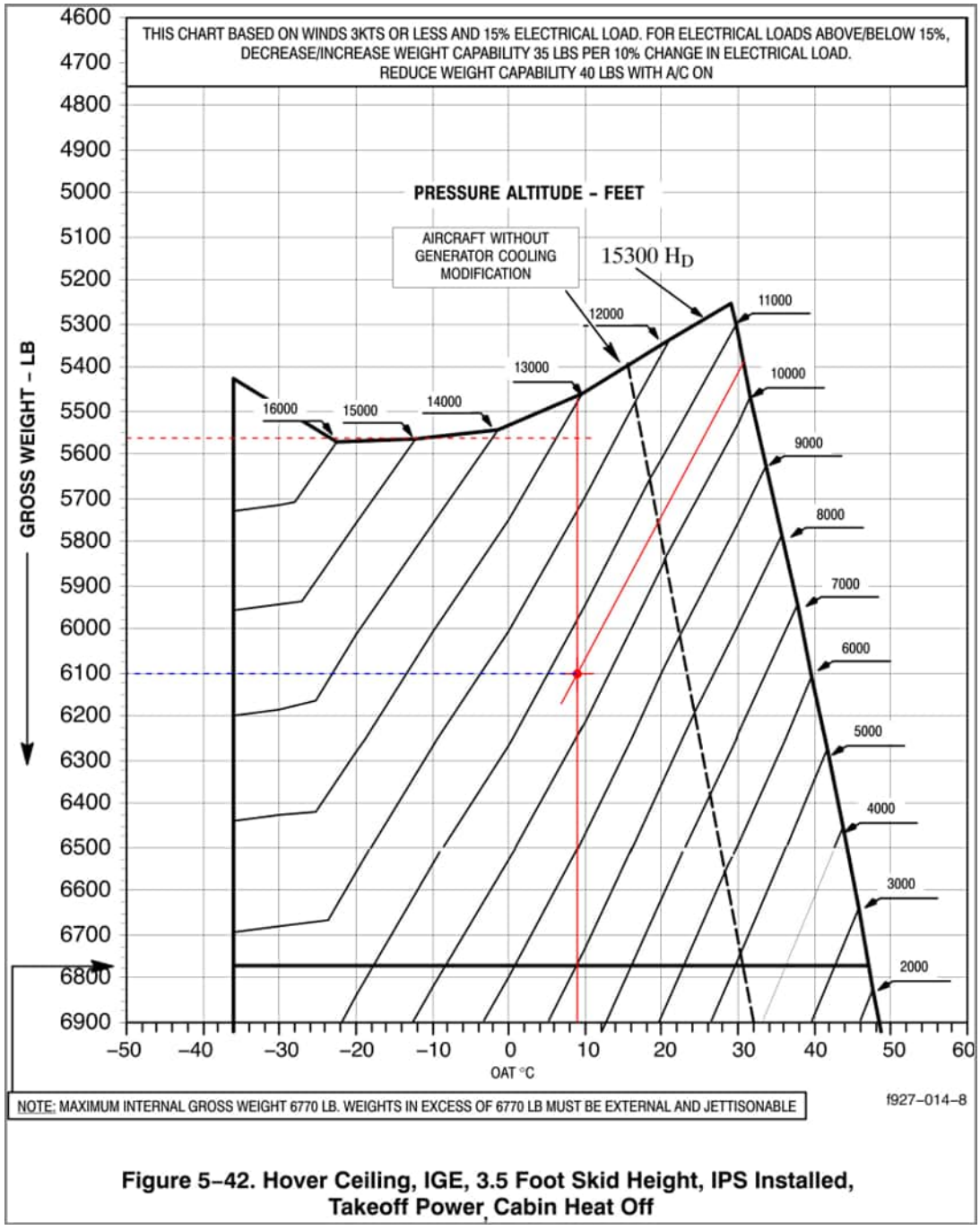

Figure 5–42. Hover Ceiling, IGE, 3.5 Foot Skid Height, IPS Installed, Takeoff Power, Cabin Heat Off

Source: MDHI RFM, supplemented by SIA

Figure 23 RFM Figure 5-44, Hover Ceiling, OGE, Flight Manual MD900

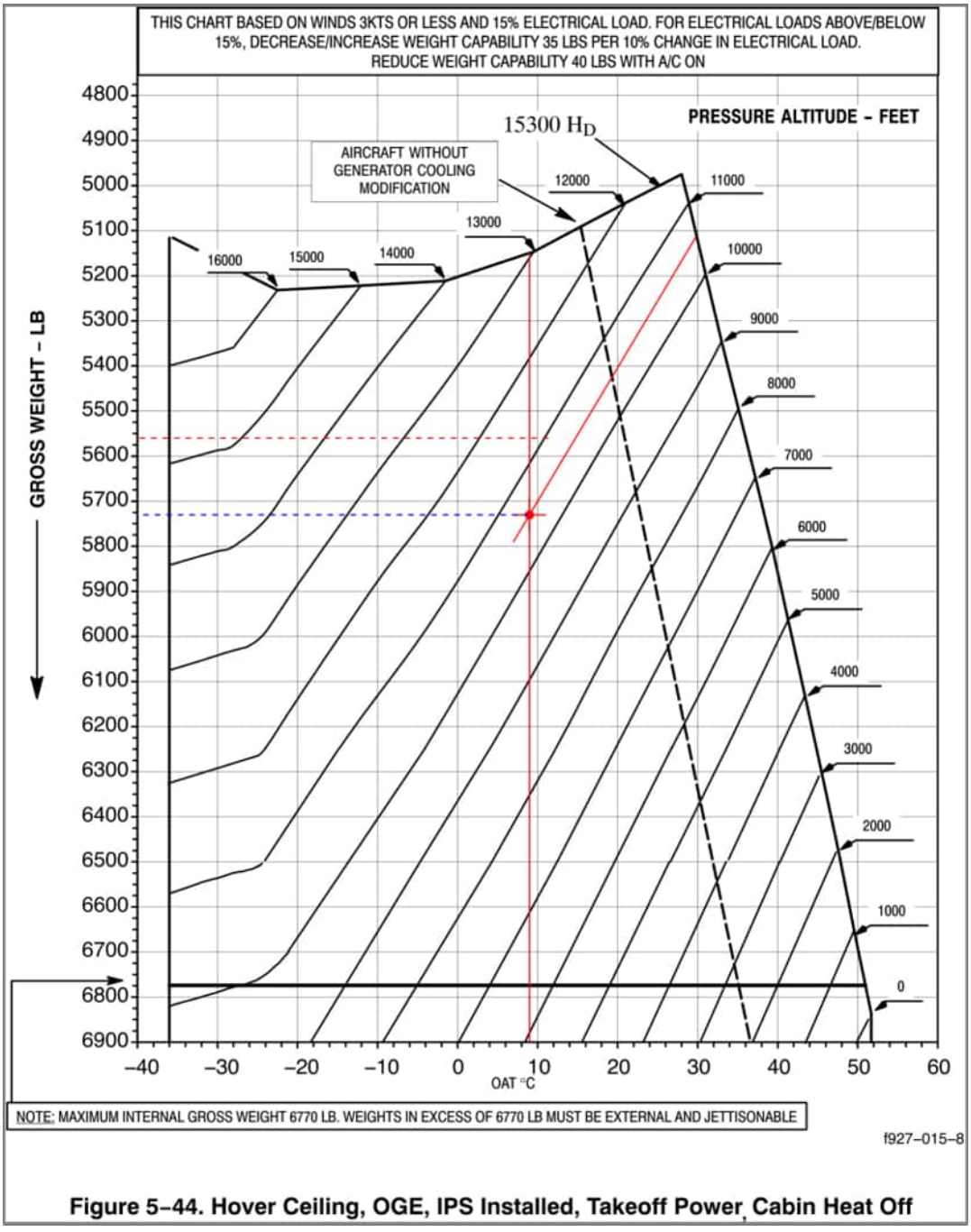

Source: MDHI RFM, supplemented by SIA

What is noticeable is that in comparison to Figure 2-2 or 5-37, altitudes are expressed as pressure altitudes. It is also noticeable that in all the diagrams from Figure 5-38 to Figure 5-45, the upper limit value is 15300 ft density altitude. This is notable for two reasons. On the one hand, because in Chapter 2 ("Limitations") the "Maximum operating altitude" is given as 20000 ft density altitude. However, there is no way to carry out a performance calculation for altitudes greater than 15300 ft, as all diagrams end there. Second, because

the diagrams relating to hover in ground effect (HIGE), e.g. Figure 5-42 (this report Figure 22), cover areas greater than 12400 ft, although operation at altitudes greater than 12400 ft in the ground effect is not permitted in accordance with the Limitations chapter. This can lead to pilots mistakenly assuming that such an operation is permissible. It would make sense to mark an operating limit in these HIGE charts at a density altitude of 12400 ft. In addition, these diagrams are based on the assumption that the wind is 3 kt or less. Since no diagrams or other information are available for stronger winds, the diagrams in Figure 5-38 to Figure 5-45 can only be used to a limited extent for the performance calculation in stronger winds.

2.4 History of flight and flight operations

The helicopter was utilized by the operator for HEMS operations and was stationed at the Matrei helicopter base in East Tyrol (LOMM). The flight departed on 1 August at around 18:04 hours from Matrei to the rescue site on the Adlersruhe. Prior to this, a proper pre-flight preparation was carried out, including weather briefing, performance calculation and mass and balance calculation. The pilot's mass calculation included an additional crew member with 85 kg who was not actually on board and approximately 40 kg more fuel than was determined by the Safety Investigation Authority during the technical examination. This results in a discrepancy between the aircraft mass of 5658 lbs (2566 kg) used by the pilot and the actual aircraft mass of 5558 lbs determined by the Safety Investigation Authority, which is advantageous for flight performance. The performance calculation was carried out in accordance with the operator’s specifications. The operator refers correctly to the RFM in the Operations Manual Part B (OM-B). However, the performance calculation sheet does not provide for an explicit consideration or calculation of the density altitude to be expected at the rescue site. The density altitude and its relevance for the operational limits is not explicitly mentioned in the OM-B either. However, this is – especially for the present MD900 helicopter model – decisive for determining the maximum attainable geographic altitude and for landing or take-off.

The density altitude corresponds to the air density at a certain location and is expressed as the equivalent of the corresponding altitude in standard atmospheric conditions. It is therefore dependent on altitude (of the rescue site) and temperature. A temperature increase of 1°C reduces the maximum possible take-off and landing altitude, for example in the present case by about 22 m (72 ft). The limits regarding the density altitude (RFM Figure 2-2) were not exceeded in the present case, based on the available weather and engine

data, but the helicopter was operated very close to the limit (12261 ft density altitude at the operating site vs. 12400 ft operating limit). In any case, it must be noted that the other environmental conditions were by no means ideal (see also section 2.3.3). The weather in high mountains is generally very changeable. Above all, the wind flowing over the mountain ridge is a factor of uncertainty that should not be neglected, as different small-scale warmings and air circulations close to the ground and walls can lead to locally different wind directions and temperature variations. Temperature fluctuations at the rescue site could also have had a noticeable influence. The temperature determined above does not represent a measurement at the rescue site, but an interpolation and interpretation of various sources around the rescue site. In addition, the approach to the landing site was carried out as a descending flight. This means that the helicopter was initially operated at a slightly higher altitude than the calculated 12261 ft for the approach. The same applies to the departure.

These factors make it difficult to determine the expected density altitude at the rescue site prior to the flight, or at least result in larger tolerances. The density altitude can also be determined in flight using conversion tables or charts[1] (conversion charts) or using a navigation computer (e.g. E6-B, electronic variants or smartphone apps). However, this requires the pilot to use one or sometimes both hands. Charts must be read with great accuracy. This is especially true if it is planned to get very close to the operational limits. This method is not very practical for HEMS operations, since in most cases it involves single pilot operations in hostile environments. However, the final assessment can only be made by the pilot directly at the operating site and is therefore indispensable. When flying in such difficult conditions, a pilot should and must devote the majority of his or her cognitive performance, attention and concentration to controlling the helicopter, navigating and communicating with the crew. Take-off and landing or flying close to the ground or close to the mountains represents an additional risk factor.

With the present MD900 helicopter model, it is possible to display the pressure altitude and the density altitude together on the alphanumeric display of the IIDS. However, these data are not shown by default and can only be displayed after navigating through the menu. The manufacturer's RFM describes this option in Chapter 7 ("System Description"). The operator's OM-B did not mention the possibility of displaying the density altitude or the use of this to determine whether the operating limits were possibly exceeded. After the accident, the operator issued a Flying Staff Instruction, making the utilization of this display mandatory. It should be noted that the alphanumeric display is also used to display

[1] Conversion chart between pressure altitude and density altitude e.g. in RFM Chapter 5 ("Performance Data").

warnings, advisories and cautions, which may be displayed with priority and can (temporarily) prevent the display of the density altitude. In this respect, the display of the density altitude on the IIDS can only be regarded as an aid and not as a permanent or primary display.

The pilot stated that he had carried out an overflight as well as a hover flight to check the actual available power before landing. In helicopters with a conventional tail rotor, this is a common procedure for determining the remaining pedal travel and power reserves. Whether a landing is possible depends in principle on the presence of the available power. If helicopters with a conventional tail rotor have sufficient power to hover outside the ground effect (HOGE), landing can be carried out safely, as less engines power is required to land in the ground effect (HIGE).

In the case of the MD900 helicopter model, however, no conclusion can be drawn about the (aerodynamic) power reserves in the ground effect (IGE) on the basis of such an overflight outside the ground effect (OGE), since the method of anti-torque generation differs fundamentally from conventional helicopter models. The helicopter behaves aerodynamically differently when approaching the ground (see sections 1.15.3 and 2.3.3). The fact that sufficient power may be available at a certain altitude, but controllability close to the ground can nevertheless be limited, is not immediately comprehensible to pilots without having been specially trained or instructed on this aerodynamic peculiarity. This is particularly true because a similar limitation as in RFM Figure 2-2 does not exist for comparable (Part 27, CS-27) helicopters.

Even though it can be seen from Figure 2-2 of the RFM that for a helicopter with a mass between 4000 and ca. 6100 lb the operating limit is constantly at 12400 ft for take-off and landing with no wind, or wind from the front, it can be assumed that a lighter helicopter is generally more favorable and can be brought closer to the operating limits. In this respect, the pilot made the correct decision to save weight by not taking the fourth crew member, who was supposed to be on board for training. Conversely, it can be assumed that the additional weight of the patient when boarding the helicopter inevitably contributed negatively to the performance balance and probably also to the accident. This is especially true if the helicopter was already moving just at the edge of the performance limit as well as in ground effect. It is not known and cannot be clearly seen from the witness video whether the lodge keeper was also (partially) standing on the skids when the patient boarded the helicopter. However, the helicopter was supported by a skid on the ground

during the period when the lodge keeper was standing by the helicopter, which would have compensated for any additional load caused by the weight of the lodge keeper.

According to Figure 2-2 of the RFM, the helicopter was always operated within the permissible range with regard to the aircraft mass and balance. The helicopter began to yaw to the right about 30-40° for the first time without any control input from the pilot when the patient entered the helicopter. This occurred at a time when the helicopter was hovering in ground effect. It can therefore be assumed that this increase in total weight (despite operation within the permissible weight range according to the RFM) was a decisive factor in causing or even triggering the helicopter to start yawing uncontrollably, even though the weight of the patient had not contributed significantly to the total mass of the helicopter when boarding. In addition, in the course of the uncontrolled rotation, the prevailing wind no longer approached the helicopter from the front, but increasingly from the left side. This deviation from the aerodynamically ideal flow from the front also contributed negatively to the aerodynamic performance.

Since the pilot could not see exactly whether the patient was already strapped in and whether the door was still open or already closed at the time the patient got in, the only way to keep the helicopter under control that seemed safest for everyone involved was to first keep it hovering with the pedal fully depressed for as long as possible and then try to gain altitude and distance from the mountain by climbing slightly. If a helicopter starts to yaw uncontrollably (due to power limits), the usual procedure is to lower the collective control stick, thereby reducing the torque on the main rotor and, as a result, losing altitude. Additionally the helicopter's nose must be pushed down with the cyclic control stick, thereby picking up speed. In the particular situation, both options posed a high risk of colliding with the terrain. Touching down on the landing site was not an option either, as no flat enough surface was available.

Since the yawing motion, which was very pronounced at this point in time, could no longer be corrected, there was no alternative to pushing the collective control stick down. Hence, this reaction is considered correct. Any attempt to the contrary to gain further altitude would have increased the yawing motion of the helicopter and would have made the aircraft even more difficult to control. As a result, the helicopter decreased in altitude and touched down very roughly on the rocky ground, still in a spinning motion. An “escape” from this situation would most likely only have been possible until shortly before the initial landing. The approach and landing were continued, as at this point the pedal deflection was not significantly increased and, according to the pilot, there was still sufficient reserve available on the pedals.

In the specific case, the pilot was unable to fully touch down the helicopter on the ground because a flat enough surface was not available for landing. He therefore had to pick up the patient while keeping the helicopter in hovering flight – supported by one skid touching the mountain slope. In general, this is a usual procedure and is common for HEMS operations in mountains, but it also poses an increased inherent risk. In this case, for example, the pilot no longer had the opportunity of easily aborting the take-off when he noticed that the helicopter could no longer be controlled around the vertical axis.

During HEMS missions, pilots have to land in most cases on unpaved areas such as meadows and fields, or on roads and pathways to pick up patients. In any case, the area-wide construction of landing pads for helicopters is not feasible in a sensible way. However, the area around the Erzherzog-Johann lodge is regularly used to pick up patients, as a popular route for climbing of Mount Grossglockner passes this area. Corresponding mission data is available from the HEMS operators. The construction of a platform[1] for helicopter landings in the vicinity of the Erzherzog-Johann lodge should be assesed in any case, especially with regard to the safety gain for HEMS operations. Had a suitable landing area been available, the pilot would have had the opportunity to land the helicopter completely and safely on the platform again at the slightest sign of an incipient spinning movement. This safety gain would not only benefit flights with the MD900 helicopter, but all HEMS flights.

[1] e.g. "Portable Heliport" from *Soloy Aviation Solutions* or similar landing platforms

2.4.1 Regulatory requirements for HEMS operations

As explained in section 1.16.2, the requirements of Regulation (EU) No. 965/2012, especially part SPA.HEMS, must be met for HEMS operations. A safe continuation of the flight requires sufficient climb performance at the respective altitude of the operating site, taking into account the helicopter weight and the temperature at the operating site. Specifically, according to the EASA Guidance Material for Regulation (EU) 965/2012 corresponding to performance class 2, if one engine fails, a minimum climb rate of 150 ft/min up to 1000 ft above the take-off point would be required. Neither the MD900 helicopter nor other comparable helicopter types meet this requirement under realistic operating conditions (weight, altitude and temperature). This deficit has already been recognized by EASA, and a change to the provisions on the performance requirements for rescue flight operations is planned (see NPA 2018-04, 2.3.2.5).

Under the designation OSD (Operational Suitability Data), EASA and the European Union maintain a concept whereby aircraft type certificate holders provide EASA and operators with certain information that is considered to be particularly important for the safe operation of the aircraft. Currently, EASA does not have any OSD FCD (Flight Crew Data) available from the type certificate holder of the MD900 helicopter. However, this would be an opportunity to point out the type-specific characteristics of the MD900 model in the course of pilot qualification and training, especially with regard to the operating limits given in Figure 2-2.

Regulation (EU) 748/2012 puts the obligation to obtain an approval for Operational Suitability Data / Flight Crew Data for holders of a type certificate only when such type certificate holders intend to deliver a new aircraft to an EU operator on or after 17 February 2014. For the MD900 model, there is therefore no legal obligation to provide Operational Suitability Data / Flight Crew Data as part of the type certification.

2.5 Safety actions

After the accident, the operator has already taken proactive measures to prevent a recurrence. These are endorsed by the Federal Security Investigation Authority and are in line with the findings of the safety investigation.

One of the measures is that the existing MD900 helicopters have been stationed differently or are being deployed in other locations, so that operating sites with a density altitude of 12400 ft are no longer within the operational radius of the respective helicopter.

In addition, a Flying Staff Instruction (FSI) was issued as part of the OM-A, which specifically refers to the limits regarding the density altitude and Figure 2-2. This FSI also requires that the density altitude display on the IIDS's alphanumeric display be activated from take-off to landing.

3 Conclusions

3.1 Findings

- At the time of the accident, natural daylight and visual meteorological conditions prevailed.
- The pilot had all the licenses and ratings required to conduct the flight.
- The pilot had sufficient flight experience both on the accident type, as well as with other types of helicopters.
- The pilot reported sufficient rest periods and was rested.
- Physical or psychological factors influencing the pilot can be excluded.
- The annual maintenance inspection, including tolerances, was exceeded by 3 days. This exceedance of the annual maintenance inspection was not causative of the accident.
- An incorrectly installed Upper Inlet Ramp was found during the investigation.
- The incorrect installation of the Upper Inlet Ramp was due to incorrect bonding, priming and painting.
- A negative influence of the detached Upper Inlet Ramp on the airflow in the tail boom cannot be proven and is therefore unlikely, but ultimately cannot be completely ruled out.
- Apart from the exceeded annual maintenance inspection and the incorrectly installed Upper Inlet Ramp, the aircraft was properly maintained.
- All the mandatory service bulletins and airworthiness directives were properly carried out.
- The certification basis for the helicopter was CFR 14 Part 27, Amendments 1 to 26.
- The controllability with respect to Figure 2-2 was an area of critical concern for airworthiness when it was first certified by the FAA (ELOS Finding TD9369LA-R/F-2) and in the course of a service bulletin review by the FAA (SB900-099R1, AD US-2009-07-13).
- An alternative method to comply with CFR 14 Part 27.143 had to be selected during certification, as the required controllability at an altitude of 7000 ft could not be demonstrated. For this purpose, the “WAT Limit and Area A Azimuth For Crosswind Operations” diagram (RFM Figure 2-2) in the flight manual was established as an operating limit.

- During the FAA's processing of Service Bulletin SB900-099R1, flight tests revealed that the actual controllability limits were inconsistent with the limits given in the WAT and Crosswind Limits chart (RFM Figure 2-2). As a result, the FAA issued Airworthiness Directive AD US-2009-07-13 for mandatory implementation.
- The information in the flight manual relating to Figure 2-2 and Figure 5-37 may be misinterpreted by pilots due to the way in which they are presented. This could inadvertently lead them to misjudge the operating limits of the helicopter.
- In the Type Certificate Data Sheet, there is no note about the limitation of 12400 ft density altitude limit for take-offs and landings or an illustration similar to Figure 2-2.
- At most HEMS operating sites, it will most likely not be possible to determine wind direction and the wind speed accurately enough, especially without windsocks or other measuring devices. Strict adherence to the wind data in Figure 2-2 would therefore likely be difficult or even impossible.
- A fourth crew member, who should have been onboard for training, was left on the ground in order to reduce the overall weight of the helicopter.
- The mass and center of gravity were within the permissible range througout the entire flight.
- The pre-flight preparation was carried out properly.
- During the entire flight sufficient engine power was always available with respect to the flight manual chapter "Performance Data" (Figures 5-38 to 5-45).
- An overflight as well as hover flight was carried out to assess the performance margins. Due to the aerodynamic characteristics and special nature of the NOTAR system, this is only suitable to a limited extent for the MD900 helicopter model to estimate the remaining safety margins with regard to controllability in the ground effect.
- The temperature at the operating/accident site was determined to be 9.2°C (ISA+16) based on the available data at the time of the accident.
- The operating/accident site lies at a geographical elevation of 11220 ft.
- The calculated density altitude at the accident site was 12231 ft at the time of the accident.
- The pilot performed a descent approach to the landing site. Consequently, the helicopter was at a higher altitude when starting the approach than the calculated density altitude of 12231 ft at the accident site. The reserve was therefore about 169 ft. The same applies to the departure.
- The operating limit for take-offs, landings and flights in ground effect is 12400 ft (density altitude) as specified by the manufacturer in the flight manual. This operating limit was not exceeded at the accident site.

- The wind at the accident site was about 12-15 kt from the front at the time of the accident according to the video evaluation.
- The measure to lower the collective stick to reduce the uncontrolled spinning movement was correct. In this specific case, it was not possible to pick up speed from the hover due to the turning motion and the proximity to the mountain.
- Determining the density altitude prior to the flight is only rarely feasible with accuracy. In most cases, the elevation of the operating site and the prevailing temperature there are not precisely known. A final assessment by the pilot at the operating site is indispensable.
- The use of navigation computers or conversion tables and charts to determine the density altitude is possible in principle. However, this represents an additional cognitive burden for pilots in HEMS operations – especially in single pilot operations – which should be avoided. Instruments that directly display the density altitude would be preferable.
- The use of the IIDS to display the density altitude is possible in principle, but is neither prescribed nor recommended by the manufacturer or the certifying authority for determining whether the operating limits are complied with. The operator prescribed this by means of a Flying Staff Instruction after the accident.
- A flat and level landing area was not available at the operating/accident site. The patient had to be picked up while the helicopter was hovering. A suitable landing area would have provided the opportunity to fully and safely touching down the helicopter again at the first indication of an uncontrolled turning motion.
- The operator has already taken proactive measures to prevent a recurrence of a similar incident.
- The requirements prescribed by the European Union and EASA on performance classes for HEMS operations (Regulation (EU) 965/2012) cannot be met at high altitudes by a number of helicopter models in use. EASA is aware of this issue and corresponding changes are already in progress.

3.2 Probable causes

Loss of yaw control around the vertical axis during take-off and in ground effect (IGE)

3.2.1 Likely factors

- Operation of the helicopter close to the limit of aerodynamic controllability around the vertical axis.
- Lack of potential landing sites near the Erzherzog-Johann lodge to fully touch down the helicopter.
- Aerodynamic peculiarity of the NOTAR system and therefore different behavior in ground effect compared to helicopters with a conventional tail rotor.
- Although properly certified by the civil aviation authorities, information regarding operating limits in the flight manual may be misinterpreted by pilots due to the way they are presented.

4 Safety recommendations

Since the operator has already taken proactive measures, no additional safety recommendation is made to the operator. With regard to the performance classes for HEMS flight operations at high altitudes, no additional safety recommendation is addressed to EASA, as this issue is already known and being processed.

No. SE/SUB/LF/6/2022, addressed to the Type Certificate Holder:

Although not considered to be the cause of the accident, it was found that the Upper Inlet Ramp had been incorrectly bonded and installed. It is recommend that all operators be made aware of the need to check the correct installation of the Inlet Ramps.

No. SE/SUB/LF/7/2022, addressed to the Type Certificate Holder:

The MD900 helicopter has a density altitude limit for take-offs, landings and operation in ground effect. Depending on the outside temperature, the density altitude may vary greatly from the pressure altitude reading on the altimeter. It is recommended that as part of the safety promotion all operators be made aware of the possibility of having the density altitude displayed directly on the IIDS. Other measures should also be explored. For example, the “Limitations” chapter of the flight manual could be supplemented with a note indicating that the IIDS display can be used to comply with the density altitude limit.

No. SE/SUB/LF/8/2022, addressed to EASA:

It was noted that Figure 2-2 from the MD900 Flight Manual, Chapter 2 “Limitations”, was properly approved by the civil aviation authorities, but some information may be misinterpreted. It is recommended that the information in Figure 2-2 should be re-evaluated and, in cooperation with the FAA and the manufacturer, that consideration be given to whether and how the relevant information in this chart can be presented more clearly, taking into account the possibility of misinterpretations. This may include, among other things, extending the text “TAKEOFF AND LANDING WAT LIMIT” to include the word “HIGE”, introducing safety margins, especially around the operating limit of 12400 ft, clarifying that wind from the front can also have a negative effect, or, if necessary, changing the title, as “[...] For Crosswind Operations” could give the wrong impression that the chart is only to be used in crosswinds conditions.

No. SE/SUB/LF/9/2022, addressed to EASA:

OSD (Operational Suitability Data) for the MD900 helicopter are not available from the type certificate holder at EASA, nor does a legal obligation exist for the MD900 type to require such. However, the operating limit regarding the aerodynamic controllability (flight manual Figure 2-2) is a peculiarity of this helicopter model and the NOTAR system, which is uncommon in this form compared to helicopter models with conventional tail rotor according to FAR Part 27 or CS-27. It is recommended to examine options, in cooperation with FAA and the type certificate holder, to make pilots aware of the aerodynamic and operational peculiarities of MD900 type helicopters.

No. SE/SUB/LF/10/2022, addressed to the Office of the Carinthian Provincial Government:

The current accident could probably have been avoided if a suitable landing area or landing platform had been available. The Erzherzog-Johann lodge is the highest lodge for and last stop before the climbing of Mount Grossglockner. It is recommended that the construction of a landing site – e.g. in the form of a mobile platform – in the vicinity of the Erzherzog-Johann lodge be examined in cooperation with the Office of the Tyrolean Provincial Government.

5 Consultation

Pursuant to Art. 16 (4) Regulation (EU) No. 996/2010, the Federal Safety Investigation Authority shall solicit comments from the authorities concerned, including EASA, the type certificate holder, the manufacturer and the operator concerned prior to publishing the final report.

In solociting such response, the Federal Safety Investigation Authority followed the international guidelines and recommendations regarding investigations of aviation accidents and incidents as approved under Article 37 of the Chicago Convention on International Civil Aviation.

Pursuant to article 14 para. 1 of the UUG [*Accident Investigation Act*] 2005 as amended, the Federal Safety Investigation Authority asked the owner of the aircraft and any survivors or victims for their written comment on the facts and conclusions pertinent to the occurrence under investigation before finalization of the report on the investigation ("Stellungnahmeverfahren").

The Federal Safety Investigation Authority received comments from the pilot, Austro Control GmbH (ACG), the European Aviation Safety Agency (EASA), the helicopter type certificate holder/manufacturer and the engine type certificate holder/manufacturer.

The responses obtained were taken into consideration and incorporated in the investigation report as applicable.

List of Tables

List of Figures

List of Regulations and Standards

Austrian Federal Law of 2 December 1957 on Aviation (**Aviation Act 1957** – [***Luftfahrtgesetz - LFG***]), Federal Law Gazette [*BGBl. I*] No. 253/1957 as amended by Federal Law Gazette [*BGBl. I*] No. 92/2017

Austrian Federal Law on Independent Safety Investigation of Accidents and Incidents (**Accident Investigation Act 2005** – [***Unfalluntersuchungsgesetz - UUG***]), Federal Law Gazette [*BGBl. I*] No. 123/2005 last amended by Federal Law Gazette [*BGBl. I*] No. 231/2021

Regulation (EU) No. 996/2010 of the European Parliament and of the Council of 20 October 2010 on the investigation and prevention of accidents and incidents in civil aviation and the repeal of Directive 94/56/EC

Regulation (EU) No. 376/2014 of the European Parliament and of the Council of 3 April 2014 on the reporting, analysis and follow-up of incidents in civil aviation, amending Regulation (EU) No. 996/2010 of the European Parliament and of the Council and repealing Directive 2003/42/EC of the European Parliament and of the Council and of Commission Regulations (EC) No. 1321/2007 and (EC) No. 1330/2007

Commission Implementing Regulation (EU) No. 923/2012 of 26 September 2012 laying down common rules of the air and operational provisions regarding services and procedures in air navigation and amending Implementing Regulation (EU) No 1035/2011 and Regulations (EC) No 1265/2007, (EC) No 1794/2006, (EC) No 730/2006, (EC) No 1033/2006 and (EU) No 255/2010. (**SERA**)

Regulation (EU) No. 965/2012 of 5 October 2012 laying down technical requirements and administrative procedures related to air operations pursuant to Regulation (EC) No 216/2008 of the European Parliament and of the Council

Code of Federal Regulations, Title 14 - Aeronautics and Space, Chapter I - Federal Aviation Administration, Department Of Transportation, Subchapter C - Aircraft, Part 27 – Airworthiness Standards: Normal Category Rotorcraft. (**14 CFR 27 – Part 27**)

Abbreviations

ACG	Austro Control GmbH
AD	Airworthiness Directive
AEO	All Engines Operative
AFM	Aircraft Flight Manual
ARC	Airworthiness Review Certificate
ASCM	Aircraft Systems Condition Monitoring
ATPL(H)	Airline Transport Pilot License, Helicopter
BMS	Balance Monitoring System
CG	Center of Gravity
CPL	Commercial Pilot License
DCU	Data Collection Unit
EASA	European Aviation Safety Agency
ECET	End of Civil Evening Twilight
EEC	Electronic Engine Control
EFB	Electronic Flight Bag
ELOS	Equivalent Level of Safety
ELT	Emergency Locator Transmitter
EMS	Emergency Medical Services
FAA	Federal Aviation Administration
FAR	Federal Aviation Requirements
FCD	Flight Crew Data (within the framework of OSD)
FI	Flight Instructor
GAFOR	General Aviation Forecast
HCM	HEMS Crew Member
HEMS	Helicopter Emergency Medical Services
HIGE	Hover in Ground Effect
HOGE	Hover out of Ground Effect
IGE	In Ground Effect
IIDS	Integrated Instrumentation Display System

IPS	Inlet Particle Separator
IR	Instrument Rating
JAA	Joint Aviation Authorities
JAR	Joint Aviation Requirements
LOMM	ICAO identifier of heliport Matrei in East Tyrol
LOWI	ICAO identifier of Innsbruck Kranebitten airport
LOWK	ICAO identifier of Klagenfurt airport
M&B	Mass & Balance
MCC	Multi Crew Coordination
MET(H)	Multi-Engine Turbine, Helicopter
METAR	Meteorological Aerodrome Report
MDHI	MD Helicopters, Inc.
MGT	Measured Gas Temperature
MSL	Mean Sea Level
MTM	Maintenance Training Manual
MTOM	Maximum Take Off Mass
NOTAR®	No Tail Rotor (registered trademark of MDHI)
NTSB	National Transportation Safety Board
OGE	Out of Ground Effect
OM	Operations Manual
OSD	Operational Suitability Data
PPL	Private Pilot License
QNH	Atmospheric pressure related to sea level in hPa
RFM	Rotorcraft Flight Manual
rpm	Revolutions per minute
SB	Service Bulletin
SERA	Standardised European Rules of the Air
SFC	Surface
SIA	Federal Safety Investigation Authority of Austria
SWC	Significant Weather Chart
TAF	Terminal Aerodrome Forecast

TAWES	Teilautomatisches-Wetter-Erfassungs-System (Semi-automatic Weather Recording System)
TCDS	Type Certificate Data Sheet
UTC	Coordinated Universal Time
VAMES	Voll-Automatisches-Meteorologisches-Erfassungs-System (Fully Automatic Meteorological Recording System)
VFR	Visual Flight Rules
VMC	Visual meteorological conditions
VSCS	Vertical Stabilizer Control System
WAT	Weight-Altitude-Temperature
WGS84	World Geodetic System 1984
W/T	Wind/Temperature
ZAMG	Zentralanstalt für Meteorologie und Geodynamik (*An Austrian weather data provider*)

ft	Feet (1 ft = 0,3048 m)
ft/min	Feet per minute (1 ft/min = 0.00508 m/s)
Hz	Hertz
in	Inch (1 in = 0,0254 m)
in-lbs	Inch-Pound (1 in-lbs = 0.1129848 Nm)
kt	Knots (1 kt = 0,514444 m/s)
lb	Pound (1 lb = 0,453592 kg)
psia	Pound-force per square inch absolute (1 psia = 0,0689476 bar)

Abbreviations related to weather observations (METAR) and forecasts (TAF) can be found in the WMO manual “Aerodrome Reports and Forecasts”, WMO-No. 782 (https://library.wmo.int/doc_num.php?explnum_id=5981).

6 Appendices

6.1 Extract from 14 CFR

"§ 27.143 Controllability and maneuverability

(a) The rotorcraft must be safely controllable and maneuverable—
  (1) During steady flight; and
  (2) During any maneuver appropriate to the type, including—
    (i) Takeoff;
    (ii) Climb;
    (iii) Level flight;
    (iv) Turning flight;
    (v) Glide;
    (vi) Landing (power on and power off) ; and
    (vii) Recovery to power-on flight from a balked autorotative approach.

(b) The margin of cyclic control must allow satisfactory roll and pitch control at Vne with—
  (1) Critical weight;
  (2) Critical center of gravity;
  (3) Critical rotor r.p.m.; and
  (4) Power off (except for helicopters demonstrating compliance with paragraph (e) of this section) and power on.

(c) A wind velocity of not less than 17 knots must be established in which the rotorcraft can be operated without loss of control on or near the ground in any maneuver appropriate to the type (such as crosswind takeoffs, sideward flight, and rearward flight), with—
  (1) Critical weight;
  (2) Critical center of gravity;
  (3) Critical rotor r.p.m.; and
  (4) Altitude, from standard sea level conditions to the maximum altitude capability of the rotorcraft or 7,000 feet, whichever is less.

(d) [...]"

(**Part 27.143, Amendment 1 to 26**)

6.2 Bundeswehr Research Institute regarding Inlet Ramps

Original German quote from the Bundeswehr Research Institute for Materials, Fuels and Lubricants regarding Inlet Ramps:

> "Die Untersuchungsergebnisse zeigen, dass die Oberseite der UIR [Anm.: *Upper Inlet Ramp*] angeschliffen wurde. Die Unterseite wurde lackiert. Diese Lackierung wurde im Randbereich grob entfernt. Anschliff und Lackierung der UIR sind ohne erkennbare Funktion. Daher ist anzunehmen, dass die Ober- und Unterseite in der Produktion vertauscht wurden. Beim Klebevorgang ist dies offenbar aufgefallen, da der Lack im Randbereich der Klebung grob entfernt wurde. Eine ausreichende Oberflächenvorbehandlung fand jedoch nicht statt, da die Klebung adhäsives Versagen an der Grenzfläche zwischen dem Heckausleger und der UIR aufweist.
>
> Damit unterscheidet sich der Klebschichtaufbau der UIR signifikant von dem der LIR [Anm.: *Lower Inlet Ramp*], der keine Lackreste aufweist. Die Klebevorschrift der Firma McDonnell Douglas besagt, dass UIR und LIR nicht angeschliffen werden sollen. Dies steht im Gegensatz zum Klebstoffdatenblatt, das ein Anrauen der Oberfläche vorsieht.
>
> Eine Aussage darüber, ob das Versagen vor bzw. nach dem Flugunfall aufgetreten ist, kann nicht getätigt werden." (Report of the Bundeswehr Research Institute for Materials, Fuels and Lubricants)

6.3 Flow simulation

The expert report prepared by flowdynamics "Investigation of the ground effect on the aerodynamic properties of a helicopter with a NOTAR system" is attached below.

Untersuchung des Bodeneffekts auf die aerodynamischen Eigenschaften eines Helikopters mit NOTAR-System

Markus Trenker Dieter Reisinger

21. November 2019

flowdynamics

Inhaltsverzeichnis

1 Einleitung

Die Strömung am Heckausleger des Helikopters MD-900, Abb. (1.1) mit NOTAR-System soll untersucht werden. Hierzu wird sowohl die Ausströmung der Luft an den Längsschlitzen des Heckauslegers als auch die vom Hauptrotor erzeugte Strömung berücksichtigt. Im Besonderen soll der Einfluss der Bodennähe auf die Umströmung des Helikopters untersucht werden. Aus den Ergebnissen der Simulationen werden sowohl Erkenntnisse über die lokale Strömung am Heckausleger als auch deren Auswirkung auf die globalen Eigenschaften des Helikopters, wie angreifende Kräfte und Momente gewonnen.

Abbildung 1.1: Helikopter MD-900 der Londoner Air Ambulance

© https://upload.wikimedia.org/wikipedia/commons/b/b2/(cropped)_London_Air_Ambulance_G-EHMS.jpg

2 Durchführung

In den nachfolgenden Kapiteln werden die einzelnen Schritte der Strömungsberechnung vorgestellt. Die Aufbereitung der Geometrie wurde in verschiedenen CAD-Programmen, unter anderem in ANSYS durchgeführt. Die Vernetzung des Strömungsgebietes wurde in ANSYS Fluent Meshing durchgeführt, und zur Berechnung der stationären Umströmung des Helikopters wurde der finite Volumen Solver ANSYS Fluent eingesetzt.

2.1 Geometrieaufbereitung

Ein Geometriemodell des Helikopters wurde bei https://hum3d.com/ in den zwei Datenformaten „stl" und „iges" erworben. Die beiden Formate unterscheiden sich in der Definition der Geometrie: Während das stl-Format die Oberflächen des Objekts als tesselierte Dreiecksflächen darstellt, speichert das iges-Format einzelne Flächen des Objekts durch die Angabe von Kontrollpunkten der Fläche ab. Mithilfe dieser Kontrollpunkte wird während des iges-imports die Fläche mit speziellen Routinen zum Zwecke der Darstellung berechnet. Abbildung Abb. (2.1) zeigt den Helikopter im stl-format, Abb. (2.2) zeigt die iges-Repräsentation.

Abbildung 2.1: stl-Repräsentation des Helikopters MD-900

In beiden Datenformaten übersteigt der Detaillierungsgrad des Modells bei Weitem den Erfordernissen für die vorgesehene Simulation. Das Modell musste deshalb vereinfacht werden. Die Längsschlitze am Heckausleger, die in der Simulation berücksichtigt werden sollen, fehlten jedoch in beiden Datenformaten. Die Modelle des Anbieters hum3d werden zumeist für die Programmierung bzw. Erweiterung von Computerspielen, Flugsimulatoren usw. eingesetzt, deren Anforderungen sich deutlich von denen einer Strömungssimulation unterscheiden:

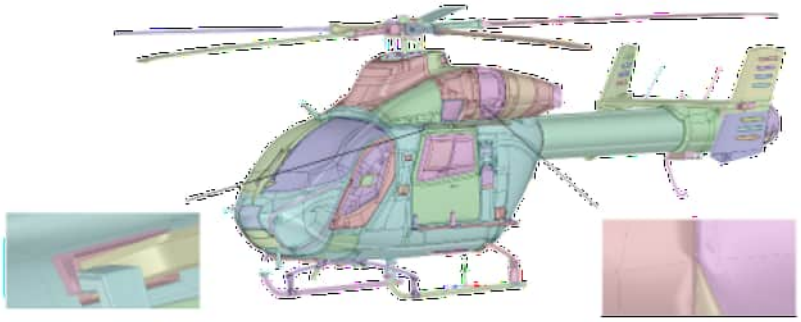

Abbildung 2.2: iges-Repräsentation des Helikopters MD-900

Während der hohe Detaillierungsgrad für realitätsnahe Computeranimationen wichtig ist, kann dieser für Strömungssimulationen oftmals störend sein, da geometrische Details aufgelöst sind, die für die vorgesehene Untersuchung unwesentlich sind und den Bearbeitungs- und Berechnungsaufwand deutlich erhöhen würden. Eine wesentliche Unterscheidung zwischen dem Modell zur Animation und dem Modell zur Strömungssimulation stellt jedoch die zwingende Bedingung der „Wasserdichtheit" für das Simulationsmodell dar.
Die übliche Vorgehensweise ist nun das Geometriemodell soweit wie notwendig zu vereinfachen und alle Flächen in einer Weise zu verbinden, so dass ein wasserdichtes Modell entsteht, ohne jedoch das globale Erscheinungsbild des Modells nicht zu stark zu verändern. Zur Berechnung der Umströmung muss in weiterer Folge ein ausreichend großer Strömungsbereich um das Modell definiert werden, von dem das Helikoptermodell durch eine Boole'sche Operation geometrisch abgezogen wird. Das auf diese Weise erhaltene, sogenannte Negativvolumen ist der Bereich in dem die Strömung berechnet wird.
Für Strömungssimulationen wird üblicherweise eine iges- bzw. stp-Repräsentation herangezogen, da sie bestens für die Bearbeitung in CAD-Programmen geeignet ist. Es zeigte sich jedoch, dass aufgrund der vielen nicht verbundenen Flächen, siehe Details in Abb. (2.2), dieses Modell nicht geeignet für die weitere Verarbeitung ist. Es wurde deshalb die stl-Repräsentation herangezogen. Die Bearbeitung der facettier-

ten stl-Geometrie stellt sich ebenfalls als schwierig heraus, da keine Flächeninformationen vorhanden sind, sondern nur die Darstellung durch Dreiecke. Das stl-Modell wurde deshalb soweit wie möglich vereinfacht und danach einem wrapping-Prozess unterzogen. Hierbei wird die stl-Geometrie mit einer numerischen „Haut" deren Steifigkeit einstellbar ist, umhüllt. Die neu generierte Oberfläche schmiegt sich an die stl-Geometrie an und erzeugt eine wasserdichte Oberfläche des Modells. Das auf diese Weise erzeugte Modell des Helikopters wird, wie bereits erwähnt, vom Umgebungsvolumen abgezogen, um so das Strömungsvolumen zu erhalten. Da das Leitwerk am Heckausleger erst bei höheren Geschwindigkeiten im Vorwärtsflug wirksam wird, wurde dieser nach Rücksprache mit dem Auftraggeber entfernt, um die Strömung an den Längsschlitzen am Heckausleger besser untersuchen zu können.

2.2 Netzgenerierung

In Abbildung (2.3) ist das erstellte Strömungsgebiet um den Helikopter dargestellt. Alle Oberflächen sind bereits mit dreieckigen Oberflächenelementen vernetzt. Am Boden des Rechengebietes wurde das Oberflächennetz im Bereich des Helikopters entsprechend verfeinert.

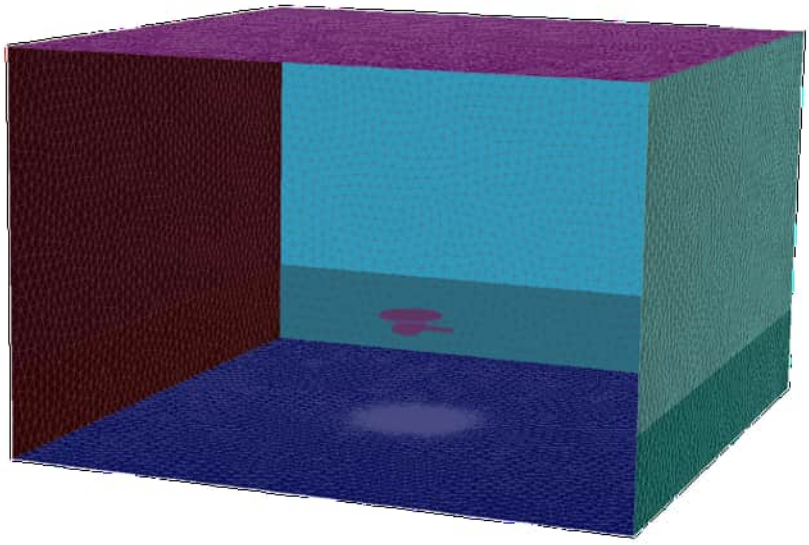

Abbildung 2.3: Das erstellte Rechengebiet, die Vorderseite ist zur besseren Sichtbarkeit entfernt.

Anstelle des Rotors wurde ein zylindrisches Volumen mit Rotordurchmesser erzeugt, dessen Basisfläche in späterer Folge mit einem Drucksprung („actuator disc") beaufschlagt wird. Der für die Berechnung schlussendlich aufbereitete Helikopter ist in Abb. (2.4) dargestellt.

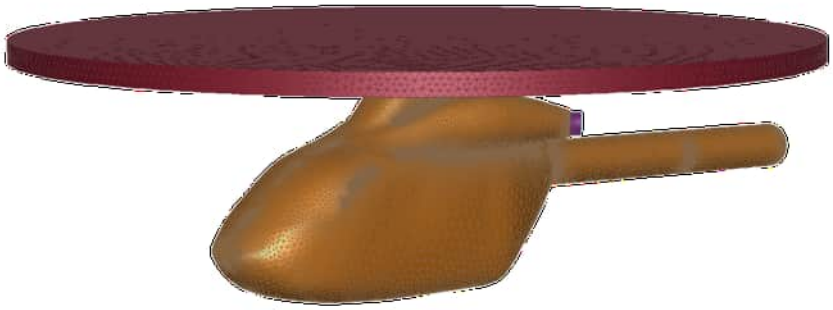

Abbildung 2.4: Der Helikopter mit dem Rotorvolumen

Nachdem alle Oberflächen mit hinreichender Qualität vernetzt sind, wird das Volumennetz im Rechengebiet erstellt. Das Netz besteht aus zirka 15 Millionen Zellen. Abbildung (2.5) zeigt einen Schnitt durch das Berechnungsgebiet.

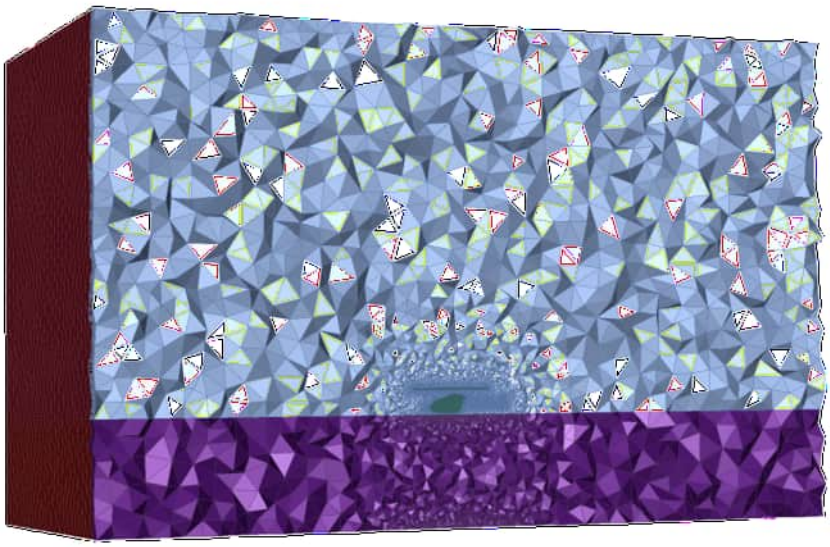

Abbildung 2.5: Das erstellte Volumennetz in einem Isoschnitt

2.3 Definition der Randbedingungen

Zur Definition der Strömungssimulation müssen nun an allen Flächen, die das Strömungsvolumen begrenzen, Strömungsparameter definiert werden. Die im Strömungsvolumen zu lösenden Erhaltungsgleichungen, inklusive der beiden Turbulenzgleichungen des $k-\omega-SST$ Turbulenzodells sind nichtlineare, partielle Differentialgleichungen 2. Ordnung (Reynolds-gemittelte Navier-Stokes Gleichungen), die iterativ gelöst werden. Die Beschreibung der zu lösenden Aufgabenstellung erfolgt neben der Geometriedefinition, durch die Beschreibung des Verhaltens der Strömung an allen begrenzenden Flächen, den Randbedingungen. Abbildungen (2.6) und (2.7) zeigen das Strömungsvolumen mit den definierten Randbedingungen.

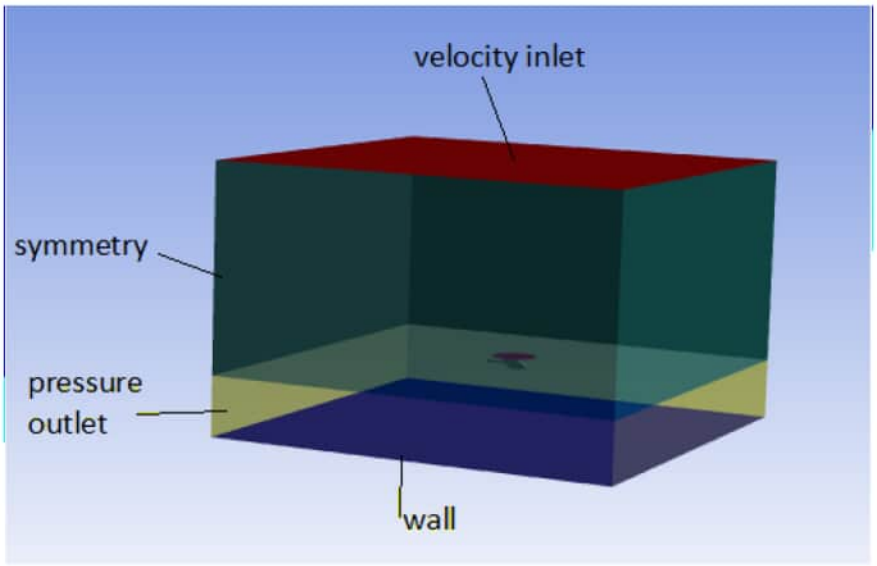

Abbildung 2.6: Definition der Randbedingungen

Die Längsschlitze am Heckausleger wurden gemäß den Angaben des Auftraggebers in das Modell eingebaut, siehe folgende Abb. (2.7).

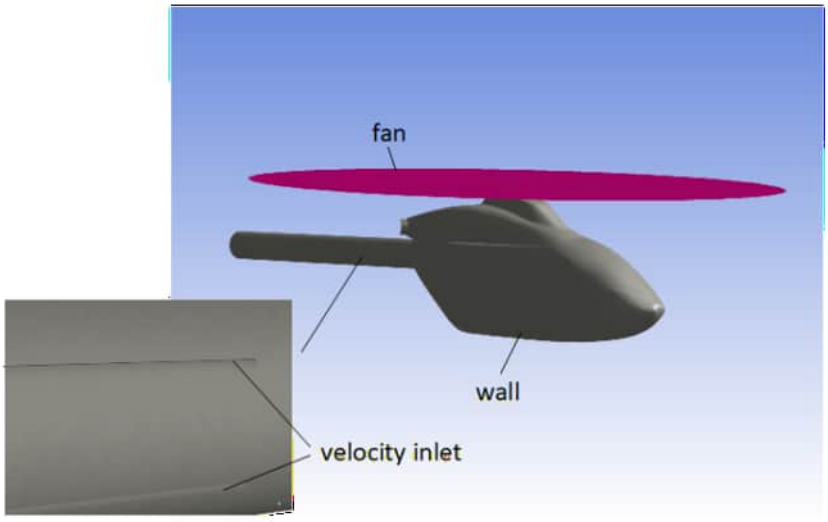

Abbildung 2.7: Definition der Randbedingungen am Helikopter. Die Detailabbildung zeigt die tangentialen Längsschlitze am Heckausleger.

Der Erdboden und die Außenflächen des Helikopters werden als reibungsbehaftete Wände („wall") mit der entsprechenden Haftbedingung modelliert. An der Randbedingung „velocity inlet" wird eine Einlassgeschwindigkeit definiert. An den beiden Längsschlitzen wurde gemäß den Angaben des Auftraggebers eine Geschwindigkeit von 60 m/s gesetzt. Diese Strömung tritt hier aus dem Helikopters aus, und ist deshalb für die Simulation der Strömung um den Helikopter eine Eintrittsgeschwindigkeit. Zur Stabilisierung des Lösungsverfahrens wurde an der Oberseite des Strömungsvolumens eine einheitliche Strömungsgeschwindigkeit von 0.5 m/s angegeben. Dies erzeugt eine vertikale Windgeschwindigkeit im gesamten Strömungsgebiet. Die Geschwindigkeit ist mit 0.5 m/s gering genug, um nicht Gefahr zu laufen, die Berechnung zu verfälschen. Diese Randbedingung dient lediglich zu einem besseren Konvergenzverhalten des Lösungsverfahrens und wurde nicht aufgrund der Flugphysik in die Berechnung eingebracht. Die Richtung der Geschwindigkeitsrandbedingungen ist stets normal zur jeweiligen Fläche.
An der „fan" Randbedingung wird ein Drucksprung von 300 Pa definiert. Dieser Wert, multipliziert mit der Fläche des Rotors von 84 m^2 ergibt eine Kraft von 25200 N, die einer Masse des Helikopters von zirka 2.5 t entspricht. An den „pressure-outlets" kann die Strömung sowohl das Strömungsgebiet verlassen als auch mit Umgebungsdruck wieder einfließen. Die Symmetrierandbedingung entspricht einer reibungsfreien Wand.
Die Luft wird als inkompressibles, ideales Gas mit einer Dichte von 0.8 kg/m^3 bei einem Umgebungsdruck von 67020 Pa angenommen. Dies entspricht in etwa einer Höhe von 3000 m.

3 Einschränkungen

Der gewählte Lösungsweg zur Berechnung der Strömung unterliegt den folgenden wesentlichen Einschränkungen:

- Die Berechnungen werden stationär durchgeführt. Es können deshalb keine Aussagen über den zeitlichen Verlauf der Bewegung des Helikopters und der Strömung gemacht werden.

- Das Leitwerk wurde nicht modelliert. Es wird davon ausgegangen, dass das Leitwerk erst ab einer Fluggeschwindigkeit von ca. 7 m/s erste Wirkung zeigt. Im Moment des Abhebens, im Schwebeflug, ist die Fluggeschwindigkeit sehr gering. Das Leitwerk ist damit nicht wirksam. Sobald sich der Helikopter in eine Drehbewegung um die Hochachse bewegt, würden die Leitwerksflächen allerdings aufgrund des Strömungswiderstandes bei seitlicher Anströmung dämpfend wirken. Eine mögliche Interferenz zwischen Rotor-Downwash und Leitwerk müsste ggf. ebenfalls berücksichtigt werden

- Die beiden Abgasströme der Turbinen wurden aufgrund nicht vorhandener Daten nicht berücksichtigt.

- Die drehbar gelagerte Schubdüse am Ende des Heckauslegers wurde nicht modelliert. Der Pilot bringt über die Anti-Torque Pedale eine Seitenkraft auf, die durch die drehbar gelagerte Schubdüse verändert werden kann. In dieser Berechnung stellen wir die Frage, ob die Umströmung des Heckauslegers an sich, in Verbindung mit der aus den Schlitzen austretenden Strömung, sich bei Annäherung an den Erdboden verändert und wenn ja wie. Das Nicht-Modellieren der Schubdüse hat daher keine Einschränkung auf die gegenständliche Fragestellung.

- Der Rotor wird durch einen konstanten Drucksprung simuliert („actuator disc"). Der Rotorabwind ist daher über den gesamten Rotordurchmesser konstant, d.h. der Abwind an den Blattspitzen ist gleich dem Abwind im Innenbereich der Rotorscheibe. In einer realen Rotorströmung muss man davon ausgehen, dass sich die Abwinde von innen nach außen verändern.

- Die Austrittsgeschwindigkeit am Heckausleger wurde konstant mit 60 m/s angenommen. Am realen Hubschrauber muss man davon ausgehen, dass sich die Austrittgeschwindigkeit am Schlitz von vorne nach hinten verändert.

- Ablösungen sind sehr von der Reynoldszahl und vom Zustand der Strömung (laminar, turbulent) und von der Oberflächenbeschaffenheit abhängig. Für die Berechnungen werden alle Oberflächen des Modells als hydraulisch glatt angenommen. Am realen Fluggerät können Verschmutzungen, vorstehende Nieten, oder Bleche und Kanten, die nicht modelliert wurden, das Strömungsbild verändern.

- Der Erdboden wird als glatte, homogene Wand definiert. Die in der Praxis oftmals bei Außenlandungen beobachteten Geländestufen oder Unebenheiten werden in der Berechnung nicht berücksichtigt.

4 Auswertung

Es wurden vier stationäre Simulationen für unterschiedliche Bodenabstände durchgeführt: Für den geringsten Abstand wurde ein Bodenabstand des Helikopters von 8 cm gewählt. Dieser Fall wird im Folgenden mit „Bodenabstand 0 m" bezeichnet. Die weiteren Abstände zwischen den Kufen des Helikopters und dem Boden wurden mit 3 m, 6 m und 15 m festgelegt.
Die folgende Auswertung zeigt Stromlinien, die aus dem erhaltenen Geschwindigkeitsfeld berechnet wurden. Die farbliche Kodierung entspricht der lokalen Geschwindigkeit $U = \sqrt{u^2 + v^2 + w^2}$ als vektorielle Summe der lokalen Geschwindigkeitskomponenten u, v, w in x, y und z-Richtung. Die Stromlinien wurden sowohl bei den beiden Schlitzen am Ausleger, die unter 80° und 135° bezogen auf die vertikale Symmetrieebene angeordnet sind, als auch vom Rotor gestartet. In allen folgenden Abbildungen wird zur besseren Sichtbarkeit nur jede 50'ste Stromlinie dargestellt. Das verwendete Koordinatensystem ist in Abb. (4.1) abgebildet.

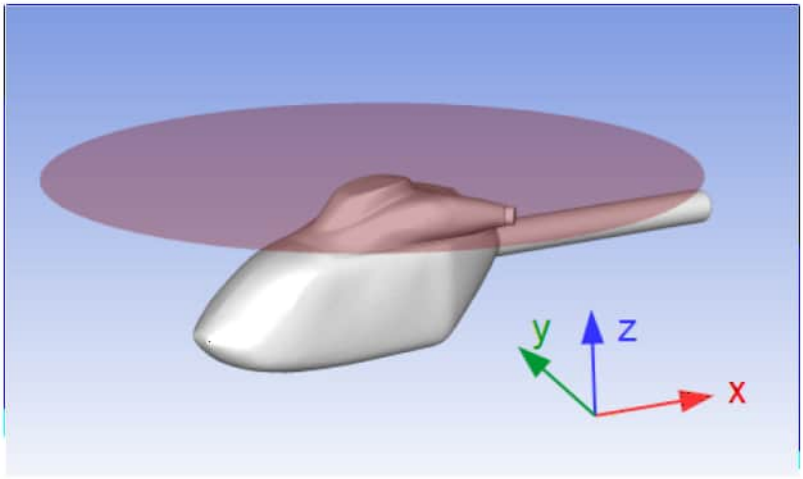

Abbildung 4.1: Helikopter mit verwendetem Koordinatensystem

4.1 Stromlinien im Strömungsfeld

Schwebehöhe 0 m

Die folgenden Abbildungen (4.2, 4.3, 4.4) und (4.5) zeigen das Ergebnis für einen Bodenabstand von 0 m, das heißt die Bodenplatte des Helikopters befindet sich 8 cm über dem Boden. Die von den Längsschlitzen am Heckausleger ausströmende Luft fließt annähernd horizontal seitlich vom Helikopter ab.

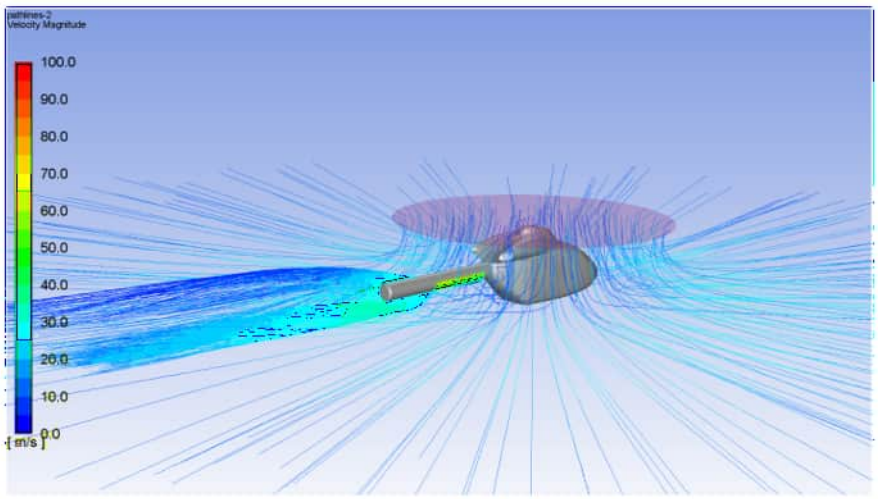

Abbildung 4.2: Stromliniendarstellung bei 0 m Bodenabstand

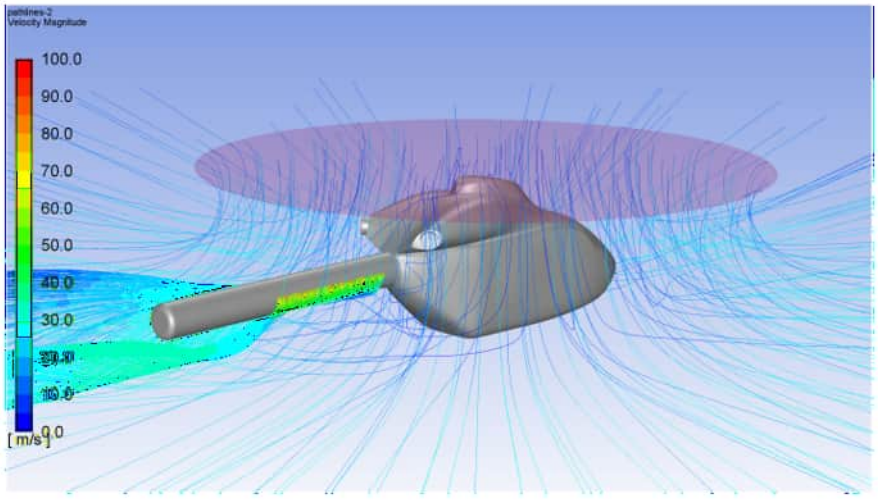

Abbildung 4.3: Detaildarstellung, Stromliniendarstellung bei 0 m Bodenabstand

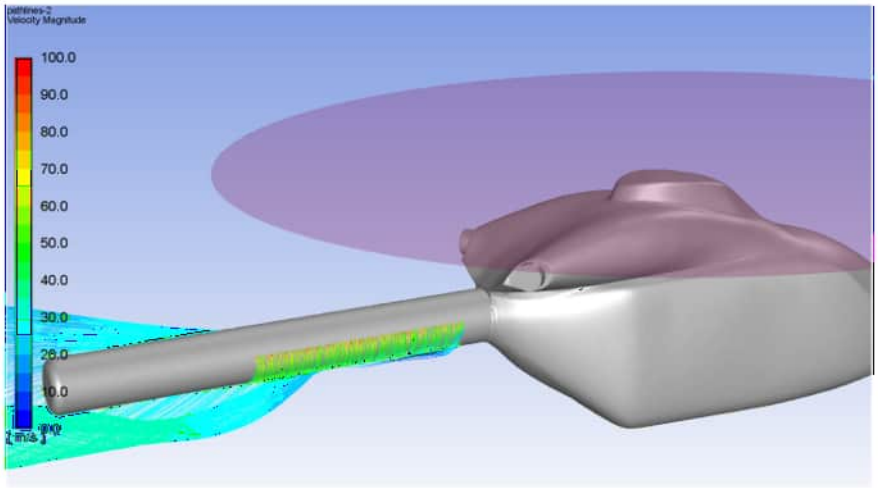

Abbildung 4.4: Detaildarstellung, Stromliniendarstellung bei 0 m Bodenabstand

In Abb.(4.5) ist eine Ablöselinie auf der Backbordseite des Helikopters zu erkennen. Am Beginn der Längsschlitze löst die Strömung bei etwa 180° bezogen auf die vertikale Symmetrieebene ab. Dieser Winkel vergrößert sich auf etwa 270° am Ende der Ausblasung. Aufgrund des instationären Charakters der Strömung muss jedoch eine, in der realen Strömung vermutliche zeitliche Veränderung dieser Linie, die in der stationären Rechnung nicht dargestellt werden kann, bei der Interpretation berücksichtigt werden.

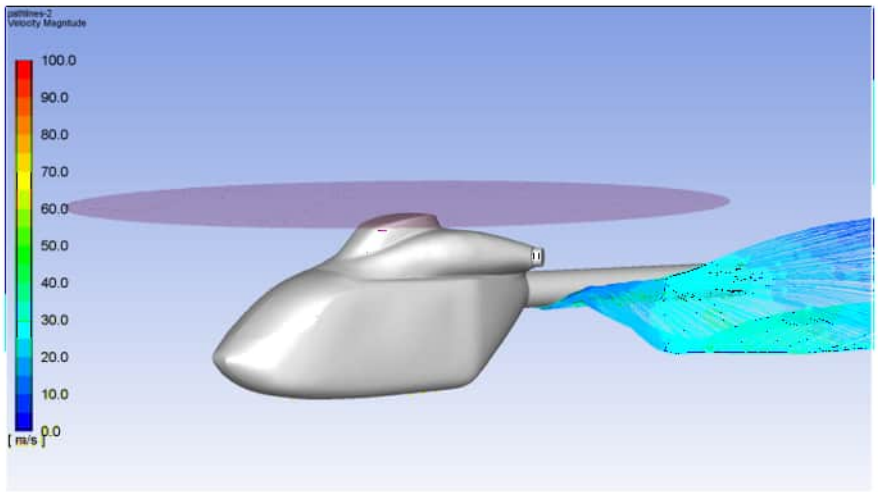

Abbildung 4.5: Detaildarstellung, Stromliniendarstellung bei 0 m Bodenabstand

Schwebehöhe 3 m

Die folgenden Abbildungen (4.6, 4.7, 4.8) und (4.9) zeigen das Ergebnis für einen Bodenabstand von 3 m. Am Heckausleger haben sich 2 großskalige Wirbel gebildet.

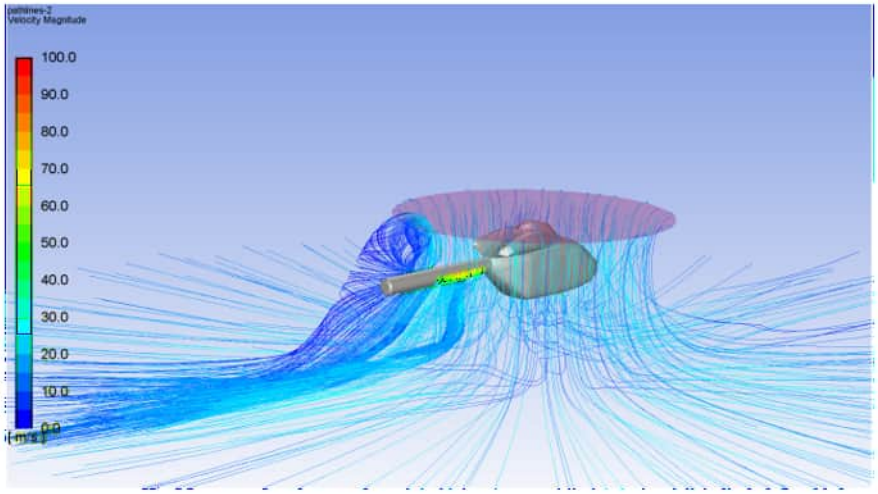

Abbildung 4.6: Stromliniendarstellung bei 3 m Bodenabstand

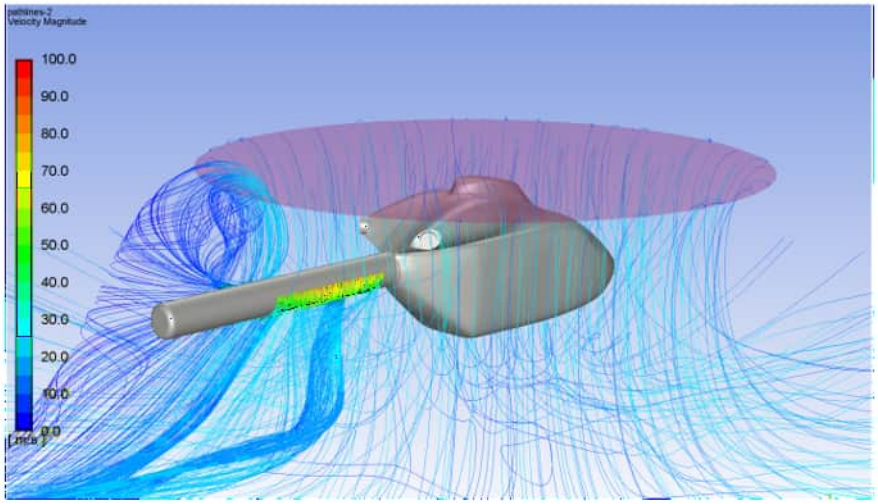

Abbildung 4.7: Detaildarstellung, Stromliniendarstellung bei 3 m Bodenabstand

Am hinteren Teil des Heckauslegers führt die tangentiale Ausblasung an den beiden Längsschlitzen zu einer Umströmung des Heckauslegers bis zirka 270° auf die Backbordseite des Helikopters, siehe Abb. (4.9). Danach löst die Strömung nach oben ab und wird durch den Rotorabwind wieder nach unten gedrückt. Der zweite Wirbel, am Beginn der tangentialen Ausblasung an den beiden Längsschlitzen, löst bereits an der Unterseite des Heckauslegers ab und bildet einen vertikalen Wirbel, dessen Geschwindigkeit höher ist als die des hinteren Wirbels.

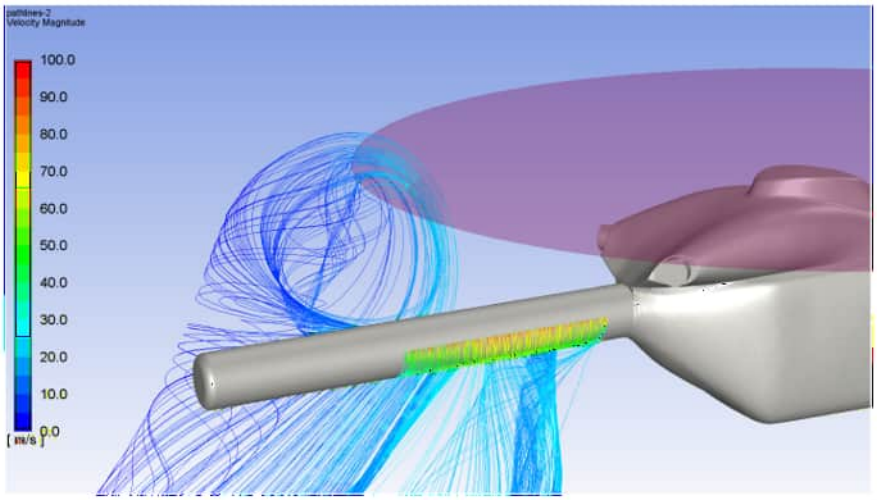

Abbildung 4.8: Detaildarstellung, Stromliniendarstellung bei 3 m Bodenabstand

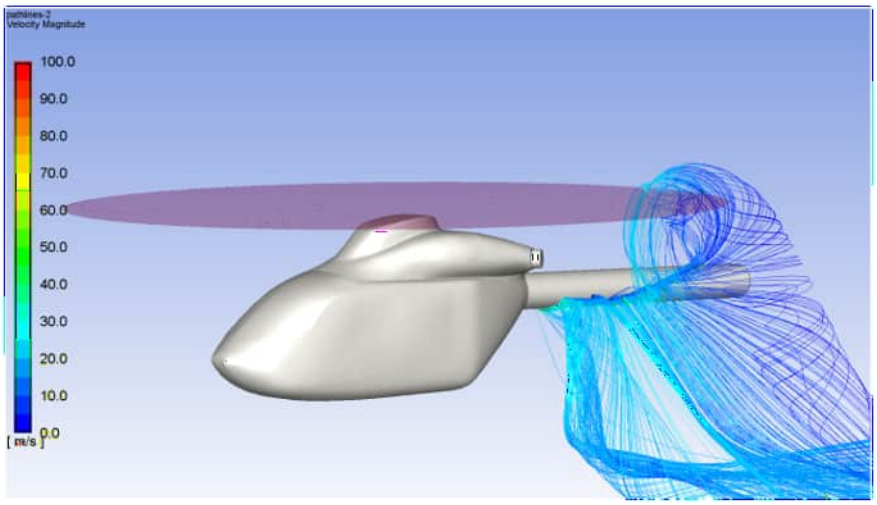

Abbildung 4.9: Detaildarstellung, Stromliniendarstellung bei 3 m Bodenabstand

Schwebehöhe 6 m

Abbildung (4.10) zeigt die Strömung bei einem Bodenabstand von 6 m.

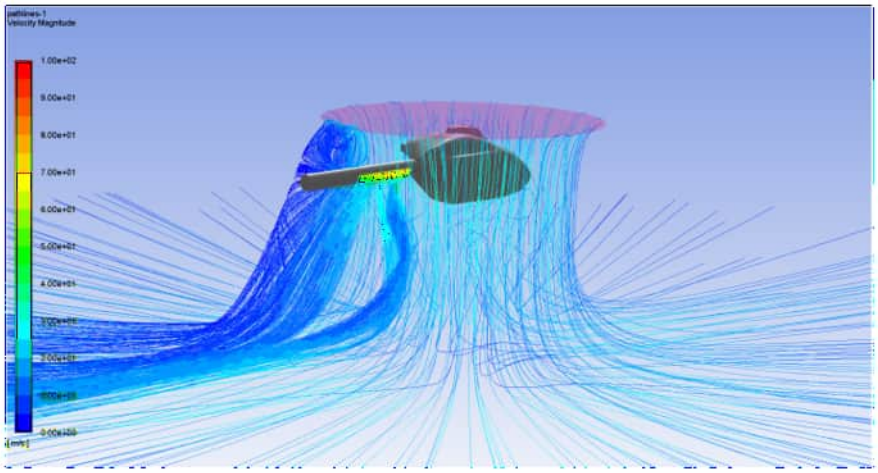

Abbildung 4.10: Stromliniendarstellung bei 6 m Bodenabstand

Der hintere Wirbel interagiert weiterhin mit dem Hauptrotor.

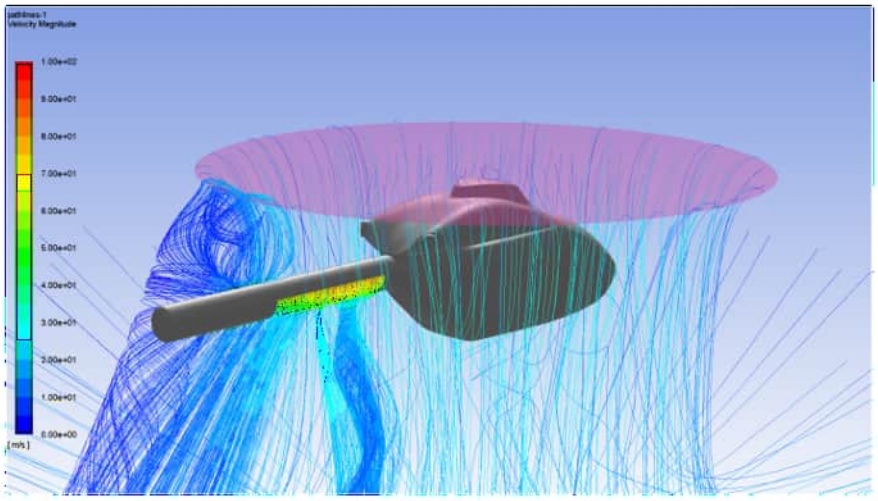

Abbildung 4.11: Detaildarstellung, Stromliniendarstellung bei 6 m Bodenabstand

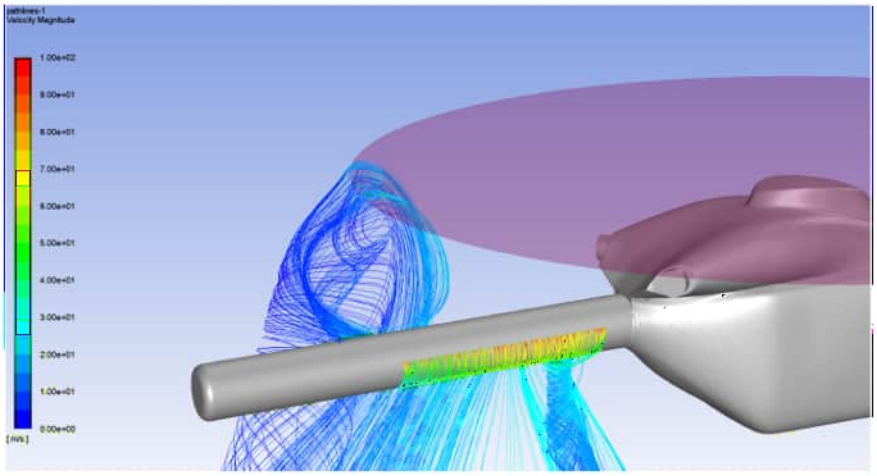

Abbildung 4.12: Detaildarstellung, Stromliniendarstellung bei 6 m Bodenabstand

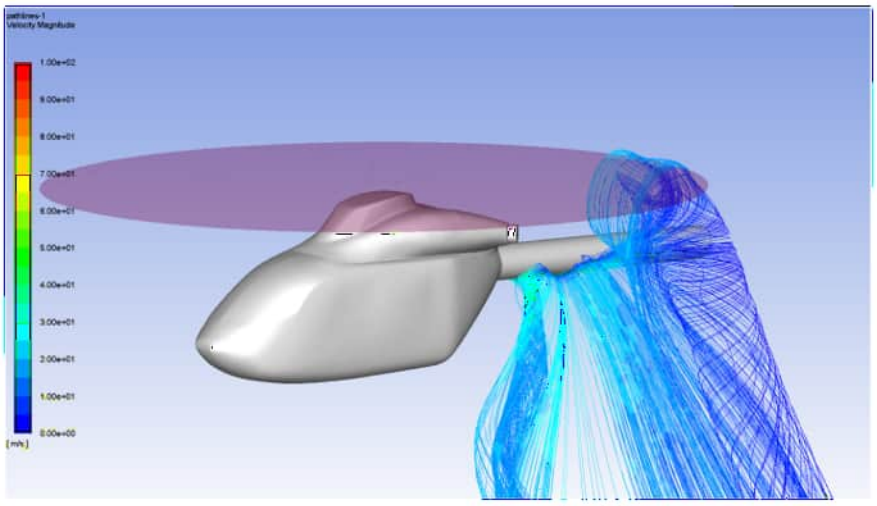

Abbildung 4.13: Detaildarstellung, Stromliniendarstellung bei 6 m Bodenabstand

Schwebehöhe 15 m

Abbildung (4.14) zeigt das Ergebnis der Simulation für die in dieser Untersuchung maximale Entfernung des Helikopters vom Boden von 15 m. Die beiden großskaligen Wirbel sind weiterhin vorhanden und dominieren das Strömungsbild.

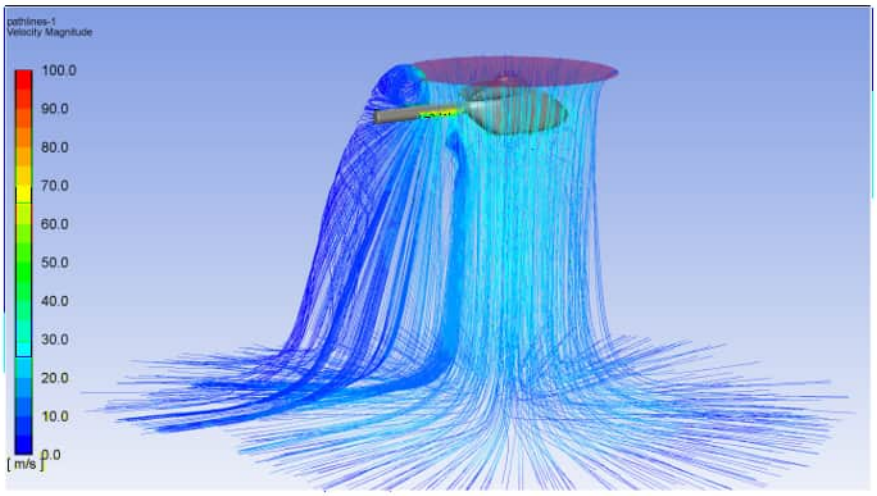

Abbildung 4.14: Stromliniendarstellung bei maximalen Bodenabstand

Die Abbildungen (4.15, 4.16) und (4.17) zeigen Detaildarstellungen dieser Wirbel.

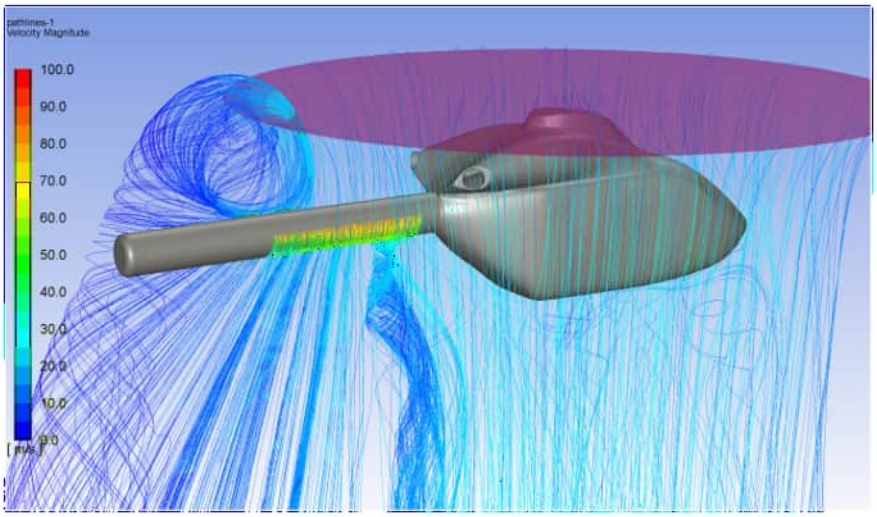

Abbildung 4.15: Detaildarstellung, Stromliniendarstellung bei maximalen Bodenabstand

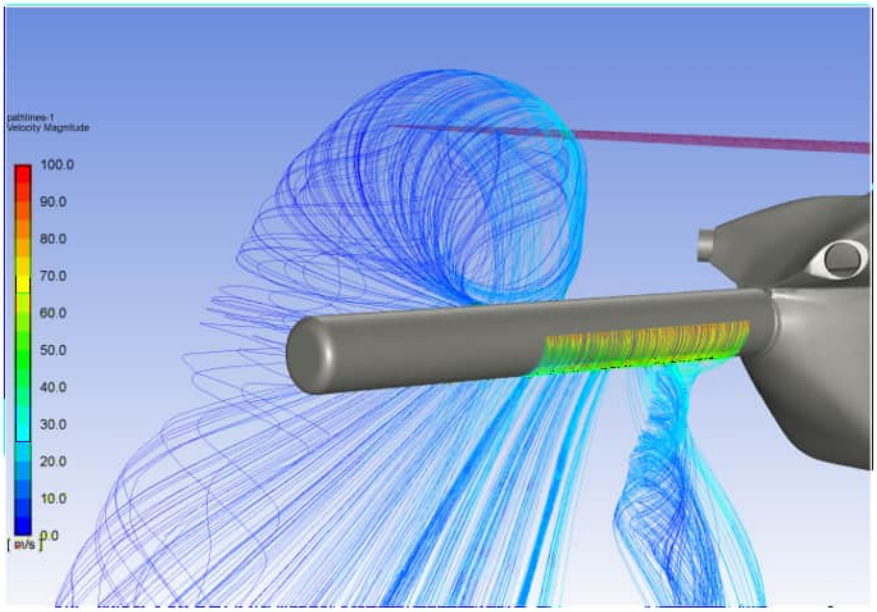

Abbildung 4.16: Detaildarstellung, Stromliniendarstellung bei maximalen Bodenabstand

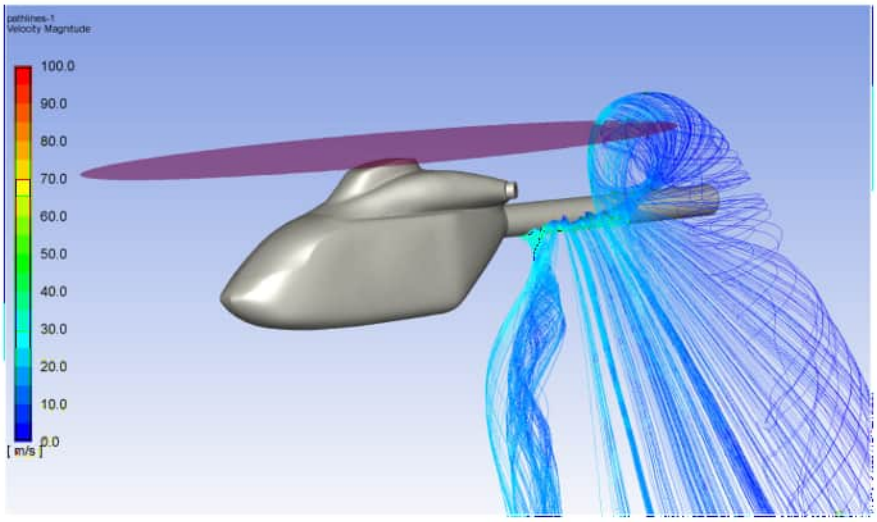

Abbildung 4.17: Detaildarstellung, Stromliniendarstellung bei maximalen Bodenabstand

Anmerkung:

Eine Frage, die sich aus den vorangegangenen Abbildungen stellt, ist, ob die beiden Wirbel Auswirkungen auf die Steuerbarkeit des Helikopters um dessen Hochachse (Gierbewegung) haben. In diesem Falle würden die Wirbel Kräfte und Momente hervorrufen, die die durch die Anti-Torque Pedale und letztlich über die Längsschlitze und Schubdüse erzeugte Seitenkraft beeinflussen. Eine Interaktion zwischen Wirbel und Rotorblatt führt im allgemeinen zunächst zu Vibrationen und zu einer Abnahme der Strömungsqualität, der Hauptrotorströmung.

4.2 Druckverteilung am Helikopter

Die folgenden Abbildungen (4.18, 4.19, 4.20) und (4.21) zeigen die statische Druckverteilung am Helikopter als Differenz zum Umgebungsdruck (p_∞ = 67020 Pa). Die farbliche Codierung ist zur besseren Vergleichbarkeit einheitlich zwischen -2000 Pa und +500 Pa gewählt. Drücke kleiner als Null bedeuten Unterdruck gegenüber der ungestörten, freien Atmosphäre.
Mit Hilfe der Differenzdrücke ist leichter nachvollziehbar, ob am Heckausleger eine Seitenkraft entsteht, und wenn ja, wie sie sich verändert. Wirbel haben im Wirbelkern niedrige Drücke und induzieren daher in der Nähe zu festen Wänden ebenfalls niedrige Drücke. Dieses Phänomen kennt man von militärischen Hochleistungsflugzeugen, wo abgelöste Wirbel über Teile der Tragfläche streichen und dadurch Wirbelauftrieb erzeugen. Im gegenständlichen Fall ist die Sache etwas anders gelagert, weil die Wirbel sich vom Heckausleger nach oben und unten entfernen und damit wenig Fläche mit Unterdruck beaufschlagen können. Die Ablösung von Wirbeln an gekrümmten Oberflächen ist von der Reynolds-Zahl abhängig.
Ein Vergleich der folgenden Abbildungen liefert folgendes Ergebnis:

- Am Rumpf des Hubschraubers gibt es kaum einen Unterschied zwischen der Druckverteilung auf der rechten und auf der linken Seite. Der Beitrag des Rumpfs auf das Giermoment ist somit vernachlässigbar.

- Am Heckausleger ist ein Unterschied in der Druckverteilung zwischen rechter und linker Seite zu beobachten, und zwar für alle Schwebehöhen. Während auf der rechten Seite vor allem Unterdrücke dominieren, sind es auf der linken Seite lokale Überdrücke. Dies lässt den Schluss zu, dass das Giermoment, und damit eine Drehbewegung um die Hochachse, durch die lokalen Druckverteilungen am Heckausleger induziert wird, wenn das durch den Rotor erzeugte Moment unberücksichtigt bleibt.

- Der lokale Druckunterschied im Ablösebereich des vorderen Wirbels nimmt mit zunehmenden Bodenabstand an Stärke zu. Auf der Steuerbordseite ist

ein Gebiet mit lokalem Unterdruck ersichtlich, welches ab 3 m Bodenabstand seine Lage nicht wesentlich ändert und im Einflussbereich des Rotor liegt. Dieses Unterdruckgebiet entsteht während des Abhebenvorganges bei einem Bodenabstand zwischen 0 m und 3 m.

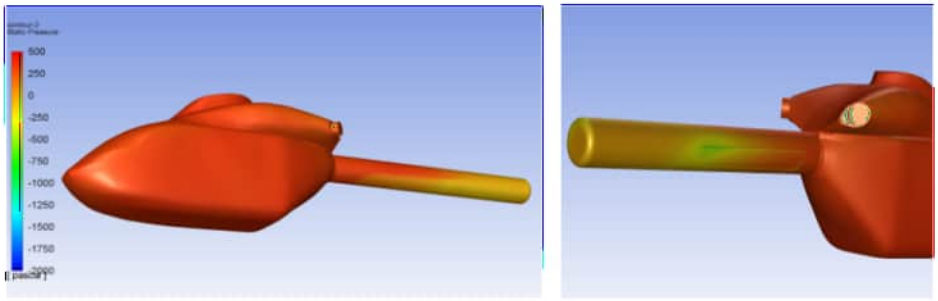

Abbildung 4.18: Druckverteilung am Helikopter bei 0 m Bodenabstand, Minimum und Maximum der Farbskala geclippt.

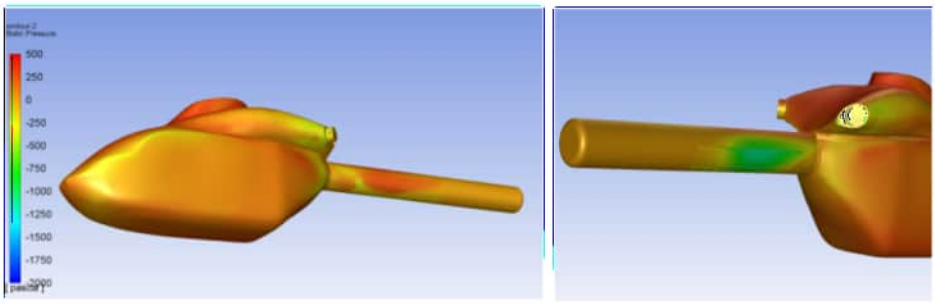

Abbildung 4.19: Druckverteilung am Helikopter bei 3 m Bodenabstand, Minimum und Maximum der Farbskala geclippt.

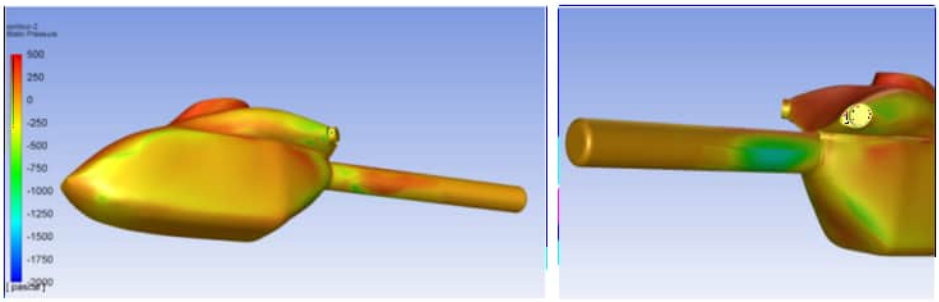

Abbildung 4.20: Druckverteilung am Helikopter bei 6 m Bodenabstand, Minimum und Maximum der Farbskala geclippt.

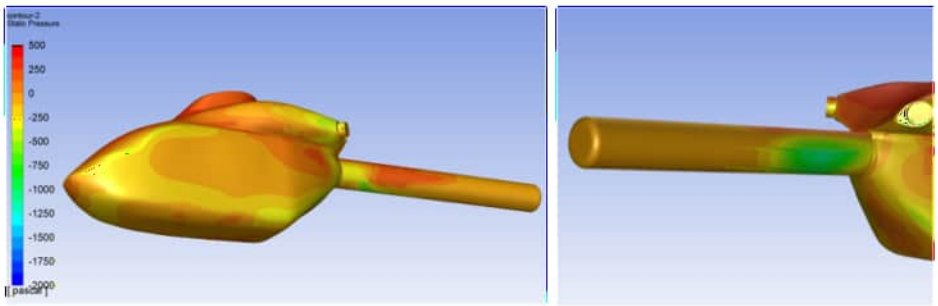

Abbildung 4.21: Druckverteilung am Helikopter bei 15 m Bodenabstand, Minimum und Maximum der Farbskala geclippt.

5 Zusammenfassung

Es wurden vier stationäre Simulationen für Schwebehöhen von 0 m, 3 m, 6 m und für 15 m durchgeführt. Im Lösungsverlauf der Simulationen zeigte sich ein zeitabhängiges Verhalten der Strömung. Die Lösungen der Simulationen bestehen aus den berechneten Strömungsgrößen, wie beispielsweise den Geschwindigkeitskomponenten und dem Druck in jedem Zellmittelpunkt des Netzes. Aus dieser Datenmenge wurden exemplarisch Stromlinien im Strömungsgebiet und Druckverteilungen an der Oberfläche des Helikopters berechnet und dargestellt. Aus den Druckverteilungen wurden die, auf den Helikopter angreifenden Kräfte und Momente in x, y und z-Richtung des kartesischen Koordinatensystems berechnet. Die Kraft F_z ist jene Kraft, welche im Wesentlichen durch den Rotorabwind entsteht. Diese Kraft muss zur Gewichtskraft addiert werden, wenn die für einen Schwebeflug erforderliche Gesamtauftriebskraft, die der Rotor aufbringen muss, bestimmt werden soll.
In Abb. (5.1) werden die Kräfte F_x, F_y und F_z über der Schwebehöhe dargestellt. Die vier simulierten Fälle sind als Knoten dargestellt und Zwecks besserer Darstellung durch kubisches Spline verbunden.

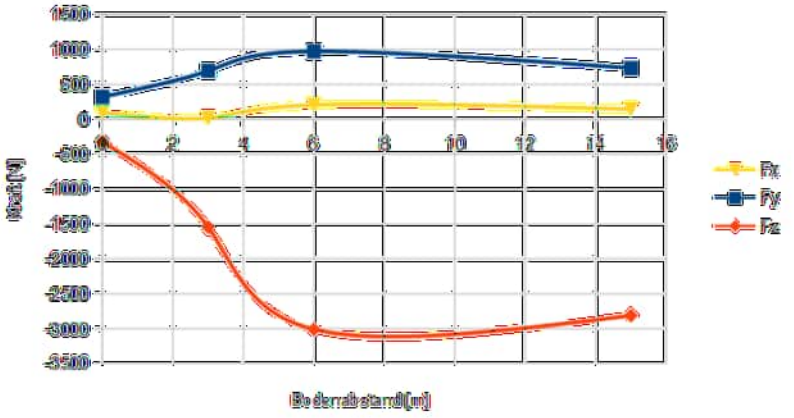

Abbildung 5.1: Kräfte F_x, F_y und F_z, orientiert als Kräfte, die von der Strömung auf den Helikopter wirken, dargestellt über dem Abstand des Helikopters vom Boden

Während die Kraft F_x, in Richtung der Längsachse des Helikopters, relativ wenig variiert und die kleinste absolute Größe über dem Bodenabstand aufweist, nimmt die Kraft F_y, die seitlich auf den Helikopter wirkt, ähnlich der Kraft F_z mit größer werdenden Bodenabstand zu.
Ebenso wie die Kraft, ist das Moment M_z jenes Moment um die Hochachse, welches von der Strömung auf den Helikopter ausgeübt wird. Da die z-Achse von der Erde weggerichtet positiv gezählt wird, ist das Moment M_z im Uhrzeigersinn drehend. Für die Auswertung des Moments wurde ein Schwerpunkt in der Rotorachse, 1.15 m über der Bodenplatte des Helikopters angenommen. Die erhaltenen Werte sind in Abb. (5.2) über dem Bodenabstand dargestellt. Das Moment M_z wächst von 1000 Nm bei 0 m Bodenabstand auf ca. 3000 Nm in 4 m Höhe. Ein Zuwachs bedeutet eine Drehbewegung um die Hochachse nach links, welche der Pilot mit rechtem Pedal ausgleichen müsste. Ab einer Schwebehöhe von zirka vier Metern hat der Abstand vom Boden keinen Einfluss mehr ($M_z \approx$ konstant). Das Moment M_y, in Richtung der Querachse, nimmt ähnlich dem Giermoment mit größer werdenden Bodenabstand zu.

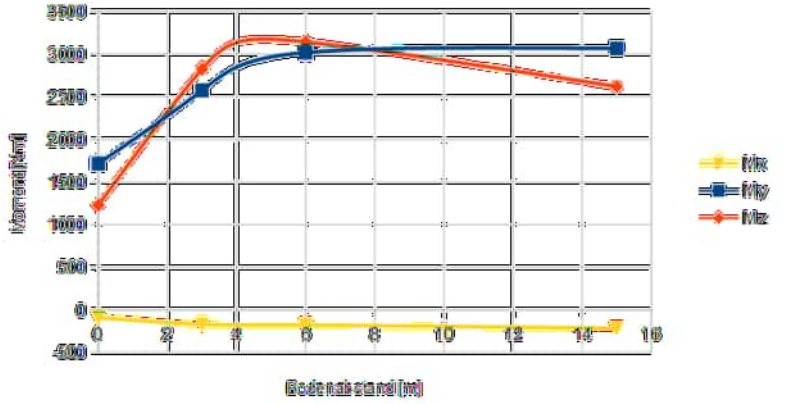

Abbildung 5.2: Momente M_x, M_y und M_z, orientiert als Momente, die von der Strömung auf den Helikopter wirken, dargestellt über dem Abstand des Helikopters vom Boden

Abbildungen (5.1) und (5.2) zeigen, dass mit der Entfernung des Helikopters vom Boden, im Zuge des Abhebevorgangs sowohl die Kräfte als auch die Momente zunehmen. Geht man also davon aus, dass der Hauptrotor unverändert dieselbe Auftriebskraft erzeugt, würde der Gesamtauftrieb des Helikopters sinken.

Aus dem Lösungsverlauf war ersichtlich, dass die Ablösung am Heckausleger stark mit dem Rotor-Downwash interagiert. Bei einem Bodenabstand zwischen 0 m und 3 m löst die Strömung vom Heckausleger an der Backbordseite ab. Während im dem Bereich des Heckauslegers, der sich im Wirkungsbereich des Rotors befindet, die Ablösung durch den Abwind des Rotors nach unten gedrückt wird, löst die Strömung am hinteren Teil des Heckauslegers, der nicht vom Rotor beaufschlagt wird, nach oben ab. Die Anwendung der λ_2-Methode zur Wirbeldetektion bestätigt den vorderen Wirbel. Während die Wirbelstärke des hinteren, größeren Wirbels, die der abfließenden Strömung nicht wesentlich übersteigt, ist die Wirbelstärke des vorderen Wirbel deutlich höher. Eine genaue Untersuchung dieser komplexen, wirbelbehafteten Strömungen ist nur bedingt mit stationären Simulationen möglich. Wirbel sind physikalisch zeitabhängige Phänomene. Eine stationäre Simulation ist zeitunabhängig und kann deshalb nur einen momentanen Zustand der Strömung berechnen. Die angegebenen Werte für Kräfte und Momente in Abhängigkeit vom Bodenabstand können daher nur als Richtwerte verstanden werden. Die Schwankungsbreiten dieser Werte können durch instationäre Simulationen über einen definierten Zeitraum bestimmt werden. Aus den so erhaltenen Werten können dann Mittelwerte und Schwankungsbreiten angegeben werden. Eine diesbezügliche Voruntersuchung zeigte, dass hierfür Zeitschrittgrößen im Bereich von 0.01 s und kleiner dafür nötig wären. Die Berechnungsdauer müsste der Dynamik der Wirbel entsprechend angepasst werden. Der rechnerische und zeitliche Aufwand zur Durchführung dieser transienten Simulation ist im Vergleich zur stationären Simulation ungleich höher.

6 Literatur

- **MD Helicopters**, technical description MD 902 Explorer https://www.mdhelicopters.com/filec/Models/MD902_Tech_Desc.pdf
- **Abmessungen und Geschwindigkeiten MD900**, [redacted], email vom 30.9.2019
  [Anm.: Name des Untersuchungsleiters]
- **Fotos**, [redacted], email vom 10.10.2019
  [Anm.: Name des Untersuchungsleiters]
- **ANSYS**, Fluent Manual v. 19.2

6.4 Pressure Altitude and Density Altitude

Pressure altitude is defined as:

> "Pressure-altitude. An atmospheric pressure expressed in terms of altitude which corresponds to that pressure in the standard atmosphere." (ICAO Annex 8, Part 1)

> "101. 'pressure-altitude' means an atmospheric pressure expressed in terms of altitude which corresponds to that pressure in the Standard Atmosphere, as defined in Annex 8, Part 1 to the Chicago Convention;" (Commission Implementing Regulation (EU) No 923/2012)

The pressure altitude can be calculated exactly using the following barometric formula, assuming a constant temperature lapse rate:

$$H = \frac{T_0}{\beta} \cdot \left[\left(\frac{p}{p_0} \right)^{-\frac{R \cdot \beta}{g_0}} - 1 \right]$$

- T_0 is the air temperature at reference level (MSL),
- β is the temperature lapse rate,
- p is the atmospheric pressure, for which the pressure altitude is to be determined,
- p_0 is the pressure at reference level (MSL),
- R is the specific gas constant for air (287 J/kgK),
- g_0 is the gravitational acceleration (9.81 m/s)

The pressure altitude H is thus obtained by inserting the wanted air pressure p and the parameters of the standard atmosphere for T_0 (288.2 K), β (-0.0065 K/m) and p_0 (1013.25 hPa).

An equivalent definition for density altitude cannot be found in ICAO Annex 8 and Commission Implementing Regulation (EU) No 923/2012. However, the FAA and the European Helicopter Safety Team of EASA defines density altitude as follows:

"Density altitude is the vertical distance above sea level in the standard atmosphere at which a given density is to be found." (FAA "Pilot's Handbook of Aeronautical Knowledge", FAA-H-8083-25B)

"Density Altitude: Density Altitude represents the combined effect of pressure altitude and temperature. DA is defined as the height in the standard atmosphere that has a density corresponding to the density at the particular location (on the ground or in the air) at which the density altitude is being measured." ("Helicopter Performance" from European Helicopter Safety Team)

The density altitude can be calculated exactly using the following barometric formula, assuming a constant temperature lapse rate:

$$H = \frac{T_0}{\beta} \cdot \left[\left(\frac{\rho}{\rho_0} \right)^{-\frac{R \cdot \beta}{R \cdot \beta + g_0}} - 1 \right]$$

- T_0 is the air temperature at reference level (MSL),
- β is the temperature lapse rate,
- ρ is the atmospheric air density, for which the density altitude is to be determined,
- ρ_0 is the density at reference level (MSL),
- R is the specific gas constant for air (287 J/kgK),
- g_0 is the gravitational acceleration (9.81 m/s)

The density altitude H is thus obtained by inserting the wanted air density ρ and the parameters of the standard atmosphere for T_0 (288.2 K), β (-0.0065 K/m) and ρ_0 (1.225 kg/m³).

Federal Safety Investigation Authority of Austrian
Radetzkystrasse 2, 1030 Vienna
+43 71162 65 0
fus@bmk.gv.at
bmk.gv.at/sub